OSCAR THE GROUCH: A ZEBRAFISH MODEL OF HERITABLE T CELL ACUTE LYMPHOBLASTIC LEUKEMIA THAT DISPLAYS APOPTOSIS RESISTANCE

by

Lynn A. Rudner

A dissertation submitted to the faculty of
The University of Utah
in partial fulfillment of the requirements for the degree of

Doctor of Philosophy

Department of Oncological Sciences

The University of Utah

May 2011

UMI Number: 3445249

All rights reserved

INFORMATION TO ALL USERS
The quality of this reproduction is dependent upon the quality of the copy submitted.

In the unlikely event that the author did not send a complete manuscript
and there are missing pages, these will be noted. Also, if material had to be removed,
a note will indicate the deletion.

UMI 3445249
Copyright 2011 by ProQuest LLC.
All rights reserved. This edition of the work is protected against
unauthorized copying under Title 17, United States Code.

ProQuest LLC
789 East Eisenhower Parkway
P.O. Box 1346
Ann Arbor, MI 48106-1346

Copyright © Lynn A. Rudner 2011

All Rights Reserved

The University of Utah Graduate School

STATEMENT OF DISSERTATION APPROVAL

The dissertation of **Lynn A. Rudner**

has been approved by the following supervisory committee members:

Nikolaus Trede	, Chair	**11/22/2010** Date Approved
Stephen Lessnick	, Member	**11/22/2010** Date Approved
Gerald Spangrude	, Member	**11/22/2010** Date Approved
Dean Tantin	, Member	**11/22/2010** Date Approved
Jerry Kaplan	, Member	**11/22/2010** Date Approved

and by **Barbara Graves**, Chair of the Department of **Oncological Sciences**

and by Charles A. Wight, Dean of The Graduate School.

ABSTRACT

T lymphocyte-derived malignancies are pediatric cancers often carrying poor prognoses. The proto-oncogenes underlying these malignancies frequently are also fundamental to normal lymphocyte development and function. Therefore, the discovery of heretofore unrecognized lymphocyte oncogenes and tumor suppressors is of potentially profound significance to both clinical medicine and scientific understanding.

To address this, we pioneered a phenotype-driven forward-genetic screen in zebrafish (*Danio rerio*). Using transgenic animals with T lymphocyte-specific enhanced green fluorescent protein (*EGFP*), we performed chemical mutagenesis, screened fish for GFP^+ tumors, and identified several lines developing heritable T cell malignancies. One of these lines, *oscar the grouch (otg)*, is characterized by recessive inheritance. Validation of *otg* as a true leukemia predisposition model was accomplished using histology, immunohistochemistry, gene expression studies, confirmation of clonality, and allogeneic transplantation.

In search of the genetic mutation underlying *otg*, we compared *in vivo* responses to glucocorticoids and γ-irradiation (therapies known to affect human T-ALL). Both dexamethasone (DXM) and irradiation treatment (XRT) were of limited or no utility in *otg*. In addition to diminished sensitivity, *otg* larvae were resistant to radiation-induced apoptosis and showed decreased activation of caspase 3. We determined this resistance is due to a block in the intrinsic mitochondrial apoptosis pathway.

To discover genetic changes that may cause T-ALL, and those contributing to relapse, we used array comparative genomic hybridization (aCGH) in both humans and zebrafish. We identified copy number aberrations (CNAs) in 17 zebrafish T-ALLs, and compared all *D. rerio* genes found in any CNA to a cohort of 75 human T-ALL samples. We found significant overlap

(62%) with genes in CNAs from the human T-ALLs. Additionally, 15 genes recurrently altered ($\geq$3 samples) in zebrafish T-ALL were also in CNAs from 5 or more human T-ALLs. Finally, we used aCGH to study CNA genes acquired during iterative allo-transplantations of 3 zebrafish malignancies. We compared these genes with human aCGH results from 23 patients who either failed induction, or had already relapsed. Again, we observed a large overlap (53%) as well as 9 genes found in 2 fish and $\geq$5 humans. These genes are candidates for causing the increased severity of these tumors.

This work is dedicated to my husband, Andy, for all of his support and patience during this long journey. Words cannot even begin to express my gratitude.

TABLE OF CONTENTS

LIST OF FIGURES

LIST OF TABLES

ACKNOWLEDGMENTS

During my time as a graduate student I have had the privilege of working for an exceptional mentor, and with a remarkable group of people who have created a supportive, thoughtful learning environment in the laboratory. I am particularly grateful for the guidance, patience, and optimism of Nick Trede, who made an extraordinary effort to create a mentoring relationship where I could feel supported, but not suffocated. I also would like to thank Kimble Frazer for his dedication to me, my learning, and to my projects. It is by watching his example that I have affirmed my wishes to become a physician scientist. I am also grateful to benefit from the ideas and counseling of my thesis committee members, and others who have unofficially helped guide this work – namely Josh Schiffman and Cicely Jette. Finally, I would like to express my appreciation for the support of the University of Utah MD/PhD program and its directors, Jerry Kaplan and Dean Li, for investing in me as a person as well as a student.

CHAPTER 1

INTRODUCTION

Background and significance

T cell acute lymphoblastic leukemia (T-ALL) is a malignant disease of developing thymocytes that affects both children and adults. It comprises 40% of all pediatric and 10% of adult ALL (Borowitz MJ 2008, Goldberg et al 2003), but is particularly prevalent as 3-4% of all pediatric cancers. Annually, 2000 cases of acute leukemia (ALL) are diagnosed in children in the US with a peak incidence at age 4, though the peak age for T-ALL in particular is during the early teenage years (Pui and Evans 2006). A clinical presentation including a mediastinal mass is classic for T-ALL, but some children also present with pallor, fatigue, fever and subcutaneous bleeds which is largely caused by the replacement of normal blood cells in the bone marrow by lymphoblasts. A life-threatening complication can arise from airway obstruction secondary to massive increase in the size of the thymus, or from organ failure caused by tumor lysis syndrome.

Over the past 50 years leukemia treatment has become increasingly efficient. In the span from the pioneering studies by Emil Frei and colleagues (Frei et al 1965) to modern-day multi-agent chemotherapy survival of patients with leukemia has improved from single digits to 80% (Silverman and Sallan 2003). Historically, though, a diagnosis of T-ALL has carried a significantly worse prognosis, with pediatric cure rates of only 70% (Pui and Evans 1998) and adult survival <40% (Larson et al 1998, Takeuchi et al 2002). While a recent review of patients with T-ALL treated at the Dana Farber Cancer Institute (DFCI) found that the use of modern treatment protocols caused leukemia remission in as great a percentage of T-ALL patients as B-

progenitor patients the patients with T-ALL remained at increased risk for therapeutic complications, including induction failure, early relapse, and isolated CNS relapse (Goldberg et al 2003). For these reasons, our current efforts are focused on devising more targeted therapies that improve treatment efficacy and limit side effects. In order to achieve this goal, we need to have a better understanding of the molecular mechanisms underlying T cell leukemia.

There are significant similarities between T-ALL and T-cell lymphomas. Indeed, many clinical oncologists believe that these two entities represent a range of the same disease (Jaffe et al 2001). This often results in clinically treating the two diseases in the same way. While an understanding of the exact molecular differences between these two diseases remains to be resolved on an individual basis, I will use the term T-ALL to refer to the range of pathology encountered in this project.

Pathogenesis of leukemia

The two main mechanisms for leukemogenesis are over-expression of a proto-oncogene and defect in a tumor suppressor (or a combination of the two). Over-expression of proto-oncogenes can be caused by chromosomal translocations resulting in activation of a gene that normally is either quiescent or controlled in normal lymphocytes (Rowley 1998). Mis-expression of genes in the absence of karyotypic changes is caused either by microscopic deletions/chromosomal rearrangements or presumably by activation of an aberrant pathway by other mechanisms. A frequent mechanism of translocation-induced T-ALL is the juxtaposition of a transcription factor or signal transduction molecule with enhancers near the TCR alpha/delta chain locus (TCRα/δ) on human chromosome 14 or the TCRβ locus on chromosome 7. In a retroviral insertion screen in mice, upregulation of divergent classes of genes caused leukemia (Suzuki et al 2002). These include transcription factors, signaling molecules, cell cycle regulators, but also structural proteins and RNA processing proteins that had previously not been identified as proto-oncogenes. In all these cases the mutation caused a dominant phenotype.

Defective expression of tumor suppressors has also been shown to cause leukemia. Here the mutation operates as a recessive trait. One allele is inherited from healthy parents; the other allele is lost (loss of heterozygosity, LOH) either physically (deletion), by inactivating point mutation, or by epigenetic silencing (Linggi et al 2002, Peng et al 2010, Sternik et al 1998). Aberrant promoter methylation has emerged as a complementary mechanism in the malignant transformation of cells, including lymphoblasts (Baylin 2005). The methylation status of some genes has also been associated with specific translocations (Baylin and Chen 2005, Garcia-Manero et al 2002, Nakamura et al 1999) with clinical presentation and molecular characteristics (Zheng 2004), and with clinical outcome (Roman et al 2001).

There is convincing epidemiologic evidence that a gene purturbation in acute leukemia involving a at least one transcription factor (such as CBF and *RARα*) is necessary for the disease phenotype (Gilliland 2001). There is equally compelling evidence that these mutations are not sufficient to cause acute leukemia, and additional mutations are required, especially in the case of diseases with long latency (Gilliland and Tsokos 2001). Regardless of the individual lesions, it appears that two events have to happen in the same cell. A hypothesis that unites these observations is known as the "two-hit model" of leukemogenesis where acute leukemia is caused by two classes of mutations. Class I mutations confer a proliferative and survival advantage to cells but do not affect hematopoietic differentiation. Class II mutations, in contrast, serve primarily to impair hematopoietic differentiation and have modest effects on proliferation and survival (Gilliland 2001).

A current understanding of T-ALL

In T-ALL chromosomal break points often involve the TCRβ enhancer (7q34) or the *TCRα*/δ enhancer (14q11), both of which are highly active in committed T cell progenitors, resulting in the deregulated expression of transcription factor genes located at the break point on reciprocal chromosomes (Ferrando and Look 2000). The transcription factors affected by these

molecular changes include basic helix-loop-helix (bHLH) family members like TAL1 (Begley et al 1989) and MYC (McKeithan et al 1986), LIM-only domain (LMO) genes LMO1 and LMO2 (McGuire et al 1992), and the orphan homeobox genes HOX11 and HOX11L2 (Dube et al 1991).

TAL1 is a master regulatory protein active during early hematopoietic development, and is required for the generation of all blood lineages (Shivdasani et al 1995). This bHLH transcription factor binds to DNA by forming heterodimers with other bHLH factors such as E2A (Baer 1993). Mice lacking E2A develop T cell leukemia (Bain et al 1997) and *Tal1* transgenic mice on an *E2A*- background also show accelerated development of the disease (O'Neil et al 2004). The LIM-only domain genes encode proteins that contain duplicated cysteine-rich LIM domains involved in protein-protein interaction. LMO1 and LMO2 can be activated by translocation to the *TCR* enhancer loci, or in the case of *LMO2*, by deletions that remove the negative regulator of *LMO2* expression (McGuire et al 1992). Homozygous disruption of *Lmo2* in mice causes the same phenotype as described above for *Tal1*-deficient mice, suggesting that these two proteins interact in the same pathway and over-expression of either of these genes transgenically in mouse thymocytes leads to T cell lymphomas (McGuire et al 1992). The interaction of these two proteins was further confirmed when it was shown that LMO2 forms a novel DNA-binding complex with GATA-1, TAL1 and E2A, and the LIM-binding protein Ldb1/NLI (Wadman et al 1997). *HOX11* was originally isolated from the site of the recurrent t(10;14)(q24;q11) translocation in T-ALL (Dube et al 1991). Similar to other *HOX* genes, *HOX11* plays an important role in embryonic development, and functions as a master transcriptional regulator necessary for the creation of the spleen (Roberts et al 1994).

The mammalian NOTCH proteins are heterodimeric transmembrane receptors that control cell proliferation, apoptosis and cell fate during the development of diverse cellular lineages (Radtke et al 2004) The protein is a transmembrane receptor whose activation occurs when ligands of the Delta-Serrate-Lag2 (DSL) family bind to one of its heterodimeric subunits and initiate a cascade of proteolytic cleavages resulting in NOTCH1 translocation to the nucleus

and formation of a large transcriptional activation complex (Logeat et al 1998, Sanchez-Irizarry et al 2004). A recent study has shown that activated NOTCH signaling is found in over 50% of human T-ALL patient samples and cell lines (Weng et al 2004). The mutations were found in all subtypes of T-ALL and are concentrated in two regions of the NOTCH1 protein. Missense mutations in the heterodimerization domain activate NOTCH signaling by altering the interaction between the transmembrane subunit and the inhibitory extracellular subunit of NOTCH1 (Malecki et al 2006). Frameshift and point mutations in the C-terminal region of the *NOTCH1* gene were also observed, which caused a deletion of the PEST domain, preventing NOTCH1 protein from being targeted for degradation by the proteosome. Similar activating mutations were also found in mouse models of T-ALL, demonstrating a conserved role for NOTCH in T-ALL and providing a model in which to test therapeutics.

Zebrafish as a cancer model system

Studies in invertebrate organisms such as flies and worms have investigated the development of abnormal cellular proliferation, but what we recognize clinically and pathologically as cancer is present almost exclusively in vertebrates. This means that to truly understand the formation, growth and spread of malignancy, vertebrate models are essential. Using mice as model organisms, we have greatly enhanced our understanding of the mechanisms of human carcinogenesis and cancer progression. Zebrafish, a vertebrate model system, combines the advantages of invertebrate organisms with those of mammalian models: large clutch sizes and the ability to visualize biologic processes *in vivo* aid in the identification of molecular genetic pathways involved in organ development and homeostasis, whereas the histology of normal tissue and cancers is highly similar to that of mouse and human samples.

The zebrafish is a unique system in which to model cancers of the immune system. Although more than 450 million years separate the last common ancestor of zebrafish and humans, the immune system in zebrafish parallels its human counterpart (Meeker and Trede

2008, Trede et al 2004). In addition, the biology of cancer also appears to be very similar in these two organisms (Amatruda and Zon 1999, Ignatius and Langenau 2009, Stoletov and Klemke 2008). Cancer commonly occurs in fish in the wild, and studies have shown that exposure to carcinogens in water can cause a wide variety of both benign and malignant tumors in virtually all organs of jawed fishes (teleosts) with histology that frequently closely resembles human tumors (Hawkins et al 1985).

The zebrafish adaptive immune system parallels that of humans

In general, the zebrafish adaptive immune system has proven to be remarkably similar to that of humans (Traver et al 2003, Trede et al 2004). The evolution of the adaptive immune system coincided with the emergence of the jawed vertebrates, far in advance of the divergence of fish from other vertebrates (Du Pasquier 2004, Laird et al 2000). Therefore, the adaptive and innate branches of the immune system are remarkably conserved across teleosts and other vertebrates, including mammals.

The adaptive immune response, composed of antibodies, specific cellular populations and secondary lymphoid organs such as the bone marrow, thymus, lymph nodes and spleen, is responsible for specific responses to specific pathogens. The thymus, which plays a major role in adaptive immunity, may have its earliest equivalent in the jawless lamprey (Amemiya et al 2007, Ardavin and Zapata 1988), but evolution of the true structural and functional equivalent of the thymus in higher vertebrates coincides with the development of the jaw, and teleost fishes are the first jawed vertebrates. Thymic organogenesis and lymphoid development are highly conserved from teleosts, including zebrafish, to mammals.

Thymic development. The overall process of thymic development as well as its separation into a cortex and medulla are well conserved through vertebrate evolution (Manley 2000). Both the ectoderm and the endoderm have been shown to be essential for the formation of functioning thymic organs in both teleosts and mammals. There are, however, interesting differences in

thymic development between fishes and humans. The most obvious is that the thymus in zebrafish remains as two distinct organs throughout development, whereas mammals have a single thymus (Trede et al 2004). Functionally, the main differences between zebrafish and mammals concern the timing of thymic development. In zebrafish, thymic development initiates at about 48 hours post fertilization (hpf), and a thymic rudiment is formed by 60 hpf, but separation into cortical and medullary compartments of the organ is not fully discernable in its conical shape until 2-3 weeks of age (Lam et al 2002) In the mouse, the interaction between thymic epithelial cells (TECs) and thymocytes, required for maturation of TECs and separation into medullary and cortical compartments, occurs as early as E15, and is complete shortly after birth (Snodgrass et al 1985). In humans, the thymus rudiment is colonized during the 6th week of gestation (Klein and Hořejší 1997)

Lymphocyte diversity. Antigen receptor genes exist in the germline in a "split" configuration and are assembled in developing B and T lymphocytes by V(D)J recombination. This site-specific recombination reaction is initiated by a complex containing the RAG1 and RAG2 proteins and completed by general DNA repair factors. *RAG1* and *RAG2,* like the adaptive immune system itself, are found exclusively in jawed vertebrates, and are thought to have entered the vertebrate genome by horizontal transmission as components of a transposable element. These clusters of functional gene segments are organized into three gene clusters located on different chromosomes. In zebrafish *rag* gene expression was first detected in the thymus at 4 days post fertilization (dpf) and in the pronephros at 21 dpf by RNA *in situ* hybridization (Willett et al 1999), although we have observed *rag* expression in the pronephros as early as 8 dpf (unpublished).

T cell development. The first detectable T cells in the zebrafish thymus by gene expression studies occur at 72 hpf at the same time the embryo hatches from its protective chorion. Immunocompetence, though, as measured by humoral response to T-dependent and –independent antigens, is not reached until 4-6 weeks after hatching. The environment for T cell

development in the zebrafish is different than the T cell population of the mouse thymus of the same developmental stage (E15) which has the advantage of a protective intrauterine environment for the first three weeks of life, with peripheral T cells appearing at about 7 days after birth (Lam et al 2002). Genomic organization of the zebrafish TCRα locus has been characterized and many gene segments sequenced, revealing over 15 Vα genes. TCRβ and γ constant regions have also been recently identified by gene expression studies (Meeker et al 2010). This general conservation suggests that the overarching diversity of rearranged TCR genes in zebrafish has the potential to be very high.

Tools for zebrafish as an experimental system

Large-scale genetic screens. Traditionally, the popularity of zebrafish as a model organism was based in the advantages it offered for studying vertebrate development. The zebrafish also has many properties that make it an ideal organism for systematic mutational approaches. It has a short generation time of 2-4 months, can be kept at high density in a small space with relatively little maintenance, resulting in reduced cost. With the development of efficient strategies to raise and maintain large numbers of independent zebrafish lines, it has become feasible to perform large-scale mutational screens. One pair of fish can sire an average of 200 progeny at weekly intervals, which greatly facilitates collection of large numbers of mutant individuals for mapping and genetic analysis. Use of zebrafish facilitates both screens employing standard crossing schemes to produce homozygous mutant embryos (classic F3 screens), and those that use gynogentic diploid embryos derived from fertilizing eggs *in vitro* using UV-inactivated sperm (early pressure screens). Classic F3 screens breed mutagenized males with wild-type females, and their offspring (F1) are interbred to yield heterzygotic carriers of the mutations (F2) (Driever et al 1996, Haffter et al 1996). The phenotypes of the recessive mutations are revealed in F3 generation offspring, in which the mutated genes are driven to homozygosity. These F3 fish can be examined at various stages of development for signs of abnormality.

Early pressure (EP) screens use embryos derived from *in vitro* fertilized eggs using UV-inactivated sperm immediately followed by inhibition of the second meiotic division by application of high atmospheric pressure (6-8000 lbs/sq inch) to break mitotic spindles. Here, both alleles of a gene are derived from either the wild type or mutated version of the meiotically duplicated maternal sister chromatids resulting in an animal homozygous for a particular locus. The advantage of this approach is that mutations that are heterozygous in the F1 female are "homozygosed," revealing mutant phenotypes immediately in the F2 generation. In addition, the resulting offspring are often viable and fertile. Viability and fertility of affected individuals are of pivotal importance for detection of immunodeficiencies or lymphoproliferative diseases because zebrafish lymphopoiesis occurs relatively late compared to other developmental processes. This technique makes it possible to use genetic screens for immunodeficiencies or lymphoproliferation beginning at 6 dpf, when T cell progenitors have typically colonized the thymus (Trede et al 2008) and continuing into adulthood (Frazer et al 2009) when the immune system, and the animal, reaches maturity as discussed above.

Transgenic animals. While the genetics underlying the development of the zebrafish lymphoid system has been an active area of investigation, functional studies to facilitate characterization of different lymphoid cell populations have been hampered by the lack of tools. In particular, there is a dearth of antibodies directed to surface receptors that are relevant to the immune system. More recently transgenic technology and lineage-restricted gene promoters have been used to drive the expression of fluorophores in specific blood cell lineages. Transgenic zebrafish lines that express genetic markers controlled by both *rag1* and *rag2* promoters (Jessen et al 2001, Long et al 1997, Meng et al 1997) have been instrumental in tracking immature T cells, but such experiments were restricted to immature rag^{+} cells, and could not be used to track mature T or B cells.

In 2004, Langenau et al. created a transgenic zebrafish in which the T-cell specific tyrosine kinase ($p56^{lck}$) gene promoter regulated GFP expression in lymphocytes (Figure 1.1).

This particular line allows for *in vivo* tracking of T cell homing and accumulation in tissues, and is amenable to forward genetic screens for mutants causing immunodeficiencies, autoimmune disease, or malignancy. Use of this line has shown that *lck* mRNA expression is first detected in T cells located in the bilateral thymic lobes by 3dpf, greatly increases in numbers by 7dpf , and, in addition, is located in cells throughout the thymus, not just cortex or medulla. Additionally, this study confirmed that lymphocytes home to the kidney, spleen, gastrointestinal lining, gills and olfactory epithelium (Figure 1.2). Mature T cells were shown to reside in the kidney marrow, and the thymus was demonstrated to harbor two distinct subpopulations of T cells at various stages of development (Figure 1.3). Varying in size, these thymocyte populations suggest that zebrafish lymphocytes likely change size as they mature, agreeing with the correlation between lymphocyte size and maturational stage of development described previously in mammals (Langenau et al 2004). The advent of similar transgenic lines, expressing fluorophores under the control of cell-specific promoters, allows us to marry the benefits of large-scale genetic screens in zebrafish with the relatively simple identification of mutants by visual inspection under fluorescence microscopy. In many cases, these screens are feasibly not only in transparent larvae, but also in adults.

Transplantation immunology. Efficient hematopoietic cell transplantation in mammals requires the ablation of the host immune system to prevent rejection and to create a niche space for engraftment of donor cells in the bone marrow. In mouse and humans, one way to achieve this ablation is by using a dose of γ-irradiation that destroys the hematopoietic system to a point where it cannot recover spontaneously, so that bone marrow infusion from a donor is required for survival. Recent studies have shown that despite the divergence of teleosts and mammals nearly 450 million years ago, a minimum lethal dose of γ-irradiation leads to hematopoietic ablation and eventually death from bone marrow failure in zebrafish (Traver et al 2004). Recent studies have also shown that lymphocytes derived from an adult zebrafish thymus homed to the thymus when injected into a 2-day-old embryo (Langenau et al 2004). Twenty-four hours after intracardiac

injection these cells were also found in the circulation. Transplantation experiments in adult, sublethally irradiated, fish have also confirmed that GFP-labeled T cells can home to the thymus, kidney, and peripheral sites where T cells are found physiologically (Langenau et al 2004). The knowledge provided by these transplantation experiments now allows us to isolate cells of interest using flow cytometry and introduce these cells into irradiated recipients to test autonomy of mutant gene function, and analyze engraftment potential of hematopoietic cell lineages in zebrafish.

Previous models of T cell acute leukemia in zebrafish

The first zebrafish ALL model utilized the zebrafish promoter to drive expression of murine *MYC* to induce disease (Langenau et al 2003). Because a GFP reporter construct was also present, the authors could determine with *in vivo* fluorescence microscopy that essentially all fish with *rag2* promoter-driven lymphoid expression of *MYC* developed T-ALL, with a mean latency of about 50 days. When this same construct was stably incorporated in the germ-line, again all fish acquired T-ALL, now with a mean latency of 32 days (Langenau et al 2005). The near-100% penetrance and short latency both support that because murine *MYC* is a potent oncogene in this system only few acquired mutations are required for leukemic transformation. However, the transgenic line could not be maintained, as fish carrying the transgene typically die of disease prior to reaching sexual maturity. Another potentially salient point is that the *MYC*-driven *D. rerio* model best represents only one human T-ALL type, the $TAL1^{+}$ late cortical thymocyte subgroup (Ferrando et al 2002, Ferrando and Look 2003, Palomero et al 2006).

A modified strategy, where Cre recombinase was used to conditionally activate murine *Myc*, circumvents the difficulty in propagating the transgenic line. However, when Cre RNA was injected into one-cell embryos of stably-transgenic *MYC* fish (to remove 'floxed' transcription stop sites preceding *Myc*), T-ALL penetrance dropped to 6%, suggesting inefficient microinjection, incomplete Cre-mediated excision, or both (Langenau et al 2005). Compound

transgenic fish with heat-shock inducible-Cre and loxP-Stop-loxP-*MYC* were a further refinement, where T-ALL rates of up to 81% could be achieved (Feng et al 2007). Again, this very high incidence attests to the oncogenic potency of murine *MYC* in *D. rerio*, and poises this system for use in suppressor screens as well. Clearly, this series of studies set an important precedent, establishing that mammalian genes can be similarly oncogenic in zebrafish lymphoid cancers.

A second transgenic zebrafish T-ALL model expressed a truncated and constitutively-active form of human NOTCH1 protein, targeted to lymphocytes through the use of the zebrafish *rag2* promoter (Chen et al 2007). Fish from this line display 40% penetrance, but have relatively long latency (disease begins at 11 months). Leukemias in this model are oligoclonal, and express a range of Notch1 target genes such as *her6* (the zebrafish orthologue of HES1) and *her9*. Although the *mMyc* models show an overexpression of the known T-ALL oncogenes *tal1/scl* and *lmo2*, the human NOTCH1-induced T cell leukemias lack appreciable expression levels of these oncogenes implying that the pathogenic mechanism of disease in these two models is distinct.

A final example of *D. rerio* ALL models used the oncogenic human *TEL-AML1* fusion gene. These lines utilized either the ubiquitous *Xenopus* elongation factor 1a (XEF), zebrafish *β-actin* (ZBA) promoters, or a lymphoid-specific zebrafish *rag2* promoter (Sabaawy et al 2006). The expression of human *TEL-AML1* from the ubiquitous XEF and ZBA promoters led to low penetrance (3%) of B cell acute lymphoblastic leukemia, with a latency of 8-12 months. No fish expressing *rag2*-driven *TEL-AML1* developed leukemia during the 36-month observation period, leading the authors to conclude that *TEL-AML1* typically acts in a B lymphocyte precursor stage prior to Rag expression, at least in the human version of this disease. This model mimics childhood $CD10^{+}$ pre-B ALL, and its long latency and low penetrance make it well suited for enhancer screens.

Goal of the dissertation

T-ALL is a particularly heterogeneous and while many pediatric malignancies have characteristic translocations, most T lymphocyte-derived diseases carry no cytogenetic hallmark. Lacking these informative lesions, insight into their molecular pathogenesis is incomplete. An increased understanding of the molecular mechanisms characterizing the pathogenesis of T-ALL will reveal critical targets, and may allow for the formulation of more specific and effective therapies. Therefore, the discovery of heretofore-unrecognized lymphocyte oncogenes and tumor suppressors is of potentially profound significance to both clinical medicine and scientific understanding. Thus, my dissertation work has sought to address several aspects of T-ALL pathogenesis using the zebrafish.

1. Can the development of heritable zebrafish T-ALL model loyally recapitulate the human form of the disease?

   Previous published models of zebrafish T-ALL rely on transgenic, known oncogenes to drive disease. In Chapter 2, I discuss a way in which we pioneered a forward genetic screen to identify new, hereditary models of T-ALL in the zebrafish. These models are driven by as-yet unknown mutations.

2. Can nonhuman models of T-ALL be used to identify leukemogenic factors in humans?

   There are many genetic studies that may be useful in further understanding the development of T-ALL, and many molecular genetic studies that can be done to identify disease targets. These types of analyses, and other large-scale therapeutic screens cannot be done in humans, or even mouse models. In Chapter 3 of my dissertation, I discuss how zebrafish models of acute leukemias are uniquely suited to help in these efforts.

3. What is the underlying mechanism of disease in *otg* fish?

Chapter 4 of my dissertation details how we determined that *otg* fish are resistant to irradiation-induced apoptosis, and how we then interrogated the apoptosis pathway to determine where functionality was lost in this mutant. We studied each step in this cascade, including double strand break repair, p53 effectors, and mitochondrial activation, to determine that *otg* mutation results in a block at the level of the mitochondria, preventing irradiation-induced apoptosis.

4. Can copy number analysis in zebrafish leukemia help identify new candidate genes that may be responsible for oncogenesis or aggressiveness in primary human T-ALLs?

   In Chapter 5 of my dissertation I discuss using array comparative genomic hybridization (aCGH) on zebrafish primary and serially passaged T-ALLs to determine genes that may contribute to transformation and oncogenesis. I also discuss the use of transplantation techniques as a proxy for relapsed human disease, and a number of genes that we have identified which are altered in both zebrafish and human T-ALLs, suggesting links between these candidate genes and T-ALL that have been conserved throughout evolution.

References

Amatruda JF, Zon LI (1999). Dissecting hematopoiesis and disease using the zebrafish. *Dev Biol* **216:** 1-15.

Amemiya CT, Saha NR, Zapata A (2007). Evolution and development of immunological structures in the lamprey. *Curr Opin Immunol* **19:** 535-541.

Ardavin CF, Zapata A (1988). The pharyngeal lymphoid tissue of lampreys. A morpho-functional equivalent of the vertebrate thymus? *Thymus* **11:** 59-65.

Baer R (1993). TAL1, TAL2 and LYL1: a family of basic helix-loop-helix proteins implicated in T cell acute leukaemia. *Semin Cancer Biol* **4:** 341-347.

Bain G, Engel I, Robanus Maandag EC, te Riele HP, Voland JR, Sharp LL *et al.* (1997). E2A deficiency leads to abnormalities in alphabeta T-cell development and to rapid development of T-cell lymphomas. *Mol Cell Biol* **17:** 4782-4791.

Baylin SB (2005). DNA methylation and gene silencing in cancer. *Nat Clin Pract Oncol* **2 Suppl 1:** S4-11.

Baylin SB, Chen WY (2005). Aberrant gene silencing in tumor progression: implications for control of cancer. *Cold Spring Harb Symp Quant Biol* **70:** 427-433.

Begley CG, Aplan PD, Davey MP, Nakahara K, Tchorz K, Kurtzberg J *et al.* (1989). Chromosomal translocation in a human leukemic stem-cell line disrupts the T-cell antigen receptor delta-chain diversity region and results in a previously unreported fusion transcript. *Proc Natl Acad Sci U S A* **86:** 2031-2035.

Borowitz MJ CJ (2008). T-lymphoblastic leukaemia/lymphoma. In: Swerdlow SH, Campos E, Harris, N.L., Jaffe, E.F., Pileri, S.A., Stein, H., Thiele J, Vardiman, J.W (ed). *WHO Classification of Tumours of Haematopoietic and Lymphoid Tissues*. IARC Press: Lyon. pp 176-178.

Chen J, Jette C, Kanki JP, Aster JC, Look AT, Griffin JD (2007). NOTCH1-induced T-cell leukemia in transgenic zebrafish. *Leukemia* **21:** 462-471.

Driever W, Solnica-Krezel L, Schier AF, Neuhauss SC, Malicki J, Stemple DL *et al.* (1996). A genetic screen for mutations affecting embryogenesis in zebrafish. *Development* **123:** 37-46.

Du Pasquier L (2004). Speculations on the origin of the vertebrate immune system. *Immunol Lett* **92:** 3-9.

Dube ID, Kamel-Reid S, Yuan CC, Lu M, Wu X, Corpus G *et al.* (1991). A novel human homeobox gene lies at the chromosome 10 breakpoint in lymphoid neoplasias with chromosomal translocation t(10;14). *Blood* **78:** 2996-3003.

Feng H, Langenau DM, Madge JA, Quinkertz A, Gutierrez A, Neuberg DS *et al.* (2007). Heat-shock induction of T-cell lymphoma/leukaemia in conditional Cre/lox-regulated transgenic zebrafish. *Br J Haematol* **138:** 169-175.

Ferrando AA, Look AT (2000). Clinical implications of recurring chromosomal and associated molecular abnormalities in acute lymphoblastic leukemia. *Semin Hematol* **37:** 381-395.

Ferrando AA, Neuberg DS, Staunton J, Loh ML, Huard C, Raimondi SC *et al.* (2002). Gene expression signatures define novel oncogenic pathways in T cell acute lymphoblastic leukemia. *Cancer Cell* **1:** 75-87.

Ferrando AA, Look AT (2003). Gene expression profiling in T-cell acute lymphoblastic leukemia. *Semin Hematol* **40:** 274-280.

Frazer JK, Meeker ND, Rudner L, Bradley DF, Smith AC, Demarest B *et al.* (2009). Heritable T-cell malignancy models established in a zebrafish phenotypic screen. *Leukemia* **23:** 1825-1835.

Frei E, 3rd, Karon M, Levin RH, Freireich EJ, Taylor RJ, Hananian J *et al.* (1965). The effectiveness of combinations of antileukemic agents in inducing and maintaining remission in children with acute leukemia. *Blood* **26:** 642-656.

Garcia-Manero G, Daniel J, Smith TL, Kornblau SM, Lee MS, Kantarjian HM *et al.* (2002). DNA methylation of multiple promoter-associated CpG islands in adult acute lymphocytic leukemia. *Clin Cancer Res* **8:** 2217-2224.

Gilliland DG (2001). Hematologic malignancies. *Curr Opin Hematol* **8:** 189-191.

Gilliland WR, Tsokos GC (2001). The clinical spectrum of anti-insulin receptor antibodies and autoimmune disease. *J Clin Rheumatol* **7:** 361-362.

Goldberg JM, Silverman LB, Levy DE, Dalton VK, Gelber RD, Lehmann L *et al.* (2003). Childhood T-cell acute lymphoblastic leukemia: the Dana-Farber Cancer Institute acute lymphoblastic leukemia consortium experience. *J Clin Oncol* **21:** 3616-3622.

Haffter P, Granato M, Brand M, Mullins MC, Hammerschmidt M, Kane DA *et al.* (1996). The identification of genes with unique and essential functions in the development of the zebrafish, Danio rerio. *Development* **123:** 1-36.

Hawkins WE, Overstreet RM, Fournie JW, Walker WW (1985). Development of aquarium fish models for environmental carcinogenesis: tumor induction in seven species. *J Appl Toxicol* **5:** 261-264.

Ignatius MS, Langenau DM (2009). Zebrafish as a model for cancer self-renewal. *Zebrafish* **6:** 377-387.

Jaffe E, Harris N, Stein H, Vardiman J (2001). Pathology and genetics of tumours of haematopoietic and lymphoid tissues. *World Health Organization classification of tumours.* IARC Press: Lyon.

Jessen JR, Jessen TN, Vogel SS, Lin S (2001). Concurrent expression of recombination activating genes 1 and 2 in zebrafish olfactory sensory neurons. *Genesis* **29:** 156-162.

Klein J, Hořejší V (1997). *Immunology* Blackwell Science: Oxford.

Laird DJ, De Tomaso AW, Cooper MD, Weissman IL (2000). 50 million years of chordate evolution: seeking the origins of adaptive immunity. *Proc Natl Acad Sci U S A* **97:** 6924-6926.

Lam SH, Chua HL, Gong Z, Wen Z, Lam TJ, Sin YM (2002). Morphologic transformation of the thymus in developing zebrafish. *Dev Dyn* **225:** 87-94.

Langenau DM, Traver D, Ferrando AA, Kutok JL, Aster JC, Kanki JP *et al.* (2003). Myc-induced T cell leukemia in transgenic zebrafish. *Science* **299:** 887-890.

Langenau DM, Ferrando AA, Traver D, Kutok JL, Hezel JP, Kanki JP *et al.* (2004). *In vivo* tracking of T cell development, ablation, and engraftment in transgenic zebrafish. *Proc Natl Acad Sci U S A* **101:** 7369-7374.

Langenau DM, Feng H, Berghmans S, Kanki JP, Kutok JL, Look AT (2005). Cre/lox-regulated transgenic zebrafish model with conditional myc-induced T cell acute lymphoblastic leukemia. *Proc Natl Acad Sci U S A* **102:** 6068-6073.

Larson RA, Dodge RK, Linker CA, Stone RM, Powell BL, Lee EJ *et al.* (1998). A randomized controlled trial of filgrastim during remission induction and consolidation chemotherapy for adults with acute lymphoblastic leukemia: CALGB study 9111. *Blood* **92:** 1556-1564.

Linggi B, Muller-Tidow C, van de Locht L, Hu M, Nip J, Serve H *et al.* (2002). The t(8;21) fusion protein, AML1 ETO, specifically represses the transcription of the p14(ARF) tumor suppressor in acute myeloid leukemia. *Nature medicine* **8:** 743-750.

Logeat F, Bessia C, Brou C, LeBail O, Jarriault S, Seidah NG *et al.* (1998). The Notch1 receptor is cleaved constitutively by a furin-like convertase. *Proc Natl Acad Sci U S A* **95:** 8108-8112.

Long Q, Meng A, Wang H, Jessen JR, Farrell MJ, Lin S (1997). GATA-1 expression pattern can be recapitulated in living transgenic zebrafish using GFP reporter gene. *Development* **124:** 4105-4111.

Malecki MJ, Sanchez-Irizarry C, Mitchell JL, Histen G, Xu ML, Aster JC *et al.* (2006). Leukemia-associated mutations within the NOTCH1 heterodimerization domain fall into at least two distinct mechanistic classes. *Mol Cell Biol* **26:** 4642-4651.

Manley NR (2000). Thymus organogenesis and molecular mechanisms of thymic epithelial cell differentiation. *Semin Immunol* **12:** 421-428.

McGuire EA, Rintoul CE, Sclar GM, Korsmeyer SJ (1992). Thymic overexpression of Ttg-1 in transgenic mice results in T-cell acute lymphoblastic leukemia/lymphoma. *Mol Cell Biol* **12:** 4186-4196.

McKeithan TW, Shima EA, Le Beau MM, Minowada J, Rowley JD, Diaz MO (1986). Molecular cloning of the breakpoint junction of a human chromosomal 8;14 translocation involving the T-cell receptor alpha-chain gene and sequences on the 3' side of MYC. *Proc Natl Acad Sci U S A* **83:** 6636-6640.

Meeker ND, Trede NS (2008). Immunology and zebrafish: spawning new models of human disease. *Dev Comp Immunol* **32:** 745-757.

Meeker ND, Smith AC, Frazer JK, Bradley DF, Rudner LA, Love C *et al.* (2010). Characterization of the zebrafish T cell receptor beta locus. *Immunogenetics* **62:** 23-29.

Meng A, Tang H, Ong BA, Farrell MJ, Lin S (1997). Promoter analysis in living zebrafish embryos identifies a cis-acting motif required for neuronal expression of GATA-2. *Proc Natl Acad Sci U S A* **94:** 6267-6272.

Nakamura M, Sugita K, Inukai T, Goi K, Iijima K, Tezuka T *et al.* (1999). p16/MTS1/INK4A gene is frequently inactivated by hypermethylation in childhood acute lymphoblastic leukemia with 11q23 translocation. *Leukemia* **13:** 884-890.

O'Neil J, Shank J, Cusson N, Murre C, Kelliher M (2004). TAL1/SCL induces leukemia by inhibiting the transcriptional activity of E47/HEB. *Cancer Cell* **5:** 587-596.

Palomero T, Odom DT, O'Neil J, Ferrando AA, Margolin A, Neuberg DS *et al.* (2006). Transcriptional regulatory networks downstream of TAL1/SCL in T-cell acute lymphoblastic leukemia. *Blood* **108:** 986-992.

Peng C, Chen Y, Yang Z, Zhang H, Osterby L, Rosmarin AG *et al.* (2010). PTEN is a tumor suppressor in CML stem cells and BCR-ABL-induced leukemias in mice. *Blood* **115:** 626-635.

Pui CH, Evans WE (1998). Acute lymphoblastic leukemia. *N Engl J Med* **339:** 605-615.

Pui CH, Evans WE (2006). Treatment of acute lymphoblastic leukemia. *N Engl J Med* **354:** 166-178.

Radtke F, Wilson A, MacDonald HR (2004). Notch signaling in T- and B-cell development. *Curr Opin Immunol* **16:** 174-179.

Roberts CW, Shutter JR, Korsmeyer SJ (1994). Hox11 controls the genesis of the spleen. *Nature* **368:** 747-749.

Roman J, Castillejo JA, Jimenez A, Bornstein R, Gonzalez MG, del Carmen Rodriguez M *et al.* (2001). Hypermethylation of the calcitonin gene in acute lymphoblastic leukaemia is associated with unfavourable clinical outcome. *Br J Haematol* **113:** 329-338.

Rowley JD (1998). The critical role of chromosome translocations in human leukemias. *Annu Rev Genet* **32:** 495-519.

Sabaawy HE, Azuma M, Embree LJ, Tsai HJ, Starost MF, Hickstein DD (2006). TEL-AML1 transgenic zebrafish model of precursor B cell acute lymphoblastic leukemia. *Proc Natl Acad Sci U S A* **103:** 15166-15171.

Sanchez-Irizarry C, Carpenter AC, Weng AP, Pear WS, Aster JC, Blacklow SC (2004). Notch subunit heterodimerization and prevention of ligand-independent proteolytic activation depend, respectively, on a novel domain and the LNR repeats. *Mol Cell Biol* **24:** 9265-9273.

Shivdasani RA, Mayer EL, Orkin SH (1995). Absence of blood formation in mice lacking the T-cell leukaemia oncoprotein tal-1/SCL. *Nature* **373:** 432-434.

Silverman LB, Sallan SE (2003). Newly diagnosed childhood acute lymphoblastic leukemia: update on prognostic factors and treatment. *Curr Opin Hematol* **10:** 290-296.

Snodgrass HR, Kisielow P, Kiefer M, Steinmetz M, von Boehmer H (1985). Ontogeny of the T-cell antigen receptor within the thymus. *Nature* **313:** 592-595.

Sternik G, Pittis MG, Gutierrez M, Diez RA, Sen L (1998). In acute lymphoblastic leukemia deletion of the tumor suppressor gene P16 is associated with abnormal interferon genes. *Medicina (B Aires)* **58:** 463-468.

Stoletov K, Klemke R (2008). Catch of the day: zebrafish as a human cancer model. *Oncogene* **27:** 4509-4520.

Suzuki H, Gabrielson E, Chen W, Anbazhagan R, van Engeland M, Weijenberg MP *et al.* (2002). A genomic screen for genes upregulated by demethylation and histone deacetylase inhibition in human colorectal cancer. *Nat Genet* **31:** 141-149.

Takeuchi J, Kyo T, Naito K, Sao H, Takahashi M, Miyawaki S *et al.* (2002). Induction therapy by frequent administration of doxorubicin with four other drugs, followed by intensive consolidation and maintenance therapy for adult acute lymphoblastic leukemia: the JALSG-ALL93 study. *Leukemia* **16:** 1259-1266.

Traver D, Herbomel P, Patton EE, Murphey RD, Yoder JA, Litman GW *et al.* (2003). The zebrafish as a model organism to study development of the immune system. *Adv Immunol* **81:** 253-330.

Traver D, Winzeler A, Stern HM, Mayhall EA, Langenau DM, Kutok JL *et al.* (2004). Effects of lethal irradiation in zebrafish and rescue by hematopoietic cell transplantation. *Blood* **104:** 1298-1305.

Trede NS, Langenau DM, Traver D, Look AT, Zon LI (2004). The use of zebrafish to understand immunity. *Immunity* **20:** 367-379.

Trede NS, Ota T, Kawasaki H, Paw BH, Katz T, Demarest B *et al.* (2008). Zebrafish mutants with disrupted early T-cell and thymus development identified in early pressure screen. *Dev Dyn* **237:** 2575-2584.

Wadman IA, Osada H, Grutz GG, Agulnick AD, Westphal H, Forster A *et al.* (1997). The LIM-only protein Lmo2 is a bridging molecule assembling an erythroid, DNA-binding complex which includes the TAL1, E47, GATA-1 and Ldb1/NLI proteins. *The EMBO journal* **16:** 3145-3157.

Weng AP, Ferrando AA, Lee W, Morris JPt, Silverman LB, Sanchez-Irizarry C *et al.* (2004). Activating mutations of NOTCH1 in human T cell acute lymphoblastic leukemia. *Science* **306:** 269-271.

Willett CE, Cortes A, Zuasti A, Zapata AG (1999). Early hematopoiesis and developing lymphoid organs in the zebrafish. *Dev Dyn* **214:** 323-336.

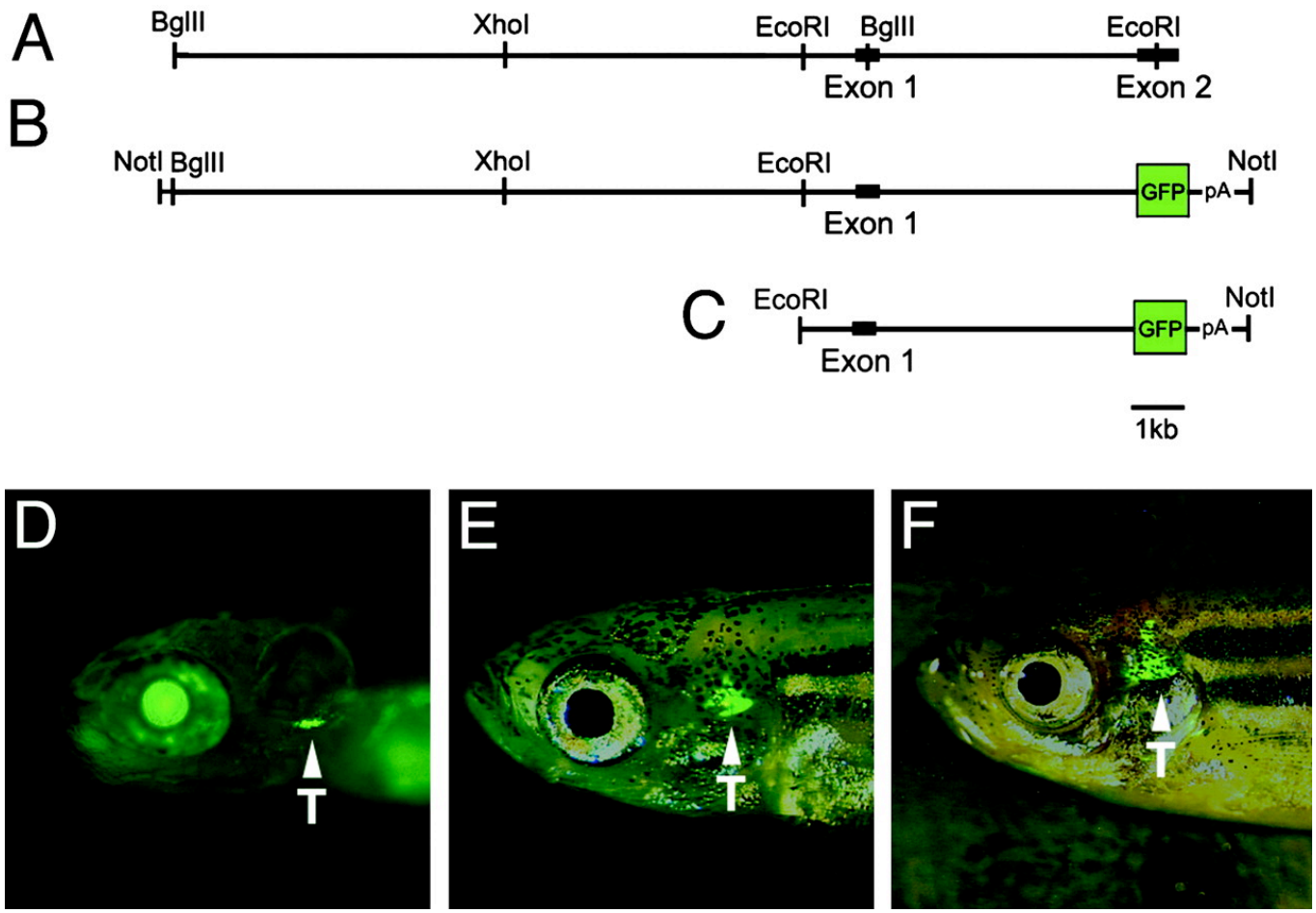

Figure 1.1. *lck::EGFP* transgenic zebrafish. Diagrams of the genomic DNA sequence comprising the lck promoter (A) and the GFP construct (B) are shown. Enzyme digest sites used for cloning and restriction mapping of the minimal promoter are shown. *lck::EGFP* transgenic fish expressing the 5.5-kb EcoRI-NotI fragment (C) are shown at 8 dpf (D), 45 dpf (E), and 80 dpf (F). Arrowheads denote GFP-labeled cells in the thymus (T). The views are lateral with anterior to the left. (Langenau et al 2004)

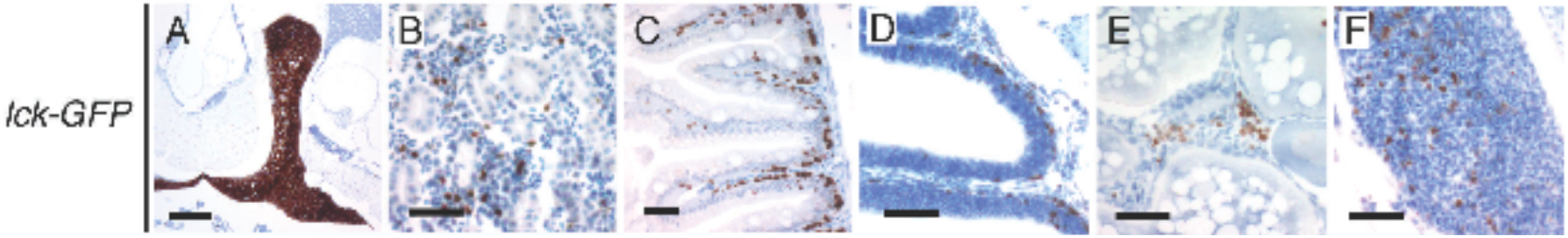

Fig 1.2. Anti-GFP immunostaining of sectioned *lck::EGFP* transgenic fish. Thymus (A), kidney (B), intestinal lining (C), nasal epithelium (D), ovary (E), spleen (F) are shown. Scale bars, 100 um (A) and 20 um (B–F) (modified from Langenau et al 2004).

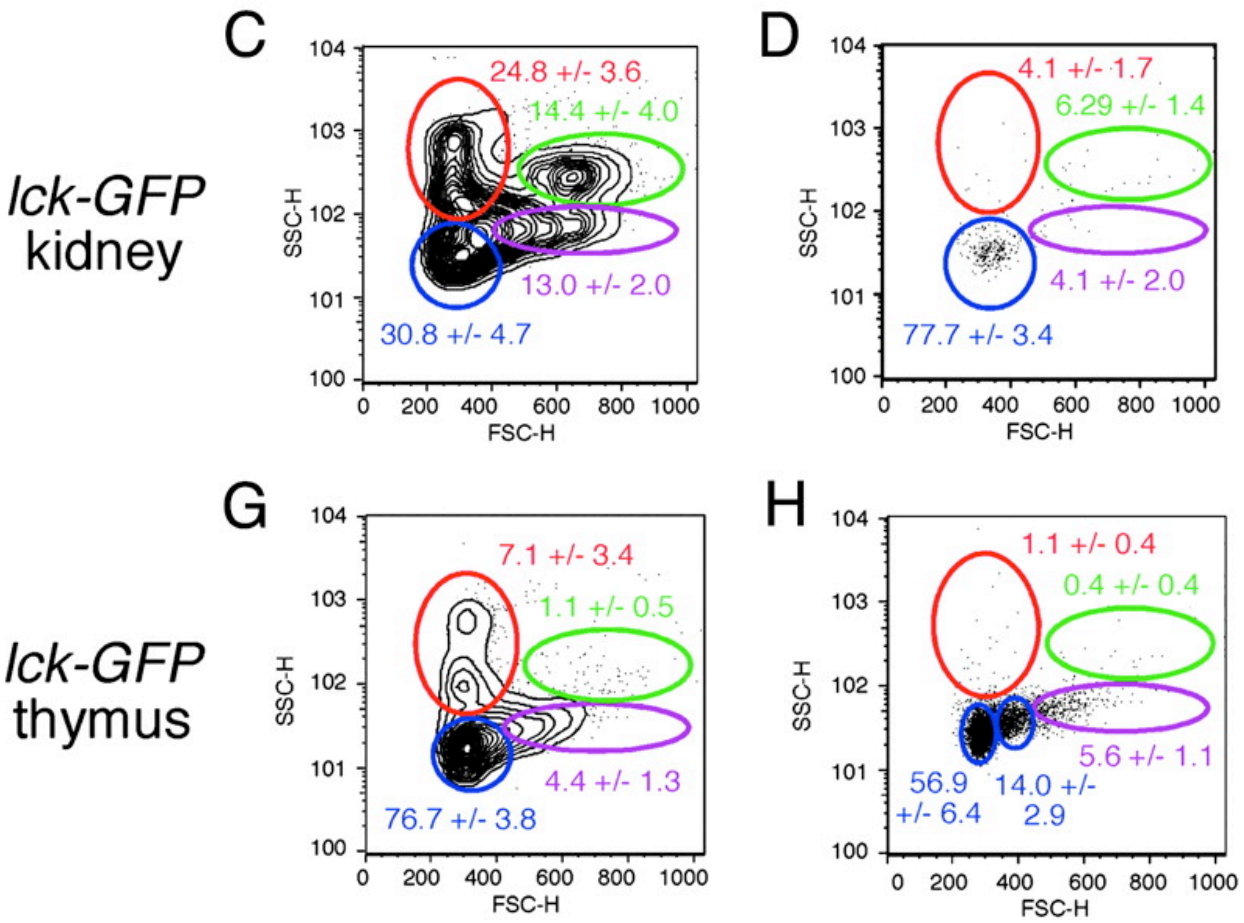

Fig 1.3. FACS analysis of cells from the kidney (C,D) and thymus (G,H) *lck::EGFP* transgenic zebrafish. Gated populations of erythrocytes (red), lymphocytes (blue), granulocytes and monocytes (green), and blood cell precursors (purple) are outlined. Populations of cells within each gate are described as percentages of total live cells (±1 SD; n = 18 for C; and n = 8 for, D, and G,H). Cell size is represented by forward scatter (FSC), and granularity is represented by side scatter (SSC). GFP-positive cells in the progenitor gate in thymus samples became confined to the lymphoid gate upon reanalysis, confirming that GFP-labeled populations in the progenitor gate are predominately lymphoid in origin. (Modified from Langenau et al 2004)

CHAPTER 2

HERITABLE T CELL MALIGNANCY MODELS ESTABLISHED IN A ZEBRAFISH PHENOTYPIC SCREEN

Reprinted with permission from: Frazer JK, Meeker ND, Rudner L, Bradley DF, Smith AC, Demarest B *et al* (2009). Heritable T-cell malignancy models established in a zebrafish phenotypic screen. *Leukemia* **23:** 1825-1835

Leukemia (2009) 23, 1825–1835
© 2009 Macmillan Publishers Limited All rights reserved 0887-6924/09 $32.00
www.nature.com/leu

ORIGINAL ARTICLE

Heritable T-cell malignancy models established in a zebrafish phenotypic screen

JK Frazer[1,2,6], ND Meeker[1,3,6], L Rudner[2,6], DF Bradley[1,2], ACH Smith[1,2], B Demarest[2], D Joshi[2], EE Locke[2], SA Hutchinson[2], S Tripp[4], SL Perkins[4,5] and NS Trede[1,2]

[1]*Department of Pediatrics, University of Utah, Salt Lake City, UT, USA;* [2]*Department of Oncological Sciences, Huntsman Cancer Institute, University of Utah, Salt Lake City, UT, USA;* [3]*Department of Internal Medicine, University of Utah, Salt Lake City, UT, USA;* [4]*ARUP Institute, Salt Lake City, UT, USA and* [5]*Department of Pathology, University of Utah, Salt Lake City, UT, USA*

T-cell neoplasias are common in pediatric oncology, and include acute lymphoblastic leukemia (T-ALL) and lymphoblastic lymphoma (T-LBL). These cancers have worse prognoses than their B-cell counterparts, and their treatments carry significant morbidity. Although many pediatric malignancies have characteristic translocations, most T-lymphocyte-derived diseases lack cytogenetic hallmarks. Lacking these informative lesions, insight into their molecular pathogenesis is less complete. Although dysregulation of the NOTCH1 pathway occurs in a substantial fraction of cases, many other genetic lesions of T-cell malignancy have not yet been determined. To address this deficiency, we pioneered a phenotype-driven forward-genetic screen in zebrafish (*Danio rerio*). Using transgenic fish with T-lymphocyte-specific expression of enhanced green fluorescent protein (*EGFP*), we performed chemical mutagenesis, screened animals for GFP$^+$ tumors, and identified multiple lines with a heritable predisposition to T-cell malignancy. In each line, the patterns of infiltration and morphological appearance resembled human T-ALL and T-LBL. T-cell receptor analyses confirmed their clonality. Malignancies were transplantable and contained leukemia-initiating cells, like their human correlates. In summary, we have identified multiple zebrafish mutants that recapitulate human T-cell neoplasia and show heritable transmission. These vertebrate models provide new genetic platforms for the study of these important human cancers.

Leukemia (2009) **23,** 1825–1835; doi:10.1038/leu.2009.116; published online 11 June 2009
Keywords: lymphoma; zebrafish; T lymphocyte; genetic screen

Introduction

In the past 50 years, acute lymphoblastic leukemia (ALL) treatment has improved dramatically. With the advent of current multi-agent chemotherapy, survival of pediatric patients with many forms of ALL has improved from single digits to over 80%,[1,2] but challenges remain. Although T-cell ALL (T-ALL) comprises only 15 and 25% of pediatric and adult cases,[3,4] it carries a significantly worse prognosis, with pediatric cure rates of only 70%[5] and adult survival $<40\%$.[6,7]

Lymphoblastic malignancies represent uncontrolled clonal proliferations of immature lymphocytes. In general, at least two mutational events must occur in the same pre-malignant cell: one arresting differentiation and a second conferring a survival and/or proliferative advantage. In some cancers, both requirements are met by bi-allelic mutation of the same gene, termed 'tumor suppressors.' In others, transformation is mediated by mutations to different genes, impacting multiple pathways. For hematological neoplasia, cooperating genetic lesions of transcription factors, tyrosine kinases and transcriptional co-activators often coincide.[8]

T-cell malignancies are molecularly heterogeneous, driven by a complex combination of genetic changes.[9] To date, the identification of specific molecular alterations that underlie lymphocyte transformation has principally come from the discovery of aberrant chromosomal translocations and pathway activations in blast cells of ALL patients.[10,11] Although several informative translocations have been described,[12] most cases lack pathognomonic cytogenetic changes.[13,14] Recent studies have clearly established roles for dysregulated transcription factors in T-ALL,[9] but the genetic lesions underlying this dysregulation are unknown. However, one common perturbation in T-ALL has been found, as aberrant NOTCH1 activation is reported to occur in more than 50% of human T-ALL patient samples and cell lines.[15] Further studies in both murine and human T-ALL have identified the *c-MYC* proto-oncogene as a direct target of NOTCH1.[16] Although these reports provide important insights into one subset of T-ALL, undoubtedly, other lesions underpinning T-ALL origin and progression have not yet been determined.

Although considerable evidence supports the role of genetic modifiers as risk factors for leukemia, few heritable mutations conferring this risk are actually known,[17,18] with most associated with bone marrow failure syndromes. Outside of these examples, 'pure familial leukemias' are quite rare, with few pedigrees transmitting disease as a Mendelian trait.[19–21] Identification of the loci responsible for these familial cases would likely provide insight into oncogenic mechanisms at work in sporadic malignancies of the same type. However, with their small sample sizes, identifying genetic risk factors in human pedigrees has been challenging. Therefore, animal models of heritable leukemic predisposition are both valuable and necessary.

Zebrafish are useful to study vertebrate development through mutational forward genetic approaches. They have also become popular models of human cancer, including hematological neoplasia.[22–24] Two important studies have used cell-specific over-expression of mammalian oncogenes to induce zebrafish T-ALL.[25,26] Both transgenic models bear striking resemblance to human disease. Their cancers are clonal, and originate in the thymus before spreading to peripheral blood. T-ALL cells from these fish efface the kidney marrow, and can engraft in irradiated hosts. But despite being innovative models, these transgenic lines are restricted in scope to the known cancer pathways used to create them.

Correspondence: Dr JK Frazer or Dr N Trede, Huntsman Cancer Institute, HCI-4264, 2000 Circle of Hope, Salt Lake City, UT 84112, USA.
E-mails: kimble.frazer@hsc.utah.edu or nikolaus.trede@hci.utah.edu
[6]These authors contributed equally to this work.
Received 12 February 2009; revised 21 April 2009; accepted 23 April 2009; published online 11 June 2009

To date, zebrafish have not been used to pursue unknown genetic lesions underlying T-cell malignancy. Here, we describe a phenotypic mutagenesis screen in a *D. rerio* line, in which the native $p56^{lck}$ promoter directs T-cell-specific expression of enhanced green fluorescent protein (*lck::EGFP*). We report three different zebrafish mutants that develop heritable T-cell malignancy. Each faithfully recapitulates human T-ALL and T-cell lymphoblastic lymphoma (T-LBL) in onset, invasion pattern, and morphology, and their neoplastic cells are clonal and transplantable. Moreover, cells can also be transplanted serially, suggesting the presence of leukemia-initiating cells (LICs). As the genetic factors that collaborate to cause these diseases are revealed, these new vertebrate models of T-ALL promise to provide exciting insights into this important class of human cancers.

Materials and methods

Zebrafish care and maintenance

Fish were housed in a colony at 28.5 °C on a 14/10-h circadian cycle. For all procedures, fish were anesthetized with 0.02% tricaine methanesulfonate (MS222). Fish were handled as per NIH guidelines, under a protocol approved by the University of Utah Animal Care and Use Committee (IACUC # 08-08005).

ENU mutagenesis screen

Male WIK strain *lck::EGFP*$^{+/+}$ zebrafish were mutagenized with ENU (*N*-ethyl-*N*-nitrosourea) as described.[27] Mutagenesis efficiency was assessed by non-complementation of the *golden (gol)* locus. Eggs from pigment-deficient *gol/gol* females were fertilized with sperm of mutagenized males. A total of 0.1% of sperm genomes ($n = 4400$) had *gol*-inactivating lesions, a rate of 30 mutations per haploid genome. Mutagenized males were then bred to non-mutagenized WIK *lck::EGFP*$^{+/+}$ females to create F1 generations for phenotypic screening by fluorescence microscopy.

Generation of gynogenetic diploids by early pressure

In vitro fertilization and pressure treatment were performed as described.[28] Sperm was UV-treated with 7×10^4 μJ using a Stratalinker (Stratagene, Cedar Creek, TX, USA). Pressures and hydraulic press equipment were as reported.[29]

Microscopy and imaging

Fish were screened for abnormal GFP patterns at 6 days, 1 month, 3 months, 4.5 months and 6 months with an Olympus szx12 fluorescent microscope and camera (Center Valley, PA, USA) and Optronics Pictureframe software (Goleta, CA, USA). Slides were imaged with a Nikon Eclipse e600 microscope (Tokyo, Japan), using a Diagnostic Instruments 14.2 color camera and Spot Imaging software (Sterling Heights, MI, USA).

Histology and immunohistochemistry

Fish were fixed in 4% paraformaldehyde, paraffin-embedded, sectioned and stained with H&E (hematoxylin and eosin) using standard techniques. For immunohistochemistry, staining was performed at 37 °C using a BenchMark XT immunostainer (Ventana Medical Systems, Tucson, AZ, USA). Anti-GFP monoclonal antibody was applied for 1 h at 1:400 dilution, with resolution of GFP$^+$ tissues using an IView DAB detection kit (Ventana). Hematoxylin was used as a counterstain.

Flow cytometry and cytology

Fish thymi, marrow and GFP$^+$ tissues were dissected and placed in Zebrafish Kidney Stromal media.[30] Cells were dissociated by pipetting, filtered with SmallParts 35 μm filters (Miramar, FL, USA), and again passed through 35 μm Filcon filters (Becton Dickinson, San Jose, CA, USA) before analysis. Flow cytometry and fluorescence-activated cell sorting (FACS) were as described[31] using a BD FACSVantage instrument (Becton Dickinson). GFP intensity, forward- and side-scatter were used for gating. Slides were made by centrifugation (800 r.p.m. × 5 min) with a Shandon Cytospin 4 (Thermo Fisher Scientific, Waltham, MA, USA) and Wright stained for 2 min.

Reverse transcription-PCR

RNA was extracted from twice FAC-sorted GFP$^+$ cells with Trizol (Invitrogen, Carlsbad, CA, USA), and TURBO DNase-treated (Ambion, Austin, TX, USA). cDNA was made with Fermentas 1st strand cDNA kit (Glen Burnie, MD, USA). Primers and PCR conditions are listed in Supplementary Material.

TCR repertoire analyses

Tumor tissue was dissected from mutant fish, and thymus and gut from a single wild-type (WT) *lck::EGFP* fish were used as a control. GFP$^+$ cells were FACS-purified as described. Total RNA was extracted with Trizol, and 5′-RACE performed using a Clontech SMART RACE Kit (Mountain View, CA, USA). Primers for *tcrβ1* constant region exon 3 were used, and are listed in Supplementary Material. PCR products were excised from ethidium bromide-stained agarose gels, and bands purified using a Qiagen QIAquick Gel Extraction Kit (Valencia, CA, USA). DNA was cloned using the TOPO TA Cloning Kit (Invitrogen) and sequenced by conventional methodologies.

Statistical analysis of tcrβ1 *sequences*

Assuming random sampling, clones were distributed as a multinomial random variable, in which the number of total clones was unknown but $\geqslant 12$ (observed number of clones from the WT control fish). A goodness-of-fit test for the following hypothesis was tested: 'Clones have a multinomial distribution with $\geqslant 12$ types of clones of equal probability.' *P*-values were then obtained from 20 000 Monte Carlo simulations.

Cell transplantation

Tumors were dissected and cells prepared as above. GFP$^+$ cells were FACS-purified, diluted in Zebrafish Kidney Stromal media and concentrations confirmed by hemocytometer counts. Using a ^{137}Cesium source, hosts were irradiated with 25 Gy, and intra-peritoneally injected 2 days later with 2.5×10^3–1×10^6 of FAC-sorted GFP$^+$ cells in injection volumes of 5–10 μl. Recipients were monitored by serial fluorescence microscopy to follow engraftment and disease progression.

Results and discussion

Identification of zebrafish mutants with T-cell malignancy predisposition

To identify genetic lesions conferring a heritable risk to T-cell malignancy, we performed a forward-genetic ENU mutagenesis screen in zebrafish (Figure 1). To detect abnormal T-cell collections, we used transgenic WIK strain fish with stably integrated *lck::EGFP*, which labels all T cells.[32] Homozygous

lck::*EGFP* males were mutagenized and bred to WT *lck*::*EGFP* females, creating over 500 F1 progeny, each with multiple unknown heterozygous mutations.[33,34]

Fish were screened by fluorescence microscopy for enlarged or extra-thymic GFP until 6 months. Atypical GFP patterns could represent T-cell malignancies, benign lymphoproliferation, autoimmune T-cell infiltrations or non-T-cell GFP expression. Regardless, F1 animals harbor dominant-acting mutations that confer an abnormal phenotype. A total of 10 F1 mutants were found and nine were studied further; two are reported here: *shrek* (*srk*) and *hulk* (*hlk*) (Figure 1a), named for green animated characters.

To determine whether the *srk* and *hlk* phenotypes were heritable, these two individuals were out-bred to WT *lck*::*EGFP* fish, creating cohorts for confirmatory testing (Figure 1b). In both, multiple F2 progeny also developed abnormal GFP$^+$ cell collections (examples shown in Figure 1c), verifying dominant inheritance, albeit with incomplete penetrance. This likely reflects a need for other acquired somatic mutations for full phenotypic penetrance, but alternate explanations such as stochastic variation in these phenotypes or additional modifier loci have not been formally excluded.

In addition, we approximated penetrance in *srk* and *hlk*. As only 50% of fish in each F2 family should inherit the mutation, our calculations presumed that half of progeny were 'carriers.' By this assumption, we estimated penetrance at 10 and 5%, respectively (Figure 1b and data not shown). We note that abnormal GFP$^+$ cell expansion is seen in WT *lck*::*EGFP* fish in $<$0.1% of animals, and heritability has not been established in these instances (our unpublished data).

To detect recessive mutations, eggs from normal F1 females underwent early pressure (EP), an induced parthenogenesis technique producing gynogenetic diploid progeny.[35] EP offspring are homozygous for maternal haplotypes, in locations where meiotic cross over did not occur. Thus, at these loci, recessive phenotypes can manifest in the F2 generation, eliminating the need for large F3 screens. We performed EP on over 100 F1 females, creating F2 families of $>$25 fish that were also screened until 6 months. One additional mutant, *oscar the grouch* (*otg*), was detected by EP (Figure 1a), in which several siblings from the same F2 family exhibited abnormal GFP patterns.

To confirm recessive inheritance in *otg*, affected EP-derived fish were bred to WT *lck*::*EGFP* animals. Here, all progeny carry one *otg* lesion. In over 300 out-bred fish, only one acquired a GFP$^+$ tumor, for a heterozygous penetrance of 0.3% (Figure 1b). In contrast, when diseased *otg* fish were in-bred to create homozygous mutants, over half of progeny showed abnormal GFP patterns (example in Figure 1c). This equated to a homozygous penetrance of 51%, and verified that *otg* acts recessively.

hlk, srk *and* otg *mutants each develop* bona fide *malignancies*

Affected fish of each mutant line were strikingly similar to T-ALL induced by oncogene over-expression.[25,26] GFP$^+$ areas were solid, intensely bright masses resembling tumors, frequently arising from the thymic region (Figure 1c). Neoplasms typically spread locally to gills and adjacent structures, and generally in a

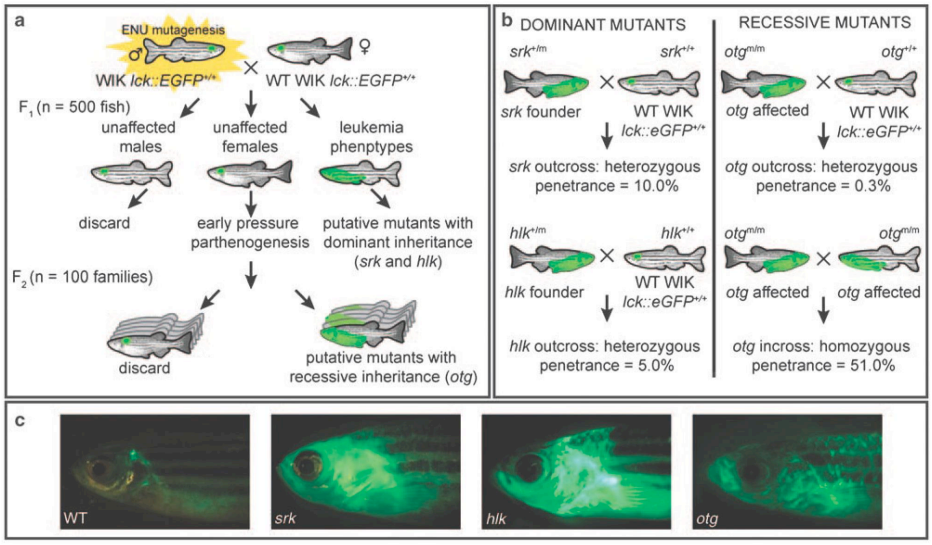

Figure 1 Heritable T-cell cancer phenotypes from an ENU mutagenesis screen. (**a**) Male homozygous *lck*::*EGFP* zebrafish were ENU treated and bred to WT female *lck*::*EGFP* fish. F1 offspring with heterozygous germline mutations were screened microscopically until 6 months. Mutants with abnormal GFP patterns were designated putatively dominant; two reported here are *shrek* (*srk*) and *hulk* (*hlk*). In addition, eggs from normal female F1 fish were subjected to early pressure parthenogenesis, creating F2 families. One family with several abnormal siblings was deemed putatively recessive, dubbed *oscar the grouch* (*otg*). (**b**) *Srk* and *hlk* were confirmed by out-breeding F1 founders to WT fish, with observation of disease in offspring. *Otg* was verified by out-breeding (only 0.3% of heterozygotes acquired disease), and in-breeding (51% of homozygotes were abnormal). (**c**) WT *lck*::*EGFP* and diseased *srk*, *hlk* and *otg* fish.

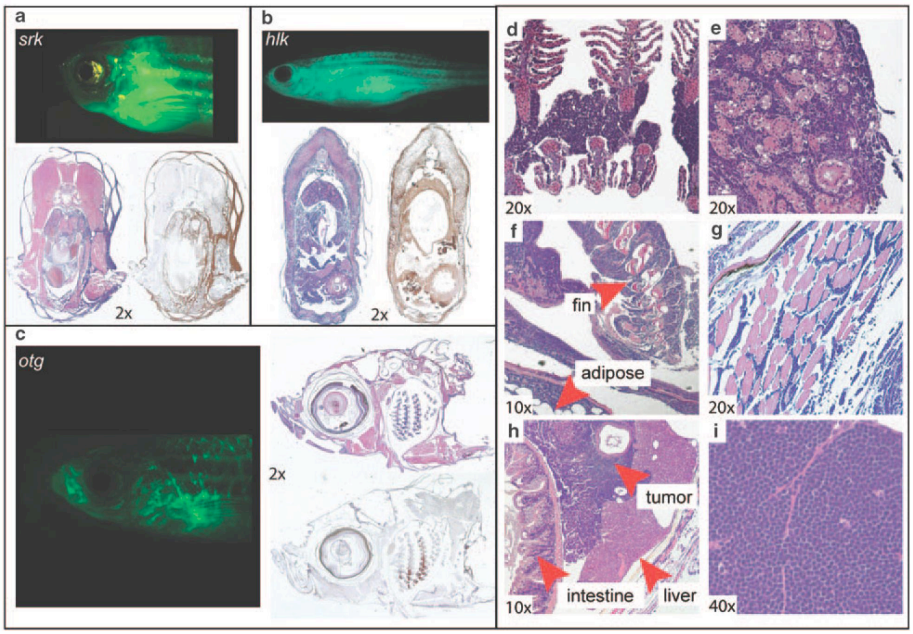

Figure 2 Histological and immunohistochemical analysis of GFP$^+$ tumors. Diseased *srk* (**a**), *hlk* (**b**) and *otg* (**c**) fish, H&E-stained sections of same fish, and sections labeled brown by α-GFP IHC. Most basophilic cells by H&E are reactive with α-GFP monoclonal antibody. H&E stains show neoplastic infiltration of (**d**) gills, (**e**) kidney-marrow, (**f**) fin and adipose, (**g**) muscle and (**h**) forming intra-abdominal tumors. Tumor tissue (**i**) has small round blue cell morphology typical of T-LBL and T-ALL. (Images have been graphically enhanced to improve color balance and brightness.)

cephalo-caudal pattern through the entire fish over weeks-to-months until generalized edema and circulatory collapse caused death (Supplementary Figure 1).

Though affected *srk*, *hlk* and *otg* fish often appeared similar, variations did occur. GFP$^+$ infiltrations of the eyes, fins, skin and tail were seen, with occasional discontinuous 'skip lesions' (Supplementary Figure 2). These patterns could reflect either multiple synchronous T-cell cancers in an individual fish, or non-contiguous spreading of a single malignancy. In particular, the skin tropism seen is reminiscent of non-Hodgkin peripheral T-cell cutaneous lymphomas, such as mycosis fungoides and Sezary syndrome.[36] In agreement with their pervasive cancer susceptibility, non-lymphocytic, GFP$^-$ tumors were also infrequently detected in *srk*, *hlk* and *otg* (Supplementary Figure 3), perhaps alluding to a general cancer predisposition.

To confirm that GFP$^+$ tumors were in fact cancerous, we performed histology and immunohistochemistry on affected animals (Figure 2). Sections from *srk*, *hlk* and *otg* fish were H&E stained, revealing infiltrating lymphocytes in tissues that coincided exactly to GFP$^+$ body areas. Notably, gills, fins, skin, muscle and fat were all distorted by a monomorphic invasive cell population with lymphocytic appearance. These cells were GFP$^+$, as shown by immunohistochemistry with α-GFP monoclonal antibody (Figures 2a–c). Fish kidney marrow (zebrafish bone marrow equivalent) was frequently effaced by these same cells, showing spread to marrow as seen in leukemia. In addition, intra-abdominal tumors of malignant lymphocytes were also seen. Tumor cells exhibited classic 'small round blue cell' morphology consistent with lymphoblasts.[37] Collectively, these phenotypes closely emulate human T-LBL and T-ALL.

Malignancies of hlk, srk *and* otg *have T-cell origin*

Despite topographical and morphological evidence that GFP$^+$ tumors were T-cell malignancies, we also examined their gene expression. To limit our analysis to only tumor cells, we isolated GFP$^+$ cells by FACS of tumors from individual *srk*, *hlk* and *otg* fish. FACS-purification was performed twice to eliminate rare mis-sorted cells. Total RNA was then interrogated for cell-specific transcripts by reverse transcription-PCR (RT-PCR; Figure 3).

All three tumors expressed *lck* and *trac* (*TCRα*), confirming T-cell identity. Cells also contained *cd4*, *cd8a* and *rag2* messages, further substantiating their T-lineage origins. It is not known whether single tumor cells co-expressed these genes, or if tumors contained different clones corresponding to multiple stages of T-cell differentiation. Of note, human T-ALL and T-LBL cells frequently co-express these same transcripts, consistent with a double-positive stage of thymocyte differentiation. However, other tumors from each of these mutants have shown gene expression profiles indicative of mature T cell differentiation (Supplementary Figure 4 and data not shown). In all malignant samples, expression of the myeloid-specific

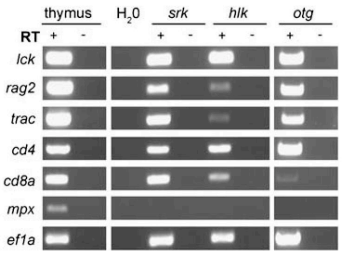

Figure 3 GFP$^+$ tumor cells have T-cell gene expression patterns. Total RNA from FACS-purified GFP$^+$ cells of *srk*, *hlk* and *otg* tumors was analyzed by RT-PCR. *D. rerio* nomenclature is listed at left (*lck*=*LCK*, *rag2*=*RAG2*, *trac*=*TCRA*, *cd4*=*CD4*, *cd8a*=*CD8A*, *mpx*=*MPO*, *ef1a*=*EEF1A1*). RNA from WT thymus and *ef1a* PCR are positive controls. H_2O-only, reactions without RT, and *mpx* are negative controls.

transcript myeloperoxidase (*mpx*; human *MPO*) was not detected, attesting to high tumor cell purities.

Malignant cells are abundant in marrow and peripheral blood

Histology often exhibited lymphocytic infiltrations in marrows of diseased *srk*, *hlk* and *otg* fish (Figure 2). To examine these cells, we performed flow cytometry on marrow and blood of affected fish. In tumor-bearing fish, we could readily identify GFP$^+$ lymphoblasts that were infrequent in WT *lck*::*EGFP* fish (Figure 4a). Malignant blasts were distinct from normal circulating T cells based on their larger average size and greater GFP intensity, but had similar granularity to T lymphocytes (Figure 4a and data not shown). Abundant GFP$^+$ cells were found in the marrow and blood of many diseased fish, and when present, were dramatically increased relative to the fraction of T cells normally seen in these two anatomic sites (Figure 4a and Supplementary Table 1).[32] Overall, several marrow and blood samples from all three mutants contained GFP$^+$ cells greater than three standard deviations above their corresponding WT mean values. This marrow infiltration and dissemination to peripheral blood is consistent with that seen in human T-cell lymphomas progressing to frank leukemias as T-ALL.[38]

To study these cells further, we made cytospin preparations from marrow, tumors, FAC-sorted GFP$^+$ cells and blood, and performed Wright stains (Figure 4b, Supplementary Figure 5, and data not shown). Marrow from affected, but not WT, fish often was effaced by lymphoblasts. Unsorted tumors had identical cells to those in the marrow, further verified by stains of FACS-purified cells from tumors, marrow and blood. Before staining, fluorescence microscopy showed that tissues consisted primarily of GFP$^+$ cells, even without FACS enrichment (Figure 4b and data not shown). Even unsorted blood smears from diseased fish had copious lymphoblasts, typical of human T-ALL. Blasts had hyperchromatic nuclei with prominent nucleoli, high nuclear:cytoplasmic ratios and intensely blue-staining cytoplasms (Figure 4b).

Malignancies show clonal TCR rearrangements

To test whether lymphoblasts were malignant clones, and not polyclonal accumulations as might be seen in benign lymphoproliferation, we performed T-cell receptor (TCR) repertoire studies to investigate their diversity. We isolated total RNA from GFP$^+$ cells of a single WT *lck*::*EGFP* fish, as well as individual *srk*, *hlk* and *otg* tumors. To minimize normal T-cell contamination, non-thymic tumors were utilized. Using 5′ rapid amplification of cDNA ends (5′ RACE), *tcrβ1* transcripts from each sample were cloned, and variable-diversity-joining (VDJ) gene segment usage were analyzed (Figure 5; sequence alignments shown in Supplementary Table 2).

The WT fish yielded 28 independently isolated sequences, comprising 12 unique clones, each captured 1–5 times in a bell-shaped distribution. This diversity was consistent with a polyclonal repertoire, surveyed incompletely in random manner ($P=0.51$). In contrast, *srk* and *otg* tumors each had highly skewed, non-random VDJ usage with a single clone representing nearly the entire *tcrβ1* cDNA pool (9/11 *srk* sequences, 14/15 for *otg*; each $P<0.001$). This bias is consistent with an oligoclonal T-cell population, as occurs in malignancy. Rarely isolated VDJ sequences from *srk* (two different clones, each obtained once) and *otg* (one clone, isolated once) may represent either less-prevalent malignant clones, or contamination by normal T cells infiltrating these tumors, as our GFP-based FACS purifications could not exclude these cells. In either case, the distribution of sequences from each tumor was highly constricted relative to WT, with sequence alignments showing that rarely detected TCR rearrangements were not related to the dominant VDJ gene segment utilized by the principal population (Supplementary Table 2).

The GFP$^+$ cells from the *hlk* tumor also showed limited *tcrβ1* diversity, showing two unrelated clones (9/15 and 6/15 of sequences). This non-random repertoire was also statistically significant ($P<0.001$), suggesting the *hlk* tumor was oligoclonal. As the two TCR rearrangements from *hlk* were unrelated (Supplementary Table 2), this could reflect two distinct malignant clones originating independently in the same animal.

Genetic characteristics of srk *and* hlk

Having shown cancers in *srk* and *hlk* to be T-cell-derived and oligoclonal, we sought to further characterize the genetics of these mutants. Extended pedigrees were created by in-breeding each line and out-crossing to other backgrounds. As our earlier penetrance estimates (Figure 1b) were deduced from small numbers, we created large families to definitively track penetrance and incidence. Animals known to carry mutations (fish having GFP$^+$ tumors) were used to create these pedigrees.

We hypothesized that when *srk* and *hlk* heterozygotes develop disease at low penetrance, acquired mutations of the second allele may facilitate transformation. If so, germline *srk* or *hlk* homozygotes might show disease at higher penetrance or with shorter latency.[39] As the *srk* and *hlk* mutations are unknown (obviating genotyping), we created homozygous mutants by in-breeding tumor bearing fish for several generations to enrich the allelic frequency of mutant loci. Validating this strategy, by the third consanguineous generation, a dramatic increase in penetrance was seen in both *srk* and *hlk* cohorts (43.0 and 40.3%, Figure 6). Although fish could not be confirmed to be uniformly homozygous at the *srk* and *hlk* loci, this finding clearly indicates that adding homozygotes to the cohort amplifies overall penetrance. The parsimonious explanation for this result is that homozygotes have higher disease rates than heterozygotes, although the possible contribution of modifier loci has not been excluded. Of interest, in-bred *srk* and *hlk* fish had normal embryonic and adult viability (data not shown), establishing that homozygous mutants are non-lethal.

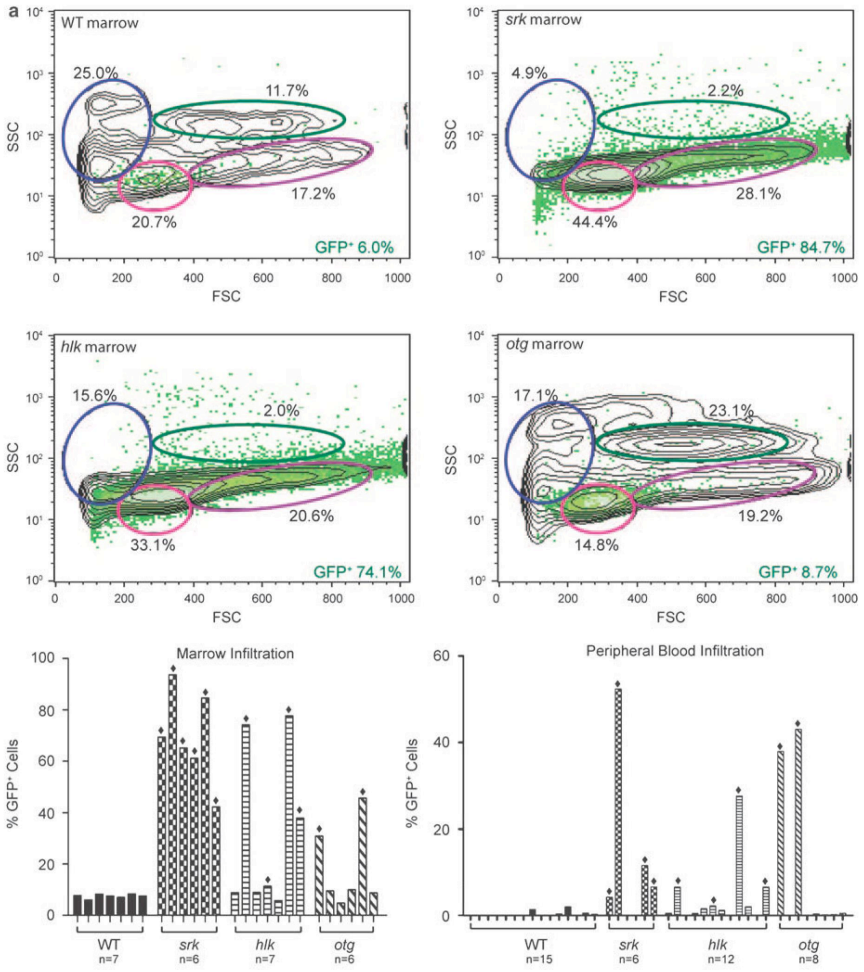

Figure 4 Neoplastic cells in marrow and blood have lymphoblast morphology. (**a**) Flow cytometry of marrow from a WT *lck*::*EGFP* fish (upper left plot) shows most GFP$^+$ cells in lymphoid (pink oval) or progenitor (purple) windows, with all T-lineage cells comprising 6.0% of total cells. Diseased *srk* (upper right plot) and *hlk* (lower left plot) fish show dramatically increased GFP$^+$ percentages (84.7 and 74.1%), with diminished erythroid (blue) and myeloid (green) fractions. *Otg* fish shows early GFP$^+$ cellular infiltration (8.7% of total), with normal erythroid and myeloid values. *x* axes: forward scatter (FSC), *y* axes: side scatter (SSC), with GFP$^+$ cells overlaid in green. Histograms at lower left show GFP$^+$ cell fraction for WT marrows (mean 7.5 ± 0.9%; $n = 7$), and multiple affected *srk, hlk* and *otg* fish. Defining abnormal as >3 s.d. above the WT mean, 6/6 *srk*, 4/7 *hlk* and 2/6 *otg* marrows showed pathological infiltrations (bars marked with diamonds). In these samples, mean GFP$^+$ fractions were 69.4% (*srk*), 50.3% (*hlk*) and 38.2% (*otg*). Histograms at right depict flow cytometry results for peripheral blood in identical format. WT fish have only rare GFP$^+$ cells (0.35 ± 0.6%, $n = 15$). Blood from affected fish had high GFP$^+$ fractions in 4/6 *srk*, 4/12 *hlk* and 2/8 *otg* samples, with mean values of 18.8, 10.8 and 40.5%, respectively. (**b**) Wright stains of malignant lymphoblasts from different tissues. Upper panels: WT (left) and *srk* (right) marrow. *Srk* sample is overrun by T-ALL neoplastic cells, and fluorescent micrograph (inset) confirms that most *srk* marrow cells are GFP$^+$. Middle panels: unsorted cells from *hlk* tumor (left) have lymphoblastic morphology; FACS-purified cells from *srk* tumor (right) are identical. High power image of GFP$^+$-sorted *hlk* tumor cells (lower left panel) shows morphological features of lymphoblasts. Blood from a diseased *srk* fish (lower right panel) shows erythrocytes (top row) and frequent malignant lymphoblasts (second row). Lymphocytes (third row) and erythrocytes (fourth row) from a WT fish are shown for comparison (*D. rerio* has nucleated RBCs). (Images graphically enhanced to improve brightness.)

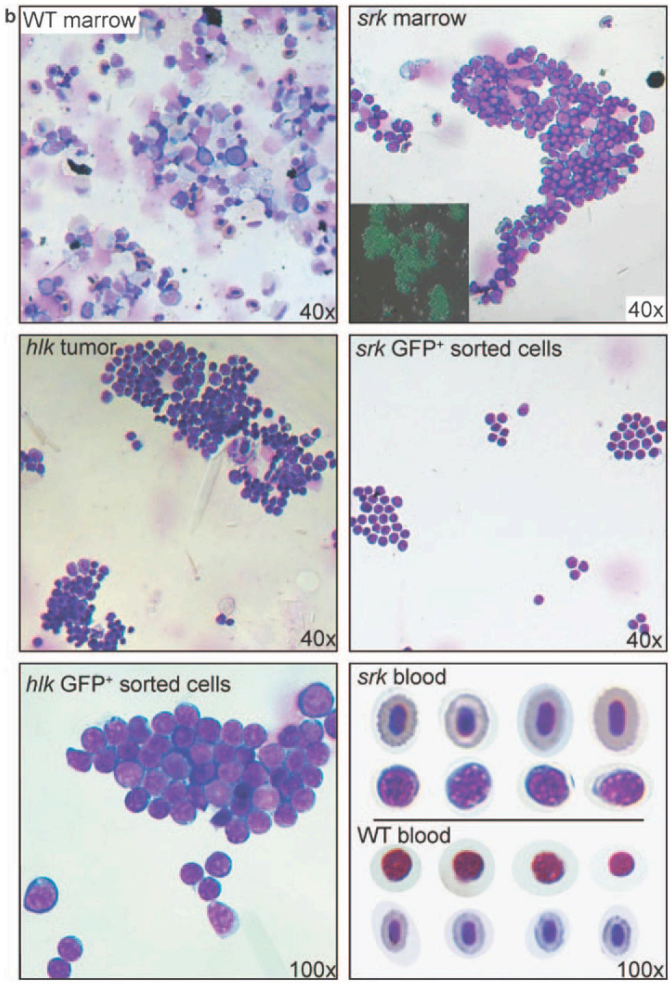

Figure 4 Continued.

To verify our earlier heterozygous penetrance figures, we used mono-allelic *srk* and *hlk* fish (affected fish with one WT parent, making them obligate heterozygotes) and bred them with WT genetic backgrounds. As 50% of gametes from mutant heterozygotes will lack the mutation, only half of these progeny were estimated to be heterozygous mutants (Figure 6: #screened vs #of carriers). In these families, *srk* and *hlk* heterozygotes had penetrance similar to original estimates (14.1 and 5.9%, Figure 6; compare with 10 and 5% in Figure 1b). Although modest, these rates are far higher than the rare T-cell neoplasias observed in WT *lck*::*EGFP* fish (<0.1%, our unpublished data). In fact, this is much higher than rates reported in transgenic zebrafish models of AML induced by *MOZ-TIF2*[40] or B-ALL caused by *TEL-AML1*.[41] More importantly, this degree of penetrance is similar to disease rates seen in rare human pedigrees of leukemia and lymphoma,[19,21,42] suggesting that *srk* and *hlk* may accurately model human familial predisposition to these diseases.

These heterozygous phenotypes verify the dominant cancer predisposition of *srk* and *hlk*. Of note, we also created *hlk* fish with transgenic *rag2*::*bcl2-EGFP*, using the native *rag2* promoter to drive lymphocyte-specific over-expression of *bcl2*.[43] Unlike NOTCH1-induced *D. rerio* T-ALL, we saw no accentuated penetrance or shortened latency in *hlk*+*rag2*::*bcl2* fish

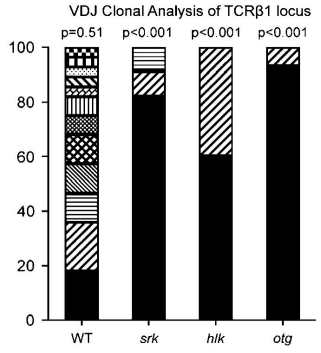

Figure 5 Tumors are clonal with shared TCRβ1 VDJ rearrangements. Total RNA from GFP$^+$ cells of a WT thymus or tumors of single *srk*, *hlk* and *otg* fish was used for 5′ RACE with *tcrβ1*-specific primers. RACE products were sequenced for VDJ analysis. From 28 WT thymus clones, 12 unique sequences were obtained, each isolated 1–5 times. From *srk* and *otg*, 9/11 (81.8%) and 14/15 (93.3%) clones were identical, suggesting oligoclonality. From *hlk*, two unrelated VDJ recombinations were detected 9/15 and 6/15 times, again showing oligoclonality. Distributions were analyzed by a goodness-of-fit test, and *P*-values calculated in 20 000 Monte Carlo simulations. *y* axis indicates percentage of clones obtained from each individual fish.

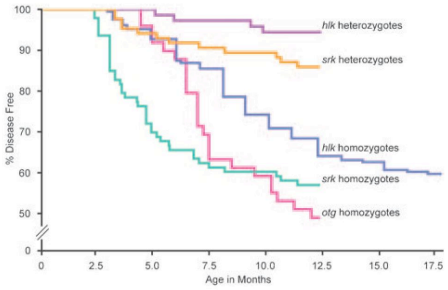

Mutant	N		Penetrance		Mean Incidence	
srk	Total # Screened	# of carriers	# Affected	%	Months	SD
Homozygotes	93	n/a	40	43.0	4.8	2.3
Heterozygotes	170	85	12	14.1	6.4	3.0
hlk						
Homozygotes	206	n/a	83	40.3	8.7	2.8
Heterozygotes	136	68	4	5.9	7.6	2.4
otg						
Homozygotes	49	n/a	25	51.0	8.2	3.2
Heterozygotes	309	n/a	1	0.3	10.3	n/a

Figure 6 Disease incidence curves for *srk*, *hlk* and *otg* mutants. Pools of fish were screened by fluorescence microscopy for T-cell malignancy. *Srk* homozygotes (green) and heterozygotes (orange) have disease penetrance of 43.0 and 14.1%, respectively. *Srk* homozygotes have shorter latency, with mean incidence of 4.8 vs 6.4 months for heterozygotes (s.d., standard deviation). *Hlk* homozygotes (blue) have 40.3% disease penetrance by 18 months (35.9% by 12 months), compared with heterozygous penetrance of 5.9% (purple). Homozygous and heterozygous *hlk* fish have similar latency (mean incidences of 8.7 and 7.6 months, respectively). *Otg* homozygotes (pink) show 51.0% penetrance by 12 months, with mean incidence of 8.2 months. Heterozygotes rarely acquire disease (0.3%), and are not depicted as a Kaplan–Meier curve.

(data not shown). Although NOTCH1 activation showed a cooperative relationship with *bcl2* in this transgenic context,[26] a similar synergy was not seen between *hlk* and *bcl2*. One possible explanation for this result is that the *hlk* mutation may perturb normal apoptosis, subverting any added effect of *bcl2* over-expression. However, thus far, apoptosis assays with *hlk* fish have failed to show any difference between *hlk* and WT animals (data not shown).

In contrast, fish with germline bi-allelic *srk* and *hlk* mutations had significantly higher penetrance. Explaining this finding, if *srk* and *hlk* are inactivating lesions, somatic mutation of the second allele may normally be required for transformation in heterozygotes. Alternatively, if the *srk* or *hlk* lesions are activating, increased homozygous penetrance may derive from gene dosage effects. Also of note, although the increased homozygous penetrance is striking, it is equally evident that neither *srk* nor *hlk* homozygotes show full penetrance. Over half of all homozygotes did not acquire disease by 1 year, implying other mutations are needed for full malignant penetrance.

Genetic characteristics of otg

Otg, identified by virtue of EP (Figure 1), was presumptively recessive, as its F1 founder was phenotypically normal. As noted above, when *otg* EP fish were out-bred, almost no T-cell neoplasia occurred (1/309 fish, 0.3%; Figure 6). One possible interpretation of this result is that somatic mutation of the second *otg* allele is infrequent relative to *srk* and *hlk*. Alternatively, a greater number of cooperating mutations may be able to potentiate *srk* or *hlk* oncogenesis. In either case, the near-absence of disease in heterozygotes confirms that *otg* behaves as a recessive trait.

Although *otg* heterozygotes were normal, progeny of in-bred *otg* EP fish showed high disease rates, even greater than *srk* or *hlk* (51.0%; Figure 6). However, despite this high penetrance, still only about half of *otg* homozygotes developed disease. As with *srk* and *hlk*, this incomplete penetrance suggests that other somatically acquired mutations are necessary for transformation.

srk, hlk *and* otg *have differing incidence patterns*

We also determined typical latencies for *srk*, *hlk* and *otg* (Figure 6). In all three mutants, tumors first developed coincident with sexual maturity (3–4 months) and peaked at 5–8 months (young adult). *Srk* homozygotes had shorter latencies than heterozygotes (4.8 vs 6.4 months), whereas *hlk* mono- and bi-allelic mutants showed similar incidence (7.6 vs 8.7 months). In *otg*, heterozygous disease was rare, preventing comparison.

As *srk* and *hlk* homozygotes show differing incidence, we infer that they have distinct genetic lesions, although the possibility of different mutations in the same gene still exists. In addition, the abbreviated latency of *srk* homozygotes implies that mutation to the second *srk* allele may be key to tumorigenesis. Still, even homozygous *srk* mutants are incompletely penetrant, proving that other somatic events are needed. Conversely, the similar incidence of *hlk* single and double mutants suggests the second *hlk* lesion impacts penetrance, but not latency. Thus, other mutations besides *hlk* are transformative. Together, these disparities in inheritance, penetrance and

incidence may suggest different cadres of cooperating mutations for all three of these models.

Malignancies can engraft and be serially passaged in allogeneic hosts

Many cancers—including zebrafish T-ALL—can engraft in allogeneic immuno-compromised hosts, and this attribute may distinguish lymphoproliferative conditions from neoplasia.[25,26] Transplantation can also determine the minimal cell number able to transmit disease, a property of LIC.[44] To test these features, we examined our models' ability to be propagated in irradiated hosts.

Zebrafish strains have limited polymorphism, but *D. rerio* are not routinely available as isogenic lines. Accordingly, immuno-suppression is used to facilitate engraftment.[45] Using this approach, WT recipients were given sub-lethal doses of 25 gray (Gy) γ-irradiation before transplant. FAC-sorted, GFP^+ tumor cells were then injected into hosts, with monitoring of engraftment by fluorescence microscopy.

Using multiple tumors from each line and a range of donor cell doses for each tumor, GFP^+ malignant cells from *srk*, *hlk* and *otg* each showed engraftment (Supplementary Figure 6). In most hosts, neoplastic cells were first seen at the site of injection, and grew to completely infiltrate the intra-abdominal and thoracic cavities, ultimately causing host demise. Many fish showed extensive dissemination before death, mimicking their donors. These features did not occur in controls injected with GFP^+ thymocytes from WT WIK *lck*::*EGFP* donors (data not shown).

We also tested whether malignancies could be serially passaged *in vivo*, and if iterative transplantation selected for more aggressive tumors—either in ability to engraft or to kill hosts. From a single *srk* tumor, FACS-purified GFP^+ cells were propagated through three transplant cycles (using 1×10^5 cells in each transplant), while monitoring host engraftment and survival. Recipients began to engraft by day 6, with the percent engrafted at 6 days increasing in each round (38.5% in cohort #1, 50.0% in cohort #2 and 58.3% in cohort #3; data not shown).

We also tracked survival, including all fish engrafted by 21 days (Figure 7). In all three transplant rounds, engrafted hosts first began to die at 11–13 days. However, net survival decreased with each transplant iteration, with mean survival 18.2 days for primary hosts, 16 days in secondary recipients and 13.5 days in tertiary hosts. Comparing Kaplan–Meier curves by the Logrank test-for-trend showed significant differences ($P = 0.0423$). These results show that cancers can serially engraft into newly irradiated fish, and that progressive transplantation selects for leukemias with increasingly malignant phenotypes. These changes may occur by the accrual of new mutations and/or alterations in gene expression that enhance tumor lethality. Alternatively, sequential transplants may select for tumors with progressively higher fractions of LIC, thereby effecting accelerated engraftment and tumor expansion.

To assess the presence and frequency of LIC, we performed transplants with cells from three different *srk* tumors (Supplementary Figure 7). Using 10-fold dilutions of GFP^+ cells in groups of five recipients each, hosts were followed for engraftment. By the linear regression model of incidence analysis, LIC values were then determined.[46] The three *srk* tumors in these experiments yielded LIC frequencies of 1:1752, 1:8159 and 1:10 373 cells, comparable to numbers reported with zebrafish T-ALL caused by murine c-MYC.[47] In addition, using cells from *in vivo*-passaged *hlk* tumors, we have seen high engraftment with as few as 2500 GFP^+ cells (data not shown).

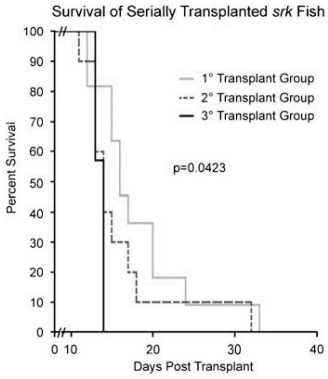

Figure 7 Serially transplanted cancers are increasingly malignant. GFP^+ cells from a *srk* tumor were sequentially transplanted into three iterations of pre-irradiated WT hosts. 1×10^5 cells were used in each transplant. Only engrafted fish are plotted (first host cohort $n = 11$; second group $n = 10$; third $n = 7$). One engrafted fish from each cohort (not included above) was used as a donor in the subsequent transplant round. Recipients had shortened survival in each round, with statistical significance of $P = 0.0423$.

These experiments establish that tumor cells from *srk*, *hlk* and *otg* can be transplanted, a common property of neoplasias. In addition, serial passaging shows that progressively more malignant phenotypes can be acquired. Further, tumors from these models contain LIC, and these cells can be quantified. Plausibly, comparisons between the same malignancy pre- and post-transplant (or following many transplant iterations) may show differences responsible for their more aggressive behavior.

Conclusion

We have used an ENU mutagenesis screen to induce and identify three *D. rerio* models of heritable T-cell cancer predisposition. These mutants emulate many clinical and molecular features of human T-ALL and T-LBL. Key characteristics and experimental advantages of these new disease models are summarized below.

Mutants have reproducible and heritable malignancy predisposition. *Srk* and *hlk* are dominantly inherited, but heterozygous penetrance is modest. Thus, these lines may represent models of familial leukemias and lymphomas, which have been reported repeatedly but are not molecularly defined.[17–20] As homozygous traits, *srk*, *hlk* and *otg* all have high penetrance (40–51%; Figure 6), facilitating production of large numbers of affected animals for study. Although antibodies against most *D. rerio* proteins are currently scarce, malignant T cells can be FACS-purified easily because they are GFP^+, simplifying their procurement.

These T-cell cancers are similar to human T-ALL and T-LBL. Mutants develop thymic tumors, akin to mediastinal masses seen in both experimental mammalian lymphoma models and human patients. Tumors often disseminate, with tropism for marrow and blood, again modeling human T-cell malignancies. Expression patterns confirm that neoplastic cells are T lineage, and TCR analyses verify their clonality. Malignant cells are

allogeneically transplantable with high rates of engraftment. Transplanted cells authentically re-establish the original disease, expediting the generation of large numbers of malignant cells. By transplantation, LIC studies are also possible. Finally, *in vivo* selection can expand clones with high LIC fractions or other desirable attributes that are currently difficult to study with mammalian models.

These studies emphasize the feasibility of forward genetic screens with adult vertebrates to discover non-embryonic phenotypes relevant to human health, such as cancer predisposition. Traditionally, zebrafish and other 'genetic' models have been used in mutational screens querying developmental phenotypes, using early embryos. By screening mutant populations into early adulthood (6 months), we show that late-manifesting conditions are also viable experimental targets. As zebrafish rarely develop spontaneous malignancy in their first 6 months, we exploited the mutagenicity of ENU and a T-cell-specific fluorochrome to detect phenotypes that would otherwise be impractical to pursue experimentally. We note that our approach is not limited to T-lymphocyte cancers. Exchanging *lck*::*EGFP* for other cell-specific markers, similar screens could investigate any number of pathological endpoints.

Using these mutants, superimposed modifier screens may be performed to identify collaborating genes affecting these phenotypes. Mutants with low penetrance and long latency (*srk* and *hlk* heterozygotes) are well suited for enhancer screens seeking more prevalent and/or earlier disease onset. Highly penetrant mutants with early incidence (*srk* homozygotes) are optimal for suppressor approaches.

These cancer-prone mutants should prove useful for dissecting the genetic changes that underlie T-cell malignancy occurrence and progression. T cells can be purified from mutant fish before tumor development (presumably before acquiring other mutations obligate to transformation). Neoplastic cells can also be purified from thymic cancers, from disseminated clones at other sites, or from highly aggressive neoplasms after serial transplantation. This should allow for comparisons between cells from each stage of disease progression. We believe these genetic cancer predisposition models will provide a platform to permit the step-by-step analysis of each crucial biological point in T-ALL and T-LBL. Ultimately, understanding the molecular events that cause neoplastic transformation—and those underlying key stages of disease progression like dissemination and engraftment—should improve our ability to treat these diseases at each and every point in their complex evolution.

Conflict of interest

The authors declare no conflict of interest.

Acknowledgements

We thank Eric Konnick and Lauren Shih for superb technical contributions to this work, Dr Kenneth Boucher for expert statistical analysis and ARUP Institute for histology and immunophenotyping. We also thank Drs Stephen Lessnick, John Parant and Joshua Schiffman for critical appraisal of the paper. JKF was supported by NICHD award K08-HD53350; NM was supported by NICHD award K12-HD001410 and an Alex's Lemonade Stand Young Investigator award; JKF and NM were both supported by the Children's Health Research Center at the University of Utah and by Primary Children's Medical Center Foundation Grants; LR was supported by NIDDK award T32-DK007115; SAH was supported by an NIH Cancer Research Training Grant and an American Cancer Society Fellowship award PF-08-105-01-LIB; NST was supported by NIAID award R21-AI079784 and the Huntsman Cancer Foundation; Huntsman Cancer Institute core facilities supported by Grant P30-CA042014 also contributed to this work.

References

1 Silverman LB, Sallan SE. Newly diagnosed childhood acute lymphoblastic leukemia: update on prognostic factors and treatment. *Curr Opin Hematol* 2003; **10**: 290–296.
2 Gaynon PS, Trigg ME, Heerema NA, Sensel MG, Sather HN, Hammond GD *et al*. Children's Cancer Group trials in childhood acute lymphoblastic leukemia: 1983–1995. *Leukemia* 2000; **14**: 2223–2233.
3 Thiel E, Kranz BR, Raghavachar A, Bartram CR, Loffler H, Messerer D *et al*. Prethymic phenotype and genotype of pre-T (CD7+/ER-)-cell leukemia and its clinical significance within adult acute lymphoblastic leukemia. *Blood* 1989; **73**: 1247–1258.
4 Goldberg JM, Silverman LB, Levy DE, Dalton VK, Gelber RD, Lehmann L *et al*. Childhood T-cell acute lymphoblastic leukemia: the Dana-Farber Cancer Institute acute lymphoblastic leukemia consortium experience. *J Clin Oncol* 2003; **21**: 3616–3622.
5 Pui CH. Recent advances in the biology and treatment of childhood acute lymphoblastic leukemia. *Curr Opin Hematol* 1998; **5**: 292–301.
6 Larson RA, Dodge RK, Linker CA, Stone RM, Powell BL, Lee EJ *et al*. A randomized controlled trial of filgrastim during remission induction and consolidation chemotherapy for adults with acute lymphoblastic leukemia: CALGB study 9111. *Blood* 1998; **92**: 1556–1564.
7 Takeuchi J, Kyo T, Naito K, Sao H, Takahashi M, Miyawaki S *et al*. Induction therapy by frequent administration of doxorubicin with four other drugs, followed by intensive consolidation and maintenance therapy for adult acute lymphoblastic leukemia: the JALSG-ALL93 study. *Leukemia* 2002; **16**: 1259–1266.
8 Gilliland DG. Hematologic malignancies. *Curr Opin Hematol* 2001; **8**: 189–191.
9 Ferrando AA, Neuberg DS, Staunton J, Loh ML, Huard C, Raimondi SC *et al*. Gene expression signatures define novel oncogenic pathways in T cell acute lymphoblastic leukemia. *Cancer Cell* 2002; **1**: 75–87.
10 Pui CH, Relling MV, Downing JR. Acute lymphoblastic leukemia. *N Engl J Med* 2004; **350**: 1535–1548.
11 Armstrong SA, Look AT. Molecular genetics of acute lymphoblastic leukemia. *J Clin Oncol* 2005; **23**: 6306–6315.
12 Ferrando AA, Look AT. Clinical implications of recurring chromosomal and associated molecular abnormalities in acute lymphoblastic leukemia. *Semin Hematol* 2000; **37**: 381–395.
13 Harrison CJ, Foroni L. Cytogenetics and molecular genetics of acute lymphoblastic leukemia. *Rev Clin Exp Hematol* 2002; **6**: 91–113; discussion 200–2.
14 Graux C, Cools J, Michaux L, Vandenberghe P, Hagemeijer A. Cytogenetics and molecular genetics of T-cell acute lymphoblastic leukemia: from thymocyte to lymphoblast. *Leukemia* 2006; **20**: 1496–1510.
15 Weng AP, Ferrando AA, Lee W, Morris JPt, Silverman LB, Sanchez-Irizarry C *et al*. Activating mutations of NOTCH1 in human T cell acute lymphoblastic leukemia. *Science* 2004; **306**: 269–271.
16 Palomero T, Lim WK, Odom DT, Sulis ML, Real PJ, Margolin A *et al*. NOTCH1 directly regulates c-MYC and activates a feed-forward-loop transcriptional network promoting leukemic cell growth. *Proc Natl Acad Sci USA* 2006; **103**: 18261–18266.
17 Gunz FW, Gunz JP, Veale AM, Chapman CJ, Houston IB. Familial leukaemia: a study of 909 families. *Scand J Haematol* 1975; **15**: 117–131.
18 Goldgar DE, Easton DF, Cannon-Albright LA, Skolnick MH. Systematic population-based assessment of cancer risk in first-degree relatives of cancer probands. *J Natl Cancer Inst* 1994; **86**: 1600–1608.
19 Horwitz M. The genetics of familial leukemia. *Leukemia* 1997; **11**: 1347–1359.

20 Segel GB, Lichtman MA. Familial (inherited) leukemia, lymphoma, and myeloma: an overview. *Blood Cells Mol Dis* 2004; **32**: 246–261.
21 Benson KF, Horwitz M. Familial leukemia. *Best Pract Res Clin Haematol* 2006; **19**: 269–279.
22 Amatruda JF, Zon LI. Dissecting hematopoiesis and disease using the zebrafish. *Dev Biol* 1999; **216**: 1–15.
23 Trede NS, Langenau DM, Traver D, Look AT, Zon LI. The use of zebrafish to understand immunity. *Immunity* 2004; **20**: 367–379.
24 Meeker ND, Trede NS. Immunology and zebrafish: spawning new models of human disease. *Dev Comp Immunol* 2008; **32**: 745–757.
25 Langenau DM, Traver D, Ferrando AA, Kutok JL, Aster JC, Kanki JP *et al*. Myc-induced T cell leukemia in transgenic zebrafish. *Science* 2003; **299**: 887–890.
26 Chen J, Jette C, Kanki JP, Aster JC, Look AT, Griffin JD. NOTCH1-induced T-cell leukemia in transgenic zebrafish. *Leukemia* 2007; **21**: 462–471.
27 Solnica-Krezel L, Schier AF, Driever W. Efficient recovery of ENU-induced mutations from the zebrafish germline. *Genetics* 1994; **136**: 1401–1420.
28 Streisinger G, Walker C, Dower N, Knauber D, Singer F. Production of clones of homozygous diploid zebra fish (*Brachydanio rerio*). *Nature* 1981; **291**: 293–296.
29 Gestl EE, Kauffman EJ, Moore JL, Cheng KC. New conditions for generation of gynogenetic half-tetrad embryos in the zebrafish (*Danio rerio*). *J Hered* 1997; **88**: 76–79.
30 Bertrand JY, Kim AD, Violette EP, Stachura DL, Cisson JL, Traver D. Definitive hematopoiesis initiates through a committed erythromyeloid progenitor in the zebrafish embryo. *Development* 2007; **134**: 4147–4156.
31 Traver D, Paw BH, Poss KD, Penberthy WT, Lin S, Zon LI. Transplantation and *in vivo* imaging of multilineage engraftment in zebrafish bloodless mutants. *Nat Immunol* 2003; **4**: 1238–1246.
32 Langenau DM, Ferrando AA, Traver D, Kutok JL, Hezel JP, Kanki JP *et al*. *In vivo* tracking of T cell development, ablation, and engraftment in transgenic zebrafish. *Proc Natl Acad Sci USA* 2004; **101**: 7369–7374.
33 Haffter P, Granato M, Brand M, Mullins MC, Hammerschmidt M, Kane DA *et al*. The identification of genes with unique and essential functions in the development of the zebrafish, *Danio rerio*. *Development* 1996; **123**: 1–36.
34 Geisler R, Rauch GJ, Geiger-Rudolph S, Albrecht A, van Bebber F, Berger A *et al*. Large-scale mapping of mutations affecting zebrafish development. *BMC Genomics* 2007; **8**: 11.
35 Trede NS, Ota T, Kawasaki H, Paw BH, Katz T, Demarest B *et al*. Zebrafish mutants with disrupted early T-cell and thymus development identified in early pressure screen. *Dev Dyn* 2008; **237**: 2575–2584.
36 Lutzner M, Edelson R, Schein P, Green I, Kirkpatrick C, Ahmed A. Cutaneous T-cell lymphomas: the Sezary syndrome, mycosis fungoides, and related disorders. *Ann Intern Med* 1975; **83**: 534–552.
37 Hicks J, Mierau GW. The spectrum of pediatric tumors in infancy, childhood, and adolescence: a comprehensive review with emphasis on special techniques in diagnosis. *Ultrastruct Pathol* 2005; **29**: 175–202.
38 Borowitz MJ, Chan JKC. T-lymphoblastic leukaemia/lymphoma. In: Swerdlow SH, Campos E, Harris NL, Jaffe EF, Pileri SA, Stein H, Thiele J, Vardiman JW (eds). *WHO Classification of Tumours of Haematopoietic and Lymphoid Tissues*. IARC Press: Lyon, 2008, pp 176–178.
39 Fay D, Spencer A. Genetic mapping and manipulation: chapter 8—dominant mutations. In: Community TCER (ed). Wormbook: Wormbook; February 17, 2006.
40 Zhuravleva J, Paggetti J, Martin L, Hammann A, Solary E, Bastie JN *et al*. MOZ/TIF2-induced acute myeloid leukaemia in transgenic fish. *Br J Haematol* 2008; **143**: 378–382.
41 Sabaawy HE, Azuma M, Embree LJ, Tsai HJ, Starost MF, Hickstein DD. TEL-AML1 transgenic zebrafish model of precursor B cell acute lymphoblastic leukemia. *Proc Natl Acad Sci USA* 2006; **103**: 15166–15171.
42 Scott RH, Homfray T, Huxter NL, Mitton SG, Nash R, Potter MN *et al*. Familial T-cell non-Hodgkin lymphoma caused by biallelic MSH2 mutations. *J Med Genet* 2007; **44**: e83.
43 Langenau DM, Jette C, Berghmans S, Palomero T, Kanki JP, Kutok JL *et al*. Suppression of apoptosis by bcl-2 overexpression in lymphoid cells of transgenic zebrafish. *Blood* 2005; **105**: 3278–3285.
44 Bernt KM, Armstrong SA. Leukemia stem cells and human acute lymphoblastic leukemia. *Semin Hematol* 2009; **46**: 33–38.
45 Traver D, Winzeler A, Stern HM, Mayhall EA, Langenau DM, Kutok JL *et al*. Effects of lethal irradiation in zebrafish and rescue by hematopoietic cell transplantation. *Blood* 2004; **104**: 1298–1305.
46 Tropepe V, Coles BL, Chiasson BJ, Horsford DJ, Elia AJ, McInnes RR *et al*. Retinal stem cells in the adult mammalian eye. *Science* 2000; **287**: 2032–2036.
47 Langenau DM, Keefe MD, Storer NY, Jette CA, Smith AC, Ceol CJ *et al*. Co-injection strategies to modify radiation sensitivity and tumor initiation in transgenic Zebrafish. *Oncogene* 2008; **27**: 4242–4248.

Supplementary Information accompanies the paper on the Leukemia website (http://www.nature.com/leu)

Supplemental Materials Reprint

Supplemental tables

	Marrow						Peripheral Blood					
	All Individuals			Affected Individuals			All Individuals			Affected Individuals		
	n	Mean % GFP$^+$ cells	SD	n	Mean % GFP$^+$ cells	SD	n	Mean % GFP$^+$ cells	SD	n	Mean % GFP$^+$ cells	SD
WT	7	7.5	0.9	0	n/a	n/a	15	0.35	0.6	0	n/a	n/a
srk	6	69.4	18.1	6	69.4	18.1	6	12.5	20.0	4	18.8	22.6
hlk	7	32.1	31.8	4	50.3	31.6	12	4.1	7.8	4	10.8	11.4
otg	6	18.2	16.3	2	38.2	10.4	8	10.3	18.7	2	40.5	3.6

Supplemental Table 2.1. Malignant involvement of marrow and blood in *srk*, *hlk*, and *otg* mutant fish. Single cell suspensions from marrow and blood of WT and tumor-bearing mutant fish were analyzed by flow cytometry, with dead cell exclusion by 7-Amino-Actinomycin D (7-AAD). WT marrows demonstrated 7.5% of viable cells to be GFP$^+$ (SD = standard deviation). Defining abnormal as >3 SD above the WT mean, 6/6 *srk*, 4/7 *hlk*, and 2/6 *otg* fish with tumors showed marrow infiltration (Marrow Affected Individuals columns), with mean values of 69.4%, 50.3%, and 38.2% of total cells, respectively. Using these same criteria, 4/6 *srk*, 4/12 *hlk*, and 2/8 *otg* fish with thymic tumors demonstrated pathologic blood involvement (Peripheral Blood Affected Individuals columns), with mean values of 18.8%, 10.8%, and 40.5% of total cells being GFP$^+$. WT *lck::EGFP* fish have only rare GFP$^+$ cells in peripheral circulation (0.35 +/- 0.6%). These results are graphically displayed in the histograms of Figure 4a.

TCRβ1 Alignment				
Zebrafish line	Variable (last 10bp)	Diversity	Joining (first 10bp)	Times Isolated (%)
WIK *lck::EGFP* (n=28)	. . . ATCGTGGCAC	CCCTGTCCCCCG	CTGTCTGGAC . . .	5 (17.9)
	. . . ATCGTGGCAC	CCCTGTCCCCCG	TCTGTACCCT . . .	2 (7.1)
	. . . ATCGTGGCAC	CCCTGTCC	TTGTACCCTT . . .	1 (3.6)
	. . . ATCGTGGCAC	CCCTGTCCCCCG	ATTATTAGAC . . .	1 (3.6)
	. . . ACGTCGAATG	CCCTGTCCCCCG	CTAGTTCGGA . . .	1 (3.6)
	. . . CGACGATCTT	CTGTCCCCC	CAGAGTCAGG. . .	5 (17.9)
	. . . ACACGTCGAT	CCTGTCC	ATGGAGACCA . . .	2 (7.1)
	. . . GACACGTCGG	TGTCCC	ATGTGACCAC. . .	3 (10.7)
	. . . ACGGTGTTCG	TCC	TTGTGACGGT . . .	3 (10.7)
	. . . TAACACGTCG	GTC	AGGTTGGTGA . . .	1 (3.6)
	. . . ACGCATAATA	GTC	TTGTGACCGT . . .	3 (10.7)
	. . . AGACGCGAAG	CTGT	TTGTGACGGT. . .	1 (3.6)
hlk (n=15)	. . . GACACGTCGA	CCCTG	CTTGTGACCG . . .	9 (60.0)
	. . . AGTCACTCAC	GTC	TGTCTGGACG . . .	6 (40.0)
srk (n=11)	. . . ACACGTCGTG	C	ATTAGAGTCA . . .	9 (81.8)
	. . . CACGGTGTTC	GTCC	TTGTGACGGT . . .	1 (9.1)
	. . . AAACACGGCG	TGTCCCCCG	GTTAATAGTT . . .	1 (9.1)
otg (n=15)	. . . GCGTCGTAGA	TG	TGTTTGAGTT . . .	14 (93.3)
	. . . AGGGAGTTTT	T	ATATTAAGGG . . .	1 (6.7)

Supplemental Table 2.2 VDJ alignments of 5'RACE products. Sequences used to compile Figure 5 are shown. Last 10 bp of each V_{b1} gene and first 10 bp of each J_{b1} gene segment are aligned. Intermediary sequences, deriving from the D_{b1} gene segment and non-templated N-segment additions/deletions that accompany recombination are listed in the Diversity column. Frequency of isolation for each VDJ sequence is listed in the far right-hand column.

Supplemental materials and methods

RT-PCR primers:

Gene	Forward Primer	Reverse Primer
lck	5'-agatgaatggtgtgaccagtgta-3'	5'-gatcctgtagtgcttgatgatgt-3'
rag2	5'-accctctcgtttgatccgtctcc-3'	5'-attcatcctcctcatcttcctcgttat-3'
trac	5'-tctgctgtgtattactgtgctctga-3'	5'-gctcatccacgctttgaaagtcacca-3'
cd4	5'-tccctggtcggtcttaaatgaaac-3'	5'-cagatgaggcggagacttgtgat-3'
cd8a	5'-tccccaccattacaaaaggcaacc-3'	5'-tttagcgtagaaacataaaagtgaacagc-3'
mpx	5'-ccagaaccagtgagcctgagacacg-3'	5'-gtgggttcttccgattgttgcaga-3'
ef1a	5'-ccaacttcaacgctcaggtcat-3'	5'-agtagagtgcccaggtttagaga-3'

RT-PCR conditions:
55°C annealing temperatures were used for *lck* and *ef1a*; 58°C for *rag2*, *trac*, *cd4*, and *cd8a*; and 59°C for *mpx*. PCR reactions were 35 cycles for *rag2*, *trac*, and *ef1a*; 38 cycles for *lck*, *cd4*, *cd8a*, and *mpx*.

5' RACE primers (from *tcrb1* constant region exon 3):

outer primer: 5'-tccgctcttagcaatggtcacgccata-3'

nested primer: 5'-tgccagcttcatccactgtgacgacttc-3'

Supplemental figures

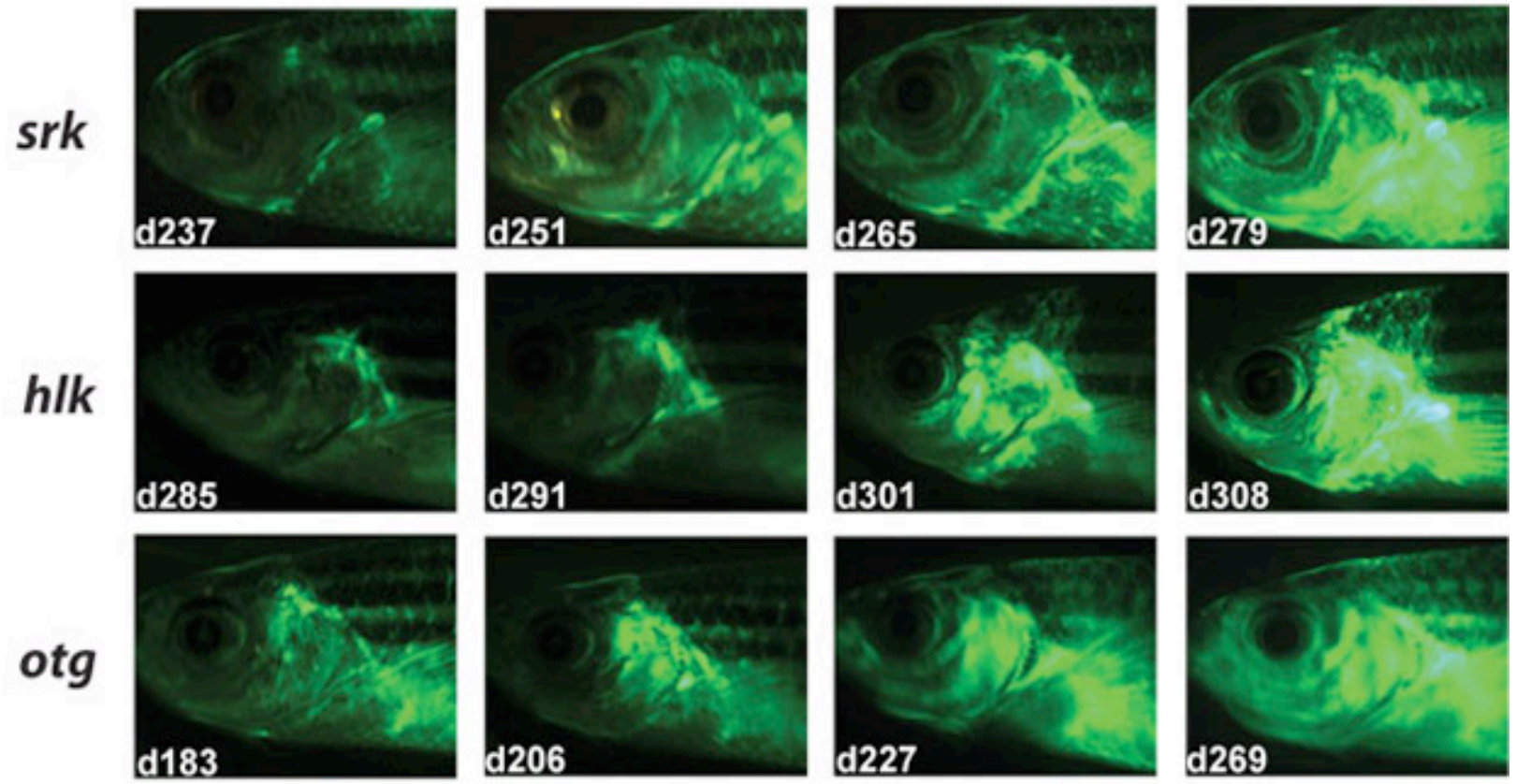

Supplemental Figure 2.1. Tumor progression in *srk*, *hlk*, and *otg* fish. Fish were serially assayed by fluorescence microscopy for thymic expression *lck::EGFP* and the development of GFP^+ tumors. Serial images of individual tumor-bearing fish from each mutant line are shown. Images were obtained at the listed age in days (d), displaying the rapid growth of tumors. Malignancies usually arise in thymus, invade gills and adjacent tissues, and spread caudally, infiltrating skin and internal organs.

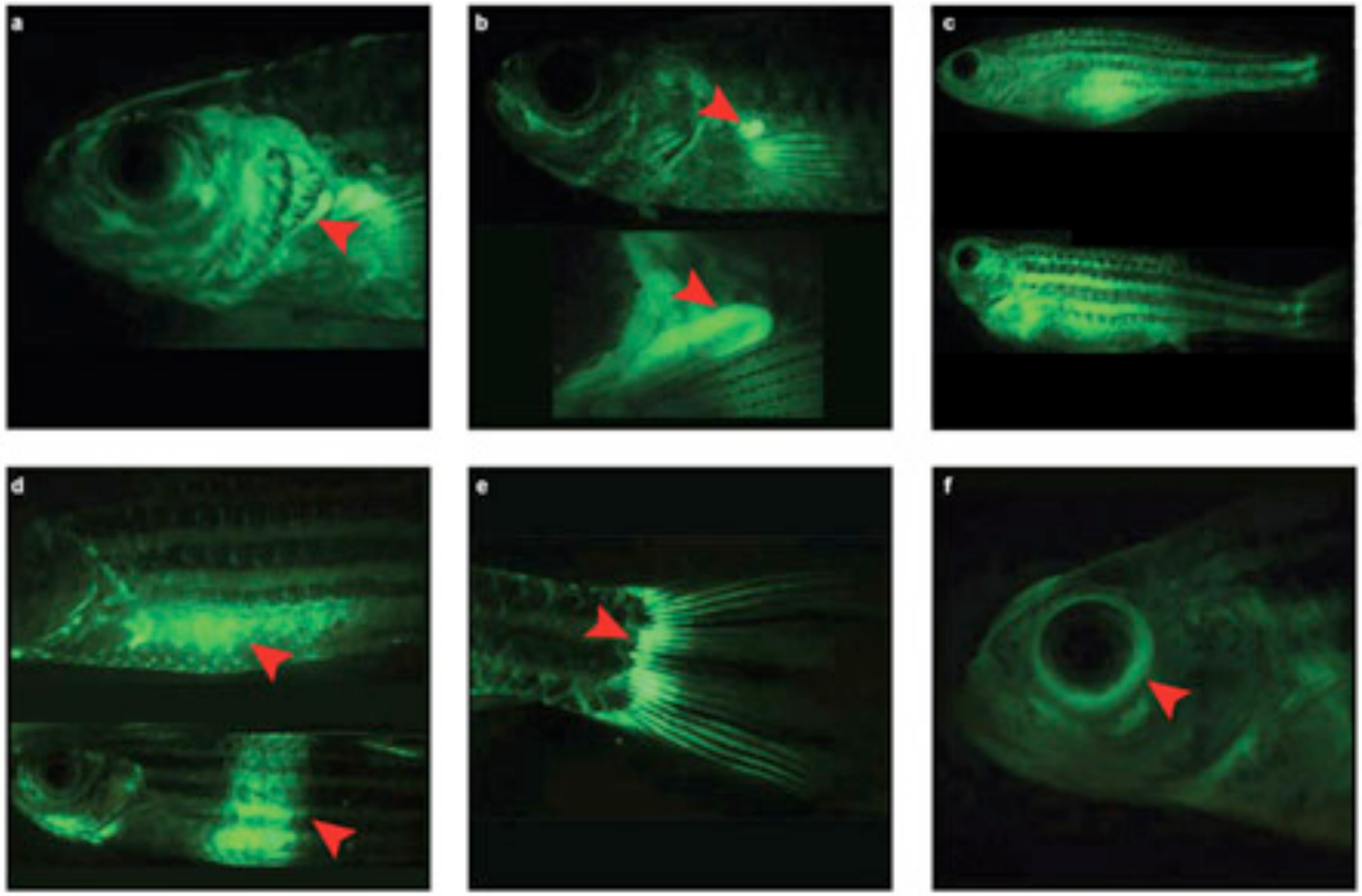

Supplemental Figure 2.2. Malignancies show diverse patterns of dissemination. Diseased *hlk* fish demonstrating common patterns of invasion. GFP^+ tumors typically have thymic origin (refer to Figure 1c and Supplemental Figure 1), and spread locally to gills (**a**) and other adjacent structures (**b**) (lower image in panel **b** shows higher magnification). Often, dissemination throughout the entire animal occurs (**c**). Skin is often heavily infiltrated (see histology in Figure 2), occasionally with discontinuous 'skip lesions' (lower fish in panel **d**). Tail (**e**) and peri-ocular tissues (**f**) are also sites of tumor tropism, the latter accompanied by proptosis.

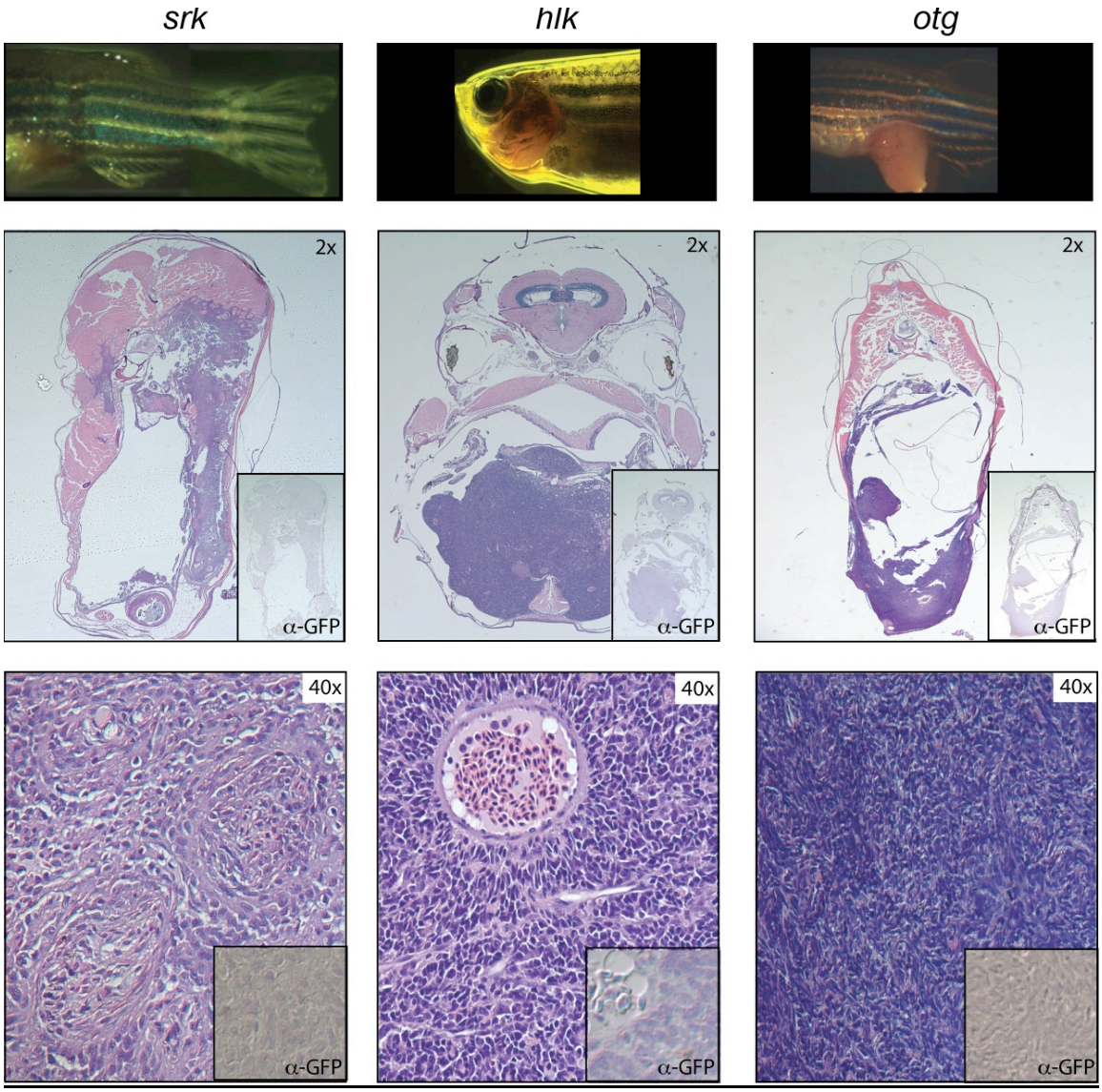

Supplemental Figure 2.3. *Srk*, *hlk*, and *otg* can also develop other malignancies. GFP^- tumors are occasionally seen in *srk*, *hlk*, and *otg* animals. At top, fish with neoplasms of the left flank (*srk*), gill (*hlk*), and peri-anal (*otg*) regions are shown; tumors were grossly GFP^- (not shown). H&E cross-sections at 2X (middle row) and 40X (bottom) display tumor involvement and non-lymphocytic morphologies. In addition to their morphologic appearance, tumors were not grossly GFP^+ (not shown) nor immuno-reactive with anti-GFP mAb (middle and bottom row inset images), suggesting they are not T cell malignancies. The *srk* tumor shows sarcoma-like histology. *Hlk*- and *otg*-derived tumors demonstrate neuroepithelial differentiation.

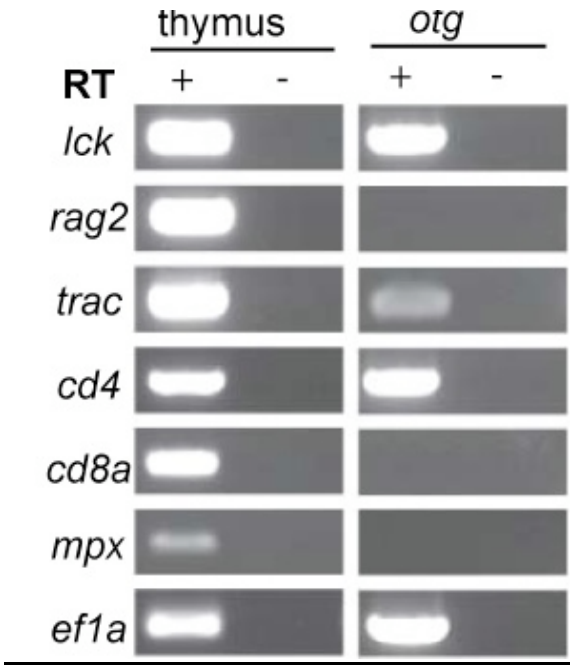

Supplemental Figure 2.4. Tumors occasionally show a mature T cell phenotype. Twice-sorted GFP$^+$ cells from a second *otg* fish were analyzed by RT-PCR (compare to Figure 3). While *lck*, *tcra*, and *cd4* again confirm T cell identity, here *rag2* and *cd8a* are not present. This expression pattern is most consistent with tumor cells having mature T cell differentiation. Other lanes and controls are as in Figure 3.

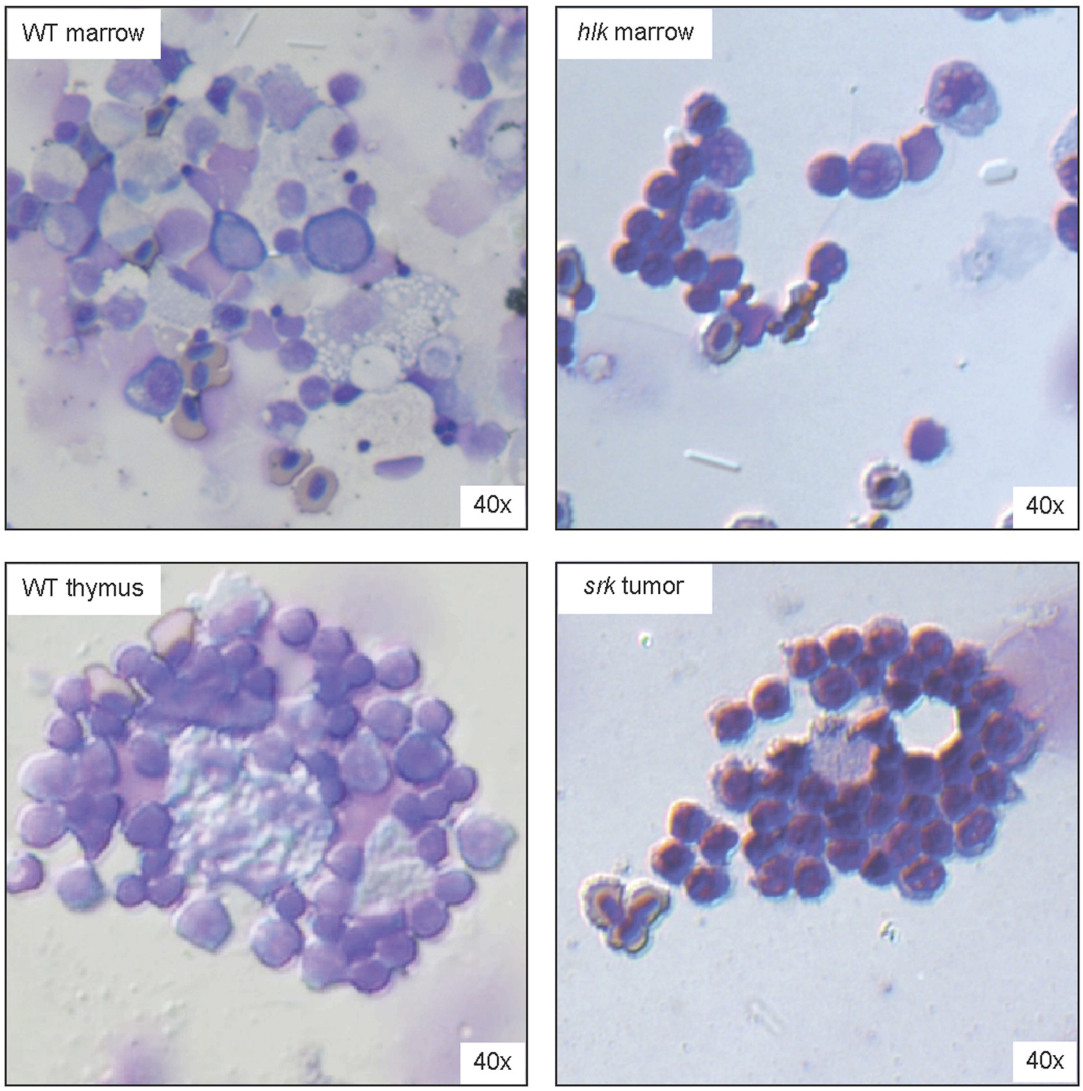

Supplemental Figure 2.5. Malignant cells have lymphoblastic morphologies. Wright-stained cytospin preparations of WT marrow (upper left) and marrow from a diseased *hlk* fish (upper right). Dark blue infiltrating lymphoblasts are seen, having similar morphologies to those shown in Figure 4b. Unsorted cells from homogenized *srk* thymic tumor (bottom right) have identical appearance. Unsorted cell suspension from WT thymus (bottom left) is shown for comparison. [Images graphically enhanced to improve brightness.]

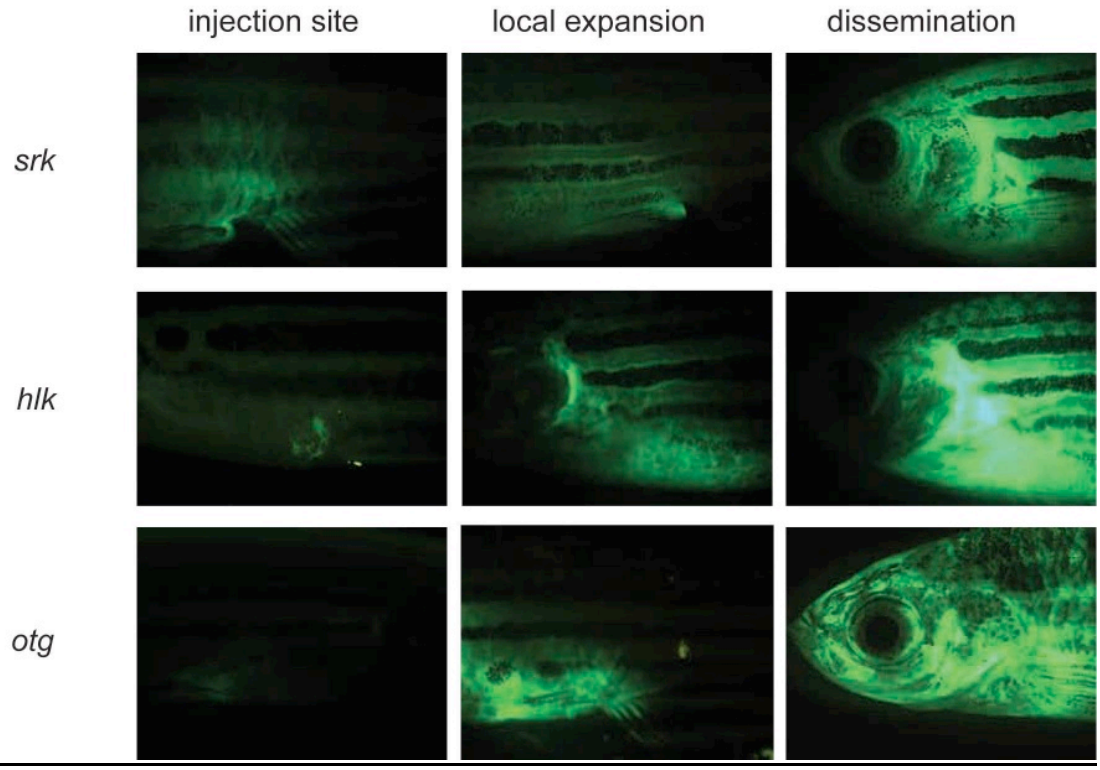

Supplemental Figure 6. Malignancies are transplantable. FAC-sorted, GFP^+ cells from *srk, hlk,* and *otg* tumors were IP-injected into irradiated WT hosts. Cell doses ranged from 2.5×10^3 to 1×10^6 GFP^+ cells, with higher doses showing higher rates of engraftment. By one week, GFP^+ cells were seen at injection sites. Subsequently, tumors spread locally and then widely disseminated, ultimately causing host death.

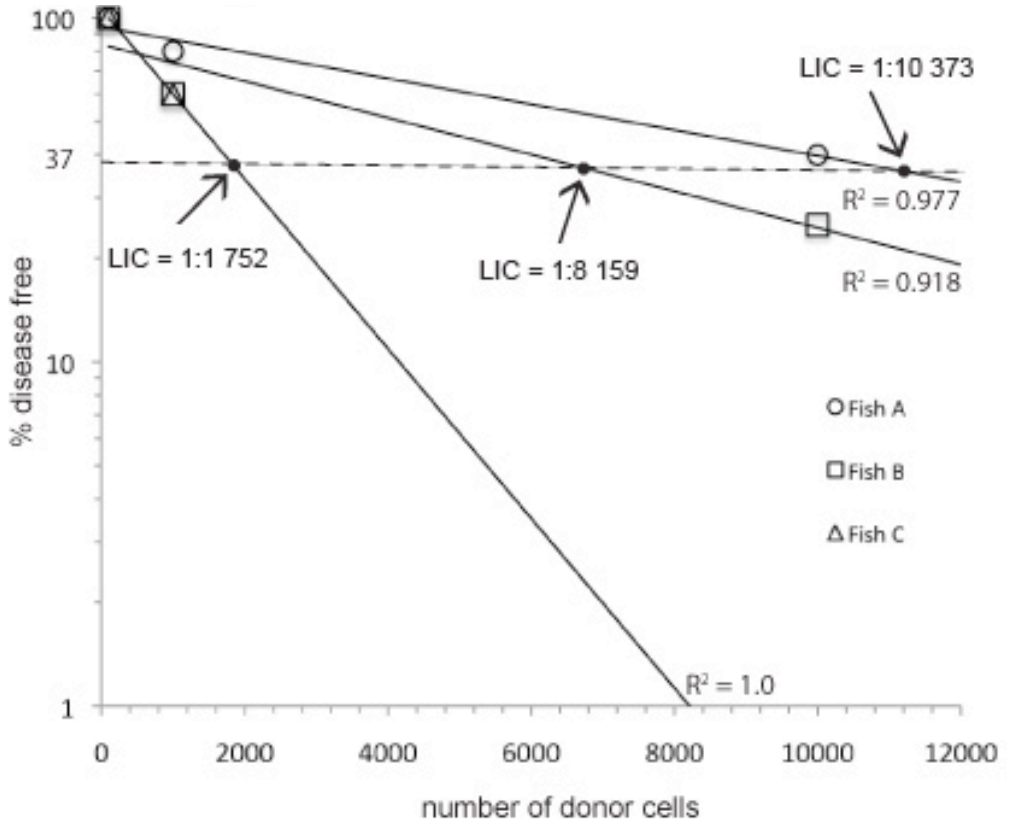

Supplemental Figure 7. Determination of leukemia-initiating cell number. The percentage of animals remaining disease-free from each transplant group (y-axis; note log scale) is plotted against injected donor cell number (x-axis). Each data point represents results from 5 recipients. Regression analysis was then used to generate straight lines fitting the dataset for each donor (fish A, circles; fish B, squares, fish C, triangles; R^2-value = 0.977, 0.918, and 1.0, respectively). Leukemia-initiating cell frequency (LIC) is determined as the number of injected cells corresponding to 37% disease-free, as previously described (Tropepe, 2000; reference #44).

CHAPTER 3

MODELING HUMAN HEMATOLOGIC MALIGNANCIES IN ZEBRAFISH: A REVIEW

Reprinted with permission from: Rudner LA, Frazer JK and NS Trede (2009). Modeling human hematologic malignancies in zebrafish: A review. *Current Trends in Immunology*. 9:119-134

Current Trends in Immunology
Vol. 10, 2009

Review

Modeling human hematologic malignancies in zebrafish: A review

Lynnie A. Rudner[*,4], J. Kimble Frazer and Nikolaus S. Trede[*,5]
Departments of Oncological Sciences and Pediatrics, Huntsman Cancer Institute, 2000 Circle of Hope, University of Utah, Salt Lake City, Utah, 84112, USA

ABSTRACT

Historically, zebrafish (*Danio rerio*) have been a powerful model organism to interrogate vertebrate development via systematic mutational and forward genetic approaches. Zebrafish have also become popular recently as an experimental system for studying human pathology, including many cancers. In the past few years, several transgenic zebrafish models have been engineered that develop hematologic malignancies, corresponding to both lymphoid and myeloid neoplasias. These transgenic lines have utilized previously known mammalian proto-oncogenes or human translocation-derived fusion proteins to initiate malignant transformation. In aggregate, these models show striking similarities to human cancers. As such, they represent useful tools for dissecting the molecular details of the pathogenic mechanisms operative in these specific diseases. Zebrafish are also amenable to large-scale phenotypic mutagenesis screens, and thus are potentially useful for detecting unknown oncogenic mutations as well. We have recently employed this experimental strategy to isolate several mutants with heritable predisposition to T cell lymphocytic cancers. Here, we review zebrafish models of human hematologic malignancy generated to date, how these systems have been exploited in the past, and the future avenues they offer to improve our understanding of leukemo- and lymphomagenesis.

*Corresponding authors
[4]lynn.rudner@hsc.utah.edu
[5]nikolaus.trede@hci.utah.edu

KEYWORDS: acute leukemia, zebrafish model, genetic screen

INTRODUCTION

Acute leukemias and their molecular pathogenesis

Acute leukemias are a heterogeneous group of malignancies of hematopoietic progenitors with differing molecular abnormalities, clinical characteristics, and variable outcomes with current treatments. Most human cases are sporadic, but rare genetic disorders or exposures to alkylating chemotherapy and ionizing radiation can also underlie these diseases [1]. While acute myeloid leukemia (AML) incidence rises linearly after age 40, acute lymphoblastic leukemias (ALL) peak between the ages of 2 and 4, decline during late childhood, adolescence and young adulthood, and have a second incidence peak in the elderly [2]. This clinical heterogeneity is complicated by an even larger network of complex molecular abnormalities including chromosomal translocations, other somatically-acquired genetic lesions, and aberrant transcription factor expression patterns–each being large classes of mutations in themselves. Although significant strides have been made in our understanding of the genetic underpinnings of leukemias and their treatment, future progress will likely need to be directed at specific molecular targets to permit the rational development of new therapies.

Acute myeloid leukemia (AML) comprises a group of neoplasms arising in precursors of the myeloid, monocytic, erythroid, or megakaryocytic

lineages. AML results from a constellation of distinct, but cooperating, genetic mutations. AML is often associated with 'fusion genes' resulting from specific chromosomal translocations. These lesions are frequently characteristic to a particular AML subtype, and confer additional prognostic and therapeutic implications. Acute lymphoblastic leukemias (ALL) likewise constitute a family of genetically-heterogeneous diseases derived from B-, T-, and NK cell-lymphocyte progenitors. B-ALL includes several cytogenetic subgroups with distinct clinical features important to patient risk stratification [3]. These subgroups account for roughly 70% of pediatric and adult cases [4]. Because it is the most common of these entities, insights into the molecular alterations that underlie acute lymphocytic leukemic transformation have primarily come from studies in B-ALL. By contrast, most T-ALL cases lack the common, near-pathognomonic translocations described for many B-ALLs. Rather, dysregulation of divergent gene classes, including transcription factors, signaling molecules, cell cycle regulators, but also structural proteins and RNA processing proteins [5] can result in T-ALL. Two primary mechanisms of leukemogenesis—and cellular transformation in general—are accentuated proto-oncogene or diminished tumor suppressor gene functioning. Oncogene over-expression can be caused by chromosomal rearrangements resulting in transcription of normally-quiescent genes in normal lymphocytes [6]. Increased oncogene function can also occur by activating point mutations, inappropriate activation of aberrant signaling pathways, or other mechanisms. Mutations in tumor suppressors also occur in leukemias [7]. In such cases the mutation can operate as a recessive trait or as a dominant negative allele.

Whether enhanced oncogene activity, lost tumor suppressor function, or both mechanisms are at play, derangements to normal cellular growth and differentiation are known to occur in leukemic cells. A theory summarizing these observations is the "two-hit model" of leukemogenesis. In this model, at least two types of mutations are thought to be required: one causing a proliferative and/or survival advantage to malignant cells (Class I) and one conferring a developmental arrest (Class II) [7-9]. One Class I-type mutation in acute leukemia was recently shown in studies identifying aberrant NOTCH1 activation in over 50% in human T-ALL patient samples and cell lines [10, 11]. Constitutive NOTCH1 signaling gives T cell precursors with these mutations a proliferative advantage over non-malignant cells. Because this type of advantage is not unique to a specific arrest point, it is logical that activating NOTCH1 lesions are seen across various T-ALL subtypes. Other pervasive proliferation- and survival-promoting mutations in ALL include deletions of *CDKN2A/CDKN2B*, *PTEN*, and related pro-apoptosis genes [12-14].

Mutations in Class I genes occur promiscuously in many different types of ALL, but acute leukemia results only when lymphoid precursors acquire both Class I and Class II genetic abnormalities. Class II type mutations, causing differentiation arrest, frequently involve the inappropriate activity of lymphoid-specific cellular developmental regulators, and there is convincing evidence that acute leukemias have altered expression of lineage-defining transcription factors [15-17]. The mis-expression of these regulators is thought to be responsible for leukemic cells' differentiation arrest and provide evidence of Class II-type mutations.

Heritable leukemias – lessons from rare pedigrees

While considerable evidence insinuates that inherited genetic traits play a role in the risk for developing leukemia [18-20], few genes conferring this heritable risk are known. Most of these genetic mutations cause defective DNA repair syndromes, and secondarily result in bone marrow failure and cancer predisposition. Absent these syndromes, familial leukemias are exceptionally rare, with few pedigrees convincingly transmitting leukemia predilection as a Mendelian trait [21]. However, this phenomenon may be under-appreciated. As early as 1968, it was recognized that relatives of patients with leukemia and lymphoma had higher incidence of these diseases [22]. More recent studies of familial chronic lymphocytic leukemia [23] and myelodysplasia [24] have revealed inherited genetic lesions within families, such as those identified in *RUNX1* [25] and *CEBPA* [26]. While we are only beginning to understand the molecular aberrations of familial leukemias, the examples set by other rare familial cancer syndromes, such as *RB* mutations in

retinoblastoma [27] or *ALK1* mutations in neuroblastoma [28-30] establish that rare pedigrees can result in discoveries that are broadly applicable to sporadic cases of the same disease.

Using zebrafish for leukemia research

Studies with invertebrates like *Drosophila* and *C. elegans* have informed our understanding of genetic pathways in cancer, like those regulating tissue specification, cell migration, and apoptosis. However, while many of these molecular pathways are preserved in invertebrates, the clinical entity we recognize as cancer seems largely restricted to vertebrates. Accordingly, murine systems represent the predominant model organism used to study carcinogenesis.

Zebrafish (*Danio rerio*) have a long history in investigations studying vertebrate development. Unlike most vertebrates (but similar to invertebrate models), zebrafish also have properties making them ideal for systematic mutational approaches. They have short generation times, are affordably housed at high density in limited space, and require little maintenance. One breeding pair can spawn over 200 progeny at weekly intervals, facilitating large pedigree analyses.

Zebrafish are also a powerful model to study cancers of the hematopoietic and immune systems. Although more than 450 million years of evolution separate the common ancestry of zebrafish and humans, the *D. rerio* immune system is remarkably similar to that of humans [31]. Evolution of an adaptive immune system coincided with the emergence of jawed vertebrates, far preceding the divergence of fish from other vertebrates [32, 33]. Hence, the adaptive and innate branches of the immune system are remarkably conserved between jawed fishes (teleosts) and other vertebrates, including mammals. In addition, cancer pathogenesis also appears to be similar between fish and mammals. Neoplasia occurs in fish in the wild, and exposure to carcinogens can cause a variety of benign and malignant tumors in virtually all organs of teleosts with histologies that closely resemble human tumors [29, 34-37]. Moreover, several mammalian oncogenes have been shown to induce zebrafish cancers closely mimicking their human counterparts [38-40].

As the pathways governing both immune system and cancer development are so highly conserved, the zebrafish is poised as a premier model for the study of human malignancy with the added benefit of many invertebrates' experimental advantages. Chief among these is the ability to perform phenotype-based, 'forward genetic' screens. Forward genetic screens can reveal new genes responsible for malignant transformation. Due to their small size and optical transparency as embryos, zebrafish also allow for simple and high-throughput detection of desired phenotypes. Once cancer-promoting mutations are found, zebrafish also provide an ideal system to perform further mutagenesis-based modifier screens to directly address the role of integrated pathways in cancer development [41]. This review will focus on recently reported zebrafish models of human leukemias, and their utility as a platform to explore mechanistic and genetic aspects of these important malignancies.

ZEBRAFISH ACUTE LEUKEMIA MODELS

Acute myelogenous leukemia (AML)

Three zebrafish models of AML have been described in recent years. These efforts were guided by a common human AML translocation that creates a fusion protein. As the most frequent chromosomal translocation in AML, the (8:21) (q22:q22) rearrangement occurs in 12-15% of patients. This fusion joins the *AML1* (also known as *CBFa2*, *RUNX1*, and *PEBPaB*) and *ETO* (also known as *MTG8*) genes [42, 43]. The chimeric protein disrupts the normal activity of RUNX1, a member of the Runt family of transcriptional regulators that are involved in many developmental processes, particularly blood development in mammals [44]. The first report of a zebrafish AML model utilized transient mosaic expression of human RUNX1-CBF2T1 during zebrafish embryogenesis [45]. Within 2 days, abnormalities were apparent in 32-41% of injected embryos. These included absent circulation accompanied by blood pooling in the aorta and ventral tail, and internal hemorrhages in the nervous system and pericardium. Examination of blood cells in the ventral tail revealed immature hematopoietic precursors and dysplastic erythroid cells. These observations were consistent with a dominant inhibition of endogenous *runx1* by the

RUNX1-CBF2T1 fusion protein, and similar to defects observed in *RUNX1-CBF2T1* knock-in mice [46]. However, general over-expression of the transgene caused embryonic lethality, precluding a more detailed analysis or the development of overt leukemia.

A similar model used an inducible human AML1-ETO fusion protein [47]. This stable line places human *AML1-ETO* under the control the zebrafish *hsp70* promoter. Transgenic *hsp70::AML1-ETO* embryos, induced by heat-shock during day 1 of life, showed no circulating blood shortly thereafter, despite beating hearts. Their cardiovascular systems were otherwise normal and, unlike the ubiquitously expressing *AML1-ETO* model [45], had a patent vasculature. The blood of inducible *AML1-ETO* embryos was dramatically enriched for immature blast-like cells that accumulated in the tail vessels and impaired circulation. While this model exhibits cytological and transcriptional hallmarks of human AML, suggesting that AML1-ETO signaling pathways are likely conserved across species, their early lethality, loss-of-circulation phenotype, and inherent hematopoietic defects make it best suited for use in repressor drug screens that restore normal differentiation and embryonic development [48].

A final zebrafish AML model was recently reported where Zhuraleva *et al.* expressed the human MYST3/NCOA2 fusion protein, a rare translocation seen in human AML, using an early myeloid gene promoter, *spi1* (PU.1) [49]. While 72% (180/250) of fish injected with the construct expressed the transgene, only 1% (2/180) of those animals developed features of AML, with a prolonged disease-free latency period (14 and 26 months). Concluding sentence: Thus, while zebrafish AML models show some promise, no convincing *D. rerio* versions of this disease have yet been described. This is in contrast to ALL, where several zebrafish models now exist.

Acute lymphoblastic leukemia (ALL)

The first zebrafish ALL model used transgenic murine *MYC* to induce disease [39]. Because a GFP reporter construct was also present, the authors could determine with *in vivo* fluorescence microscopy that essentially all fish with lymphoid expression of *MYC* developed T-ALL, with a mean latency of about 50 days. When this same construct was incorporated in the germ-line, again all fish acquired T-ALL, now with a mean latency of 32 days [50]. The near-100% penetrance and short latency both support that murine *myc* is a potent oncogene in this system. and that because of its powerful oncogenic drive only few acquired mutations are required. However, the line could not be maintained, as fish carrying the transgene typically die of disease prior to reaching sexual maturity. Another potentially salient point is that the *MYC*-driven *D. rerio* model best represents only one human T-ALL type, the *TAL1*$^{+}$ late cortical thymocyte subgroup [16, 17, 51].

A modified strategy, where *Cre* was used to conditionally activate murine *Myc*, circumvents the difficulty in propagating the transgenic line. However, when *Cre* RNA was injected into one-cell embryos of stably-transgenic *Myc* fish (to remove 'floxed' transcription stop sites preceding *Myc*), T-ALL penetrance dropped to 6%, suggesting inefficient microinjection, *Cre*-mediated excision, or both [50]. Compound transgenic fish with heat-shock inducible-*Cre* and floxed-Stop-*Myc* were a further refinement, where T-ALL rates of up to 81% could be achieved [52]. Again, this very high incidence attests to the oncogenic potency of murine *Myc* in *D. rerio*, and poises this system for use in suppressor screens as well. Clearly, this series of studies set an important precedent, establishing that mammalian genes could be similarly oncogenic in zebrafish lymphoid cancers.

A second transgenic zebrafish T-ALL model expressed a truncated and constitutively-active form of human NOTCH1 protein, targeted to lymphocytes through the use of the zebrafish *rag2* promoter [40]. Fish from this line display 40% penetrance, but have relatively long latency (disease begins at 11 months). Leukemias in this model are oligoclonal, and express a range of Notch1 target genes such as *her6* (the zebrafish orthologue of HES1) and *her9*. Although the mMyc models show an overexpression of the known T-ALL oncogenes *tal1/scl* and *lmo2*, the human NOTCH1-induced T cell leukemias lack appreciable expression levels of these oncogenes

implying that the pathogenic mechanism of disease in these two models is distinct.

A final example of *D. rerio* ALL models used the oncogenic human *TEL-AML1* fusion gene. These lines utilized either the ubiquitous *Xenopus* elongation factor 1a (XEF) or zebrafish *b-actin* (ZBA) promoters, or a lymphoid-specific zebrafish *rag2* promoter [38]. The expression of human *TEL-AML1* from the ubiquitous XEF and ZBA promoters led to low penetrance (3%) of B cell acute lymphoblastic leukemias, with a latency of 8-12 months. No fish expressing *rag2*-driven *TEL-AML1* developed leukemia during the 36-month observation period, leading the authors to conclude that *TEL-AML1* typically acts in a B lymphocyte precursor stage prior to *RAG* expression, at least in the human version of this disease. While this model mimics childhood $CD10^+$ pre-B ALL, its long latency and low penetrance make it well suited for enhancer screens.

New models of zebrafish T-ALL

The previously cited models can contribute to our understanding of the molecular mechanisms underlying leukemogenesis. However, because they rely on over-expression of known oncogenes, their scope is restricted to the known cancer pathways used to create them. To expand the range of zebrafish leukemia models, and probe the possibility of unknown genes that could be oncogenic in nature, we have taken an unbiased approach, generating the first zebrafish T-ALL models from a forward genetic screen [36].

To facilitate detection of T-ALL, we used transgenic zebrafish, where the native $p56^{lck}$ promoter directs T cell-specific expression of enhanced green fluorescent protein (*lck::EGFP*) [53]. Homozygous *lck::EGFP* males were mutagenized with *N*-ethyl-*N*-nitrosourea (ENU) and bred to WT *lck::EGFP* females, creating over 500 F1 progeny, each with multiple *de novo* heterozygous mutations [54, 55] (Figure 1a). Fish were screened by fluorescence microscopy for thymic tumors or extra-thymic EGFP-expressing cellular accumulations until 6 months of age. All F1 animals with abnormal phenotypes were out-bred to verify heritability of the trait. A total of 10 F1 mutants were found to have inherited abnormalities of EGFP expression and nine were studied further. Two dominant lines, *hulk* (*hlk*) and *shrek* (*srk*), showed particularly high penetrance and were analyzed in greater detail.

To detect recessive mutations, eggs from normal-appearing F1 females were subjected to induced parthenogenesis by early pressure (EP), a technique producing gynogenetic diploid progeny [56]. EP offspring are homozygous at maternal haplotypes in genomic locations where meiotic crossovers did not occur. Thus, at these loci, recessive traits can exhibit mutant phenotypes in the F2 generation, obviating the need for large F3 screens. We performed EP on over 100 F1 females, creating F2 families that were also screened until 6 months. One additional mutant, *oscar the grouch* (*otg*), was detected in an EP-derived family where several siblings demonstrated abnormal GFP patterns (see example in Figure 1b).

Because atypical GFP patterns could represent T cell malignancy, benign lymphoproliferation, T cell accumulations caused by infection, autoimmune T cell infiltrations, or non-T cell GFP expression, we assessed a number of visual and molecular hallmarks of malignancy. We assessed the cellular composition of the blood, kidney marrow, and tumor tissue of these fish, and determined that these organs (and others, in some cases) were infiltrated by small-round-blue cells characteristic of lymphoblasts (Figure 1c). Additionally, clonality of GFP^+ cells, a hallmark of lymphoid neoplasia. Was assessed using 5' rapid amplification of cDNA ends (5' RACE) to test whether *tcrb1* transcripts from tumor cells from each of the *hlk*, *srk*, and *otg* lines were clonal. Highly skewed, non-random VDJ usage of a one or two dominant *tcrb1* clones was seen in each case. These results are consistent with a clonal T-cell population, as occurs in human T cell malignancies.

The three mutant lines described each have a propensity to develop GFP^+ thymic lymphomas and leukemias (T-ALL) as juvenile-to-young adult fish (3-8 months). As affected fish are fertile, these lines are simply propagated by natural breeding methods. The dominantly inherited lines, *srk* and *hlk*, have high homozygous penetrance rates (43 and 40%, compared to 14 and 6%, respectively, in heterozygotes), facilitating the accrual of large numbers of diseased animals. However, because

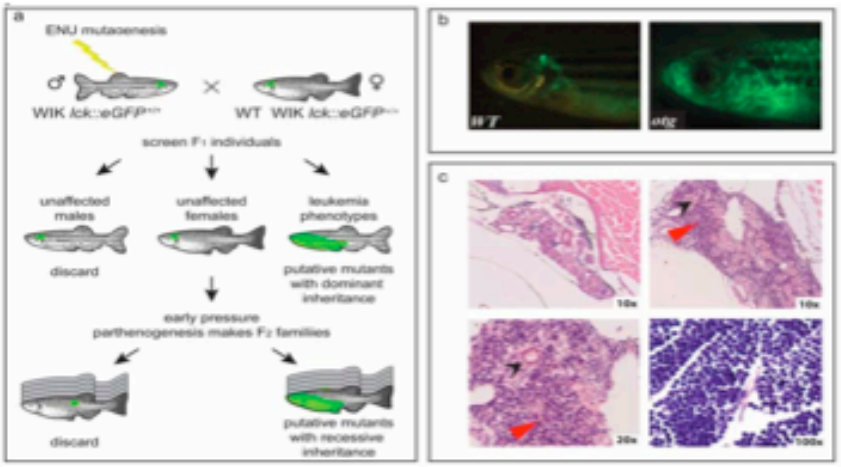

Figure 1. Heritable T-cell cancer phenotypes from an ENU mutagenesis screen. (a) Male homozygous lck::EGFP zebrafish were treated with ENU and bred to wild-type female lck::EGFP fish. Heterozygous germline mutants were identified from offspring by microscopic screening microscopically until 6 months. Eggs from normal-appearing F1 females were subjected to early pressure parthenogenesis, creating F2 families. (b) One family with several abnormal siblings was deemed putatively recessive, dubbed oscar the grouch (*otg*). (c) Histological analysis of zebrafish kidneys infiltrated by lymphoblasts from a wildtype fish, and a diseased fish at 10x, 20x (same fish). The black arrowhead represents a kidney tubule; the red arrowhead represents a lymphoblast. A 100x view of lymphoblasts invading kidney marrow, from a second diseased fish.

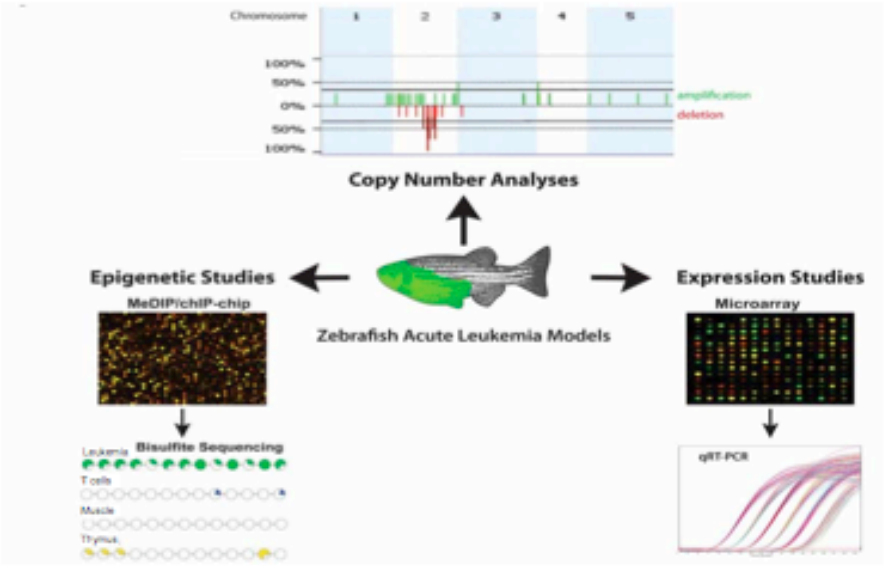

Figure 2

not all homozygotes develop T-ALL, this implies that other genetic changes are required. The recessive *otg* mutant has 50% homozygous T-ALL penetrance. Thus, *otg* fish also depend upon somatically acquired secondary events for malignant transformation, similar to natural events occurring in human T-ALL. In all three lines, then, natural disease progression is mimicked as secondary mutations contribute to oncogenesis by cooperating with the underlying inherited *srk*, *hlk*, or *otg* genetic lesions.

In addition to their timing and location of disease onset, the clinical behavior of these cancers is similar to that of human T-ALL. Fish develop thymic tumors, emulating mediastinal masses seen in both experimental mammalian models and human patients. On a morphological level, these zebrafish cancers resemble human lymphoblasts as well (Figure 1c). Tumors often disseminate, homing to marrow (Figure 1c) and blood as in human T cell neoplasia. Gene expression studies confirmed that malignancies have T lineage origin, as GFP^+ cells express both *lck* and *trac (TCRa)*, markers unique to T cells. Additionally, many tumors examined expressed *cd4*, *cd8a* and *rag2* messages, further substantiating their assignment as T-ALL. These types of studies can be taken further, as well, to globally investigate these cancers (Figure 2) and will be discussed in detail in the next section.

To examine the malignant nature of these diseases, we performed allogeneic transplants of EGFP-sorted cells, testing for serial engraftment, a hallmark of leukemia-initiating cells (LICs) [57]. Leukemic cells showed rapid engraftment and dissemination into irradiated recipients, ultimately causing their demise. We also determined that malignancies could be serially passaged *in vivo*, and observed that iterative transplantation resulted in decreased time to disease engraftment and duration of host survival with each round (Figure 3). This increasingly malignant behavior may occur by the *in vivo* selection of new mutations and/or altered gene expression patterns that enhance tumor lethality. Alternatively, sequential transplants may select for tumors with progressively higher LIC fractions, thereby effecting accelerated engraftment and tumor growth.

This study represents the first use of a zebrafish forward phenotypic screen to identify genetic models of T-ALL. While the genetic mutations conveying these leukemic predispositions are still being determined, this study proves the feasibility of forward genetic screens with adult vertebrates to discover phenotypes pertinent to human health. Apart from the discovery of the *hlk*, *srk*, and *otg* mutations themselves, these models provide tools to reveal other oncogenic events in T cell malignancy. In terms of their utility in other screening approaches, mutants with low penetrance and long latencies (*srk* and *hlk* heterozygotes) are well suited for enhancer screens seeking more prevalent and/or earlier disease onset. Conversely, highly-penetrant mutants with early incidence (*srk* and *otg* homozygotes) are optimal for suppressor approaches. Moreover, because all three mutants depend upon other somatically acquired genetic events for full phenotypic penetrance, these models are useful for the identification of other oncogenes and tumor suppressors that can collaborate with *hlk*, *srk*, and *otg* to mediate leukemogenesis.

CASTING THE NET FOR OTHER ONCOGENIC ZEBRAFISH MUTATIONS

Cancer is a multi-step process that requires a constellation of abnormalities to bring about outright malignant transformation. These abnormalities come in many forms: genetic point mutations, genomic amplifications and deletions, epigenetic gene silencing, inappropriate transcriptional activation, and other deviances from normal cellular biology. Because the *hlk*, *srk*, and *otg* mutants all carry inherited predisposition for T-ALL, but not all fish acquire cancer, we suspected that other events were contributing to disease. This raises the possibility of using these lines for the discovery of additional contributory

Legend to Figure 2. Emerging technologies can be used in conjunction with zebrafish acute leukemia models. Primary cancers and transplanted malignancies can be used to determine copy number, transcriptional, and epigenetic profiles of malignant cells. Cancer copy number variations, methylomes and transcriptomes can be compared against wild type signatures.

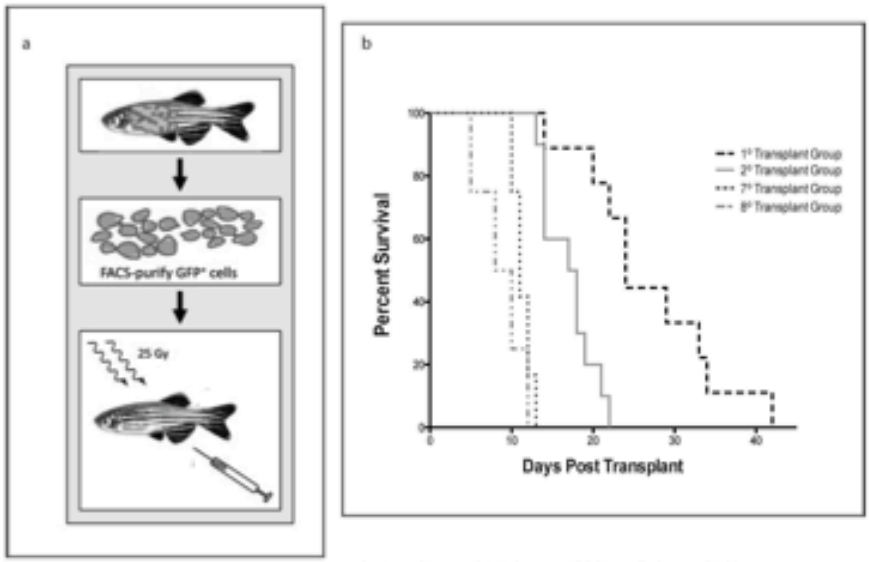

Figure 3. Serially transplanted cancers are increasingly malignant. (a) Schema of GFP+ cells from a *hlk* tumor were sequentially transplanted into pre-irradiated WT hosts where $1x10^5$ cells were used in each round. (b) Only engrafted fish are plotted. One engrafted fish from each cohort (not included above) was used as a donor in the subsequent transplant round. Recipients had shortened survival between early and late rounds, with statistical significance $p=<0.001$.

lesions. Among the types of study that can exploit the advantages of these models are the search for genetic modifiers using enhancer or suppressor screens and the application of emerging technologies such as array comparative genomic hybridization (aCGH), transcriptional profiling, and epigenetic analysis, to reveal associated acquired mutations. Furthermore, zebrafish ALL models should be able to contribute to pre-clinical testing of novel targeted therapies.

Genetic modifier screens

Traditionally, zebrafish phenotypic screens have been used to identify developmental phenotypes, and are often performed in early embryos. However, almost all of the zebrafish leukemia models discussed above have onset beyond the first week or two of life, making their application to screens more challenging (Table 1). Nonetheless, despite their incidence peaks in juvenile to young adult fish, these models can provide platforms for genetic modifier screens. As mentioned previously, mutants with lower penetrance and longer latency (*srk* and *hlk* heterozygotes) are well suited for screens seeking collaborative mutations that enhance disease penetrance and/or shorten latency. Conceptually, one would predict that such mutations would negate tumor suppressors or activate proto-oncogenes. Conversely, highly penetrant mutants with early incidence (murine *Myc* transgenics; *srk*, and *otg* homozygotes) are optimal for suppressor screens aimed at identifying mutations that delay or prevent disease onset. Here, activation of a tumor suppressor or, more likely, inactivation of a cooperating proto-oncogene are the probable molecular targets that cause the altered phenotype. Undoubtedly, the identification of modifier genes may reveal clinically relevant mutations with prognostic and therapeutic implications.

Emerging technologies

The study of acute leukemias goes beyond approaches interrogating specific candidate

Table 1. Zebrafish models of acute leukemias.

	Model	Human Disease	ZF phenotype	Penetrance	Latency	Literature
AML						
	pCS2mv-RUNX1-CBF2T1	(8;21)(q22;q22) present in 15% of AML patients (AML-ETO)	Lack circulation; blast cell pooling; hemorrhages in nervous and cardiac systems	32-41% of injected embryos	2 days, though expression is transient and mosaic; fish die before sexual maturity	Kalev-Zalinska, *et al* 2002
	zhgs7f:AML-ETO stable transgenic	(8;21)(q22;q22) present in 15% of AML patients (AML-ETO)	Lack circulation in the presence of lumenized cardiovascular system; blood enriched with lymphoblasts	100% when heat-shock induced at 18-19.5hpf	Inducible between 14-19.5hpf; all with early death before advanced disease development	Yeh, *et al* 2008
	zspi-MYST3/NCOA2-EGFP	Inv(8)(p11q13) MYST3/NCOA2 fusion representing 8% if AML stage 4/5	Myeloid blast cells invade kidney and spleen; 1 of 2 fish showed an abdominal tumor	72% of injected embryos expressed transgene, but only 1% of expressors got disease	14-26 months	Zhuravleva, *et al* 2008
ALL						
T-ALL	*zRag2*-EGFP-mMYC	TAL+ late cortical thymic subgroup	Gross tumors of the abdomen, pectoral fin; lymphoblasts completely efface kidney marrow; invasion of gut, gills, and muscle with blasts	100% if present in germline	Mean of 50dpf and 32dpf with subsequent death before sexual maturity	Langenau, *et al* 2003, 2005
	Rag2-promoter regulated lox-dsRED2-lox-EGFP-mMyc	TAL+ late cortical thymic subgroup	Same as above	Cre injection required at the 1-cell stage, rates of disease can reach 81%	Mean 120 +/- 42 dpf after heat shock at 3dpf; disease begins as T-LBL which rapidly progressed to T-ALL within 2-24 weeks	Feng, *et al* 2007

Table I continued.

	Rag2-ICN1-EGFP	T(7;9)(q34;q34.3) translocation. 60% T-ALL carry deletions and/or mutations in the NOTCH1 gene.	Lymphoblast infiltration of most tissues and organs, including a 7-fold increase in blood cells in kidney and 5-fold increase in spleen	40% penetrance	11 months	Chen, *et al.* 2007
	srk	Gene not yet identified	Lymphoblast infiltration into kidney and blood; monoclonal tumor tissue expressing T cell markers; serially transplantable.	Homozygote penetrance of 43%, heterozygote penetrance of 15%	Dominant inheritance, with disease onset at 3-4 months.	Frazer, *et al.* 2009
	tilk	Gene not yet identified	Lymphoblast infiltration into kidney and blood; oligoclonal tumor tissue expressing T cell markers; serially transplantable.	Homozygous penetrance of 40%, heterozygous penetrance of 6%	Dominant inheritance, with disease onset at approximately 8 months.	Frazer, *et al.* 2009
	otg	Gene not yet identified	Lymphoblast infiltration into kidney and blood; monoclonal tumor tissue expressing T cell markers.	Homozygous penetrance 50%, heterozygous penetrance 0.4%	Recessive inheritance, with leukemia appearing at 6 months	Frazer, *et al.* 2009
B-ALL	*zEJCTEGFP-EL-AML1* and *zbcl-EGFP-TEL-AML1* and *zRag2-EGFP-TEL-AML1*	T(12;21)(p13;q22) translocation is present in 25% of childhood pre-B ALL cases. Mimics childhood CD10+ pre-BALL	B-lymphoid differentiation arrest in kidney marrow	3% penetrance under control of ubiquitous promoters; no disease in fish with T cell specific promoters	8-12 months in fish with ubiquitously expressed promoters;	Sabaawy, *et al.* 2006

lesions to those that globally approach these questions. Techniques representing global approaches to identifying somatically acquired changes in malignant cells include array comparative genomic hybridization (aCGH), epigenetic analyses, and transcriptional profiling (Figure 3). In aggregate, these methodologies can provide a more comprehensive picture of the aberrations that distinguish leukemic cells from normal cells. Zebrafish models of acute leukemia, especially those where tumors are fluorescently labeled, are prime candidates to apply these techniques because individual cancer-bearing fish can yield large numbers of tumor cells by fluorescence activated cell sorting (FACS) purifications. Biologic replicates from the same tumor isolate can be assayed by each type of analysis, and these data can then be correlated within that particular malignancy. In addition, multiple leukemias from each line can be studied in concert. This should reveal a broader picture of the range of associated changes that can occur in the context of a given uniformly inherited "first hit" mutation that reproducibly results in leukemia.

Array CGH: Genomic amplifications and deletions are hallmarks of cancers, and array CGH has been a useful tool in the detection of genomic imbalances associated with human cancers [58], as well as those modeled in other species like rodents [59], canines [60], and even worms [61]. A bacterial artificial chromosome (BAC)-based *D. rerio* aCGH platform enriched with genes orthologous to human oncogenes and tumor suppressor genes has been reported [62]. An important feature of this array is that all included BAC clones were assigned a precise cytogenetic location by fluorescent *in situ* hybridization (FISH). This hybridization platform was used to examine T-ALL samples from the murine *c-Myc* model discussed above, as well as other tumors from zebrafish models of melanoma and rhabdomyosarcoma. Comparing DNA from tumor cells and normal tissue (from the tail of the same fish) revealed between 1 and 17 genomic imbalances per T-ALL sample [62]. We have also employed aCGH to study 8 T-ALLs from *hlk*, *srk*, and *otg* fish (Figure 3, top). Using a high resolution, commercially-available zebrafish oligonucleotide array, all malignancies exhibited at least 4 copy number aberrations (CNAs), with some neoplasms having >50. In human ALL, CNAs are associated with chemotherapy resistance and relapse [63], demonstrating that these genetic lesions can have important biologic consequences. Furthermore, loci showing recurrent CNAs by aCGH in a particular disease can also identify previously unknown oncogenes relevant to that cancer type. One recent example of this has been the discovery of an increase in copy number of the ALK kinase in human neuroblastoma [28-30]. This aCGH finding then led to directed sequencing efforts of *ALK* from other non-amplified neuroblastoma samples, demonstrating frequent activating mutations in *ALK* from these cases. In this way, aCGH can reveal genes pertinent to oncogenesis to help understand the mechanisms behind relapse and therapeutic resistance.

Epigenetic studies: DNA hypermethylation of CpG islands within gene promoters is an epigenetic modification frequently seen in silenced genes [64]. Typically, DNA methylation studies have investigated individual candidate genes in malignant solid tumors [65], but increasingly, genome-wide approaches are being conducted. For instance, DNA 'methylomes' were recently reported for two genetic classes of pediatric pre-B ALL (*ETV6/RUNX1* and high hyperdiploidy). Using a platform with over 28,000 CpG islands, more than 8,000 genes were identified with significant CpG island methylation in these patients [66]. Zebrafish leukemia models are likewise amenable to epigenetic studies, and offer practical advantages over primary patient samples. Human samples are genetically heterogeneous, such that it is only feasible to study common disease types, like the pre-B ALL classes cited above. Zebrafish models have greater molecular uniformity, allowing *Myc*-, *NOTCH1*-, or *hlk, srk,* or *otg* mutant-derived epigenetic changes to be studied in isolation, for example. Human leukemia specimens also frequently suffer from limited purity, where marrow or peripheral blood samples are comprised of blast-enriched cell populations, but normal cells are also present. Because *D. rerio* transgenics (for example *lck:*:EGFP) have fluorescently-labeled malignant

cells, cancer specimens have almost no contamination by normal cells. A related limitation of human studies is that diagnostic samples are often compared to remission samples from the same patient, where the treatment effects may alter the epigenetic profiles of ostensibly normal cells. Using zebrafish, non-malignant cells from genetically near-identical healthy animals are readily available for comparison. Overall, zebrafish are particularly well-suited for epigenetic studies as gene silencing mechanisms are conserved in higher eukaryotes, including not only DNA methylation, but also the constellation of histone modifications that govern gene expression [64]. Importantly, for optimal statistical analyses of genome-wide datasets, large numbers of malignant samples with multiple biologic and technical replicates should be performed in these studies. This is eminently-feasible with zebrafish. Finally, because several zebrafish T-ALL models now exist, epigenetic patterns can be compared across the different genetic models. Methylated (or de-methylated) genes in more than one type may be pervasively deranged in all T-ALL, and these epigenetic changes may reflect consistent secondary hits in the oncogenic process.

Transcriptional analyses: The first study to address human leukemia classification by cDNA microarray was the pioneering work of Golub et al., who reported gene expression profiles for acute lymphoid and myeloid leukemias [67]. This seminal study demonstrated that accurate categorization of these cancers could be accomplished using their mRNA expression patterns. Beyond classification schema, expression arrays have also been used repeatedly to define transformational pathways in acute lymphoblastic leukemias and lymphomas [17]. While these studies highlight the use of transcriptional microarray as an end to itself, expression profiling may be even more powerful when used in conjunction with other technologies. Results of aCGH experiments that locate putative CNA regions can be confirmed by transcriptional microarrays where amplification would be predicted to correlate with increased transcripts, and deletions would lead to diminished expression. Like genomic deletions, promoter hyper-methylation can also cause transcriptional down-regulation and this, too, can be confirmed by expression microarray analysis. Similarly, gene de-methylation predicts increased expression levels in microarrays. In concert, the use of these three technologies is rapidly expanding our knowledge about acute leukemias and the molecular genetic disturbances that contribute to malignant transformation. Cooperative use of these complementary methodologies is becoming the standard for global studies of acute leukemia [68] and the genetic utility of the zebrafish model, along with its high fecundity and easy care, make it an ideal organism in which to advance the field.

Treatment studies

Thus far, this review has focused upon zebrafish leukemia models as a means to discover oncogenic pathways operative in these diseases. However, at a practical level, zebrafish also provide a simple and affordable animal model for pre-clinical testing. Chemical and radiation treatments of both embryos and adult fish are straightforward in *D. rerio*. In this respect zebrafish can be a versatile model in the search for cancer therapeutics. With their small size, zebrafish embryos can be arrayed in multi-well plates and are therefore ideally suited for *in vivo* small-molecule screens. Proof of principle comes from studies where embryos were incubated with compounds from a small molecule library during the first 3 days of life [69] where phenotypic effects were then visually assessed and a study where a panel of biologically active compounds was screened for effects on stem cell induction in the zebrafish aorta-gonad-mesonephros region [70]. Taking this technique one step further, mutants with an embryonic phenotype, such as the zebrafish Ras-induced melanoma model that manifests in the larval stages as melanotic expansion of pigment cells [71] can be used as an initial readout for a small-molecule screen. Then, if a compound which reverts this phenotype is identified, that compound can be tested to see if it affects the adult cancer phenotype. Another example of this is an in-progress study of the *bmyb* mutant *crash and burn (crb)* that was used to identify the novel compound persynthamide

that rescued *crb*'s embryonic phenotype by delaying S-phase, and a study of the effectiveness of this in the adult would be the next phase [72]. Additionally, models of zebrafish who harbor well known translocations that are commonly found in patients, like AML1-ETO, can be used as the basis of chemical modifier screens to uncover chemical modifiers of oncogene-regulated hematopoietic differentiation [48].

Radiation treatment is also an established therapeutic intervention in lymphoid malignancies. The intent of radiation is to induce irreparable DNA damage in rapidly-dividing and highly-susceptible malignant cells, with loss of replicative capacity and eventual cellular necrosis or apoptosis. Studies examining the ability of tyrosine kinase inhibitors to modulate radiation responses have used zebrafish embryos to great advantage [73, 74]. A number of the zebrafish models of lymphoid disease presented here have the benefit of fluorescently-labeled tumor cells that can be easily detected. Hence, disease responses to different therapeutic interventions can be simply monitored by fluorescence microscopy. When adult zebrafish with *NOTCH1*-induced T-ALL were irradiated, decreases in tumor burden were readily apparent [40]. Radiation treatments have also been used to monitor the kinetics of thymic reconstitution [53] and can be similarly applied to monitor relapse kinetics. Going forward, candidate radiation-sensitizing agents could be administered to diseased fish, and these agents' effects in promoting treatment responses, as well as their general toxicity, can be easily observed.

CONCLUSION

The genetic tractability, amenability to microscopy-based phenotypic screens, and ability to produce large numbers of affected animals quickly make zebrafish an ideal system for the study of acute leukemias. These neoplasia models should accelerate the discovery of genomic, genetic, and epigenetic changes that result in leukemogenesis and disease progression. Models discussed in this review, and others yet to be developed, will provide platforms to better understand the underlying causes of human leukemias. In addition, they may soon provide experimental substrates for testing of new therapies in a pre-clinical setting.

REFERENCES

1. Scheinberg, D. A., Maslak, P., and Weiss, M. 2001, In Cancer: Principles and Practice of Oncology, (Ed.) DeVita, V. T., Hellman, S., S. A., Rosenberg. Philadelphia: Lippincott Williams and Wilkins.
2. Gilliland, D. G., and Tallman, M. S. 2002, Cancer Cell,1, 417-20.
3. Flanagan, M. B., Sathanoori, M., Surti, U., Soma, L., and Swerdlow, S. H. 2008, Am J. Clin. Pathol., 130, 620-7.
4. Pui, C. H., and Evans, W. E. 2006, N. Engl. J. Med., 354, 166-78.
5. Suzuki, H., Gabrielson, E., Chen, W., Anbazhagan, R., van Engeland, M., Weijenberg, M. P., Herman, J. G., and Baylin, S. B. 2002, Nat. Genet., 31,141-9.
6. Rowley, J. D. 1998, Annu. Rev. Genet., 32, 495-519.
7. Hakem, R., and Mak, T. W. 2001, Annu. Rev. Genet., 35, 209-41.
8. Gilliland, D. G. 2001, Curr. Opin. Hematol., 8, 189-91.
9. Gilliland, D. G. 1998, Leukemia, 12 (Suppl. 1), S7-12.
10. Weng, A. P., Ferrando, A. A., Lee, W., Morris, JPt, Silverman, L. B., Sanchez-Irizarry, C., Blacklow, S. C., Look, A. T., and Aster, J. C. 2004, Science, 306, 269-71.
11. Lee, S. Y., Kumano, K., Masuda, S. Hangaishi, A., Takita, J., Nakazaki, K., Kurokawa, M., Hayashi, Y., Ogawa, S., and Chiba, S. 2005, Leukemia, 19, 1841-3.
12. Gutierrez, A., Sanda, T., Grebliunaite, R., Carracedo, A., Salmena, L., Ahn, Y., Dahlberg, S., Neuberg, D., Moreau, L. A., Winter, S. S., Larson, R., Zhang, J., Protopopov, A., Chin, L., Pandolfi, P. P., Silverman, L. B., Hunger, S. P., Sallan, S. E., and Look, A. T. 2009, Blood, 114, 647-50.
13. Sulong, S., Moorman, A. V., Irving, J. A., Strefford, J. C., Konn, Z. J., Case, M. C., Minto, L., Barber, K. E., Parker, H., Wright, S. L., Stewart, A. R., Bailey, S., Bown, N. P., Hall, A. G., and Harrison, C. J. 2009, Blood, 113,100-7.

14. Palomero, T., Sulis, M. L., Cortina, M., Real, P. J., Barnes, K., Ciofani, M., Caparros, E., Buteau, J., Brown, K., Perkins, S. L., Bhagat G., Agarwal, A. M., Basso, G., Castillo, M., Nagase, S., Cordon-Cardo, C., Parsons, R., Zuniga-Pflucker, J. C., Dominguez, M., and Ferrando, A. A. 2007, Nat. Med., 13, 1203-10.
15. Ferrando, A. A., and Look, A. T. 2000, Semin. Hematol., 37, 381-95.
16. Ferrando, A. A., and Look, A. T. 2003, Semin. Hematol., 40, 274-80.
17. Ferrando, A. A., Neuberg, D. S., Staunton, J., Loh, M. L., Huard, C., Raimondi, S. C., Behm, F. G., Pui, C. H., Downing, J. R., Gilliland, D. G., Lander, E. S., Golub, T. R., and Look, A. T. 2002, Cancer Cell, 1, 75-87.
18. Wang, S. S., Slager, S. L., Brennan, P., Holly, E. A., De Sanjose, S., Bernstein L., Boffetta, P., Cerhan, J. R., Maynadie, M., Spinelli, J. J., Chiu, B. C., Cocco, P.L., Mensah, F., Zhang, Y., Nieters, A., Dal Maso, L., Bracci, P. M., Costantini, A. S, Vineis, P., Severson, R. K., Roman, E., Cozen, W., Weisenburger, D., Davis, S., Franceschi, S., La Vecchia, C., Foretova, L., Becker, N., Staines, A., Vornanen, M., Zheng, T., and Hartge, P. 2007, Blood, 109, 3479-88.
19. Trevino, L. R., Yang, W., French, D., Hunger, S. P., Carroll, W. L., Devidas, M., Willman, C., Neale, G., Downing, J., Raimondi, S. C., Pui, C. H., Evans, W. E., and Relling, M. V. 2009, Nat. Genet., 41, 1001-5.
20. Papaemmanuil, E., Hosking, F. J., Vijayakrishnan, J., Price, A., Olver, B., Sheridan, E., Kinsey, S. E., Lightfoot, T., Roman, E., Irving, J. A., Allan, J. M., Tomlinson, I. P., Taylor, M., Greaves, M., and Houlston, R. S. 2009, Nat. Genet., 41, 1006-10.
21. Horwitz, M. 1997, Leukemia, 11, 1347-59.
22. Rigby, P. G., Pratt, P. T., Rosenlof, R. C., and Lemon, H. M. 1968, Arch. Intern. Med., 121, 67-70.
23. Yuille, M. R., Matutes, E., Marossy, A., Hilditch, B., Catovsky, D., and Houlston, R. S. 2000, Br. J. Haematol., 109, 794-9.
24. Owen, C., Barnett, M., and Fitzgibbon, J. 2008, Br. J. Haematol., 140, 123-32.
25. Song, W. J., Sullivan, M. G., Legare, R. D., Hutchings, S., Tan, X., Kufrin, D., Ratajczak, J., Resende, I. C., Haworth, C., Hock, R., Loh, M., Felix, C., Roy, D. C., Busque, L., Kurnit, D., Willman, C., Gewirtz, A. M., Speck, N. A., Bushweller, J. H., Li, F. P., Gardiner, K., Poncz, M., Maris, J. M., and Gilliland, D. G. 1999, Nat. Genet., 23, 166-75.
26. Smith, M. L., Cavenagh, J. D., Lister, T. A., and Fitzgibbon, J. 2004, N. Engl. J. Med., 351, 2403-7.
27. Knudson, A. G. Jr. 1971, Proc. Natl. Acad. Sci. USA, 68, 820-3.
28. Mosse, Y. P., Laudenslager, M., Longo, L., Cole, K. A., Wood, A., Attiyeh, E. F., Laquaglia, M. J, Sennett, R., Lynch, J. E, Perri, P., Laureys, G., Speleman, F., Kim, C., Hou, C., Hakonarson, H., Torkamani, A., Schork, N. J., Brodeur, G. M., Tonini, G. P., Rappaport, E., Devoto, M., and Maris, J. M. 2008, Nature, 455, 930-5.
29. Chen, Y., Takita, J., Choi, Y. L., Kato, M., Ohira, M., Sanada, M., Wang, L., Soda, M., Kikuchi, A., Igarashi, T., Nakagawara, A., Hayashi, Y., Mano, H., and Ogawa, S. 2008, Nature, 455, 971-4.
30. George, R. E., Sanda, T., Hanna, M., Frohling, S., Luther, W. 2nd, Zhang, J., Ahn, Y., Zhou, W., London, W. B., McGrady, P., Xue, L., Zozulya, S., Gregor, V. E., Webb, T. R., Gray, N. S., Gilliland, D. G., Diller, L., Greulich, H., Morris, S. W., Meyerson, M., and Look, A. T. 2008, Nature, 455, 975-8.
31. Traver, D., Herbomel, P., Patton, E. E., Murphey, R. D., Yoder, J. A., Litman, G. W., Catic, A., Amemiya, C. T., Zon, L. I., and Trede, N. S. 2003, Adv. Immunol., 81, 253-330.
32. Laird, D. J., De Tomaso, A. W., Cooper, M. D., and Weissman, I. L. 2000, Proc. Nat. Acad. Sci. USA, 97, 6924-6.
33. Du Pasquier, L. 2004, Immunol. Lett., 92, 3-9.
34. Hawkins, W. E., Overstreet, R. M., Fournie, J. W., and Walker, W. W. 1985, J. Appl. Toxicol., 5, 261-4.
35. Lam, S. H., and Gong, Z. 2006, Cell Cycle, 5, 573-7.

36. Frazer, J. K., Meeker, N. D., Rudner, L., Bradley, D. F., Smith, A. C., Demarest, B., Joshi, D., Locke, E. E., Hutchinson, S. A., Tripp, S., Perkins, S. L., and Trede, N. S. 2009, Leukemia, 23, 1825-35.
37. Berghmans, S., Murphey, R. D., Wienholds, E., Neuberg, D., Kutok, J. L., Fletcher, C. D, Morris, J. P, Liu, T. X., Schulte-Merker, S., Kanki, J. P., Plasterk, R., Zon, L. I., and Look, A. T. 2005, Proc. Natl. Acad. Sci. USA, 102, 407-12.
38. Sabaawy, H. E., Azuma, M., Embree, L. J., Tsai, H. J., Starost, M. F., and Hickstein, D. D. 2006, Proc. Natl. Acad. Sci. USA, 103, 15166-71.
39. Langenau, D. M., Traver, D., Ferrando, A. A., Kutok, J. L., Aster, J. C., Kanki, J. P., Lin, S., Prochownik, E., Trede, N. S., Zon, L. I., and Look, A. T. 2003, Science, 299, 887-90.
40. Chen, J., Jette, C., Kanki, J. P., Aster, J.C., Look, A. T., and Griffin, J. D. 2007, Leukemia, 21, 462-71.
41. Faucherre, A., Taylor, G. S., Overvoorde, J., Dixon, J. E., and Hertog, J. 2008, Oncogene, 27, 1079-86.
42. Downing, J. R. 1999, Br. J. Haematol., 106, 296-308.
43. Peterson, L. F., and Zhang, D. E. 2004, Oncogene, 23, 4255-62.
44. Westendorf, J. J., and Hiebert, S. W. 1999, J. Cell Biochem. Suppl., 32-33, 51-8.
45. Kalev-Zylinska, M. L., Horsfield, J. A., Flores, M. V., Postlethwait, J. H., Vitas, M. R., Baas, A. M., Crosier, P. S., and Crosier, K. E. 2002, Development, 129, 2015-30.
46. Yergeau, D. A., Hetherington, C. J., Wang, Q., Zhang, P., Sharpe, A. H., Binder, M., Marin-Padilla, M., Tenen, D. G., Speck, N. A., and Zhang, D. E. 1997, Nat. Genet.,15, 303-6.
47. Yeh, J. R., Munson, K. M., Chao, Y. L., Peterson, Q. P., Macrae, C. A., and Peterson, R. T. 2008, Development,135, 401-10.
48. Yeh, J. R., Munson, K. M., Elagib, K. E., Goldfarb, A. N., Sweetser, D. A., and Peterson, R. T. 2009, Nat. Chem. Biol., 5, 236-43.
49. Zhuravleva, J., Paggetti, J., Martin, L., Hammann, A., Solary, E., Bastie, J. N., and Delva, L. 2008, Br. J. Haematol., 143, 378-82.
50. Langenau, D. M., Feng, H., Berghmans, S., Kanki, J. P., Kutok, J. L., and Look, T. 2005. Proc. Natl. Acad. Sci. USA, 102, 6068-73.
51. Palomero, T., Odom, D. T., O'Neil, J., Ferrando, A. A., Margolin, A., Neuberg, D. S., Winter, S. S., Larson, R. S., Li, W., Liu, X. S., Young, R. A., and Look, A. T. 2006, Blood, 108, 986-92.
52. Feng, H., Langenau, D. M., Madge, J. A., Quinkertz, A., Gutierrez, A., Neuberg, D. S., Kanki, J. P., and Look, A. T. 2007, Br. J. Haematol., 138, 169-75.
53. Langenau, D. M., Ferrando, A. A., Traver, D., Kutok, J. L., Hezel, J. P., Kanki, J. P., Zon, L. I., Look, A. T., and Trede, N. S. 2004, Proc. Natl. Acad. Sci. USA, 101, 7369-74.
54. Geisler, R., Rauch, G. J., Geiger-Rudolph, S., Albrecht, A., van Bebber, F., Berger, A., Busch-Nentwich, E., Dahm, R., Dekens, M. P., Dooley, C., Elli, A. F., Gehring, I., Geiger, H., Geisler, M., Glaser, S., Holley, S., Huber, M., Kerr, A., Kirn, A., Knirsch, M., Konantz, M., Kuchler, A. M., Maderspacher, F., Neuhauss, S. C., Nicolson, T., Ober, E. A., Praeg, E., Ray, R., Rentzsch, B., Rick, J. M., Rief, E., Schauerte, H. E., Schepp, C. P., Schonberger, U., Schonthaler, H. B., Seiler, C., Sidi, S., Sollner, C., Wehner, A., Weiler, C., and Nusslein-Volhard, C. 2007, BMC Genomics, 8, 11.
55. Haffter, P., Granato, M., Brand, M., Mullins, M. C., Hammerschmidt, M., Kane, D. A., Odenthal, J., van Eeden, F. J., Jiang, Y. J., Heisenberg, C. P., Kelsh, R. N., Furutani-Seiki, M., Vogelsang, E., Beuchle, D., Schach, U., Fabian, C., and Nusslein-Volhard, C. 1996, Development, 123, 1-36.
56. Trede, N. S., Ota, T., Kawasaki, H, Paw, B. H., Katz, T., Demarest, B., Hutchinson, S., Zhou, Y., Hersey, C., Zapata, A., Amemiya, C. T., and Zon, L. I. 2008, Dev. Dyn., 237, 2575-84.
57. Jamieson, C. H., Ailles, L. E., Dylla, S. J., Muijtjens, M., Jones, C., Zehnder, J.L., Gotlib, J., Li, K., Manz, M. G., Keating, A., Sawyers, C. L., and Weissman, I. L. 2004, N. Engl. J. Med., 351, 657-67.
58. Pinkel, D., and Albertson, D. G. 2005. Annu. Rev. Genomics Hum. Genet., 6, 331-54.

59. Hodgson, G., Hager, J. H., Volik, S., Hariono, S., Wernick, M., Moore, D., Nowak, N., Albertson, D. G., Pinkel, D., Collins, C., Hanahan, D., and Gray, J. W. 2001, Nat. Genet., 29, 459-64.
60. Thomas, R., Duke, S. E., Bloom, S. K. Breen, T. E., Young, A. C., Feiste, E., Seiser, E. L., Tsai, P. C., Langford, C. F., Ellis, P., Karlsson, E. K., Lindblad-Toh, K., and Breen, M. 2007, J. Hered., 98, 474-84.
61. Maydan, J. S., Flibotte, S., Edgley, M. L., Lau, J., Selzer, R. R., Richmond, T. A, Pofahl, N. J., Thomas, J. H., and Moerman, D. G. 2007, Genome. Res., 17, 337-47.
62. Freeman, J. L., Ceol, C., Feng, H., Langenau, D. M., Belair, C., Stern, H. M., Song, A., Paw, B. H., Look, A. T., Zhou, Y., Zon, L. I., and Lee, C. 2009, Genes Chromosomes Cancer, 48, 155-70.
63. Mullighan, C. G., Phillips, L. A., Su, X., Ma, J., Miller, C. B., Shurtleff, S. A., and Downing, J. R. 2008, Science, 322, 1377-80.
64. Esteller, M. 2007, Hum. Mol. Genet, 16 Spec. No., 1, R50-9.
65. Esteller, M. 2007, Nat. Rev. Genet., 8, 286-98.
66. Garcia-Manero, G., Jeha, S., Daniel, J., Williamson, J., Albitar, M., Kantarjian, H. M., and Issa, J. P. 2003, Cancer, 97, 695-702.
67. Golub, T. R., Slonim, D. K., Tamayo, P., Huard. C., Gaasenbeek, M., Mesirov, J. P., Coller, H., Loh, M. L., Downing, J. R., Caligiuri, M. A., Bloomfield, C. D., and Lander, E. S. 1999, Science, 286, 531-7.
68. Davidsson, J., Lilljebjorn, H., Andersson, A., Veerla, S., Heldrup, J., Behrendtz, M,. Fioretos, T., and Johansson, B. 2009, Hum. Mol. Genet., 18, 4054-65.
69. Peterson, R. T., Link, B. A., Dowling, J. E., and Schreiber, S. L. 2000, Proc. Natl. Acad. Sci. USA, 97, 12965-9.
70. North, T. E., Goessling, W., Walkley, C. R., Lengerke, C., Kopani, K. R., Lord, A. M., Weber, G. J., Bowman, T. V., Jang, I. H., Grosser, T., Fitzgerald, G. A., Daley, G. Q., Orkin, S. H., and Zon, L. I. 2007, Nature, 447, 1007-11.
71. Michailidou, C., Jones, M., Walker, P., Kamarashev, J., Kelly, A., and Hurlstone, A. F. 2009, Dis. Model Mech., 2, 399-411.
72. Stern, H. M., Murphey, R. D., Shepard, J. L., Amatruda, J. F., Straub, C. T., Pfaff, K. L., Weber, G., Tallarico, J. A., King, R. W., and Zon, L. I. 2005, Nat. Chem. Biol., 1, 366-70.
73. Kari, G., Zengin, A.Y., Ryan, A., Rodeck, U., and Dicker, A. P. 2006, International Journal of Radiation Oncology •Biology •Physics, 66.
74. McAleer, M. F., Davidson, C., Davidson, W. R., Yentzer, B., Farber, S. A., Rodeck, U., and Dicker, A. P. 2005, Int. J. Radiat. Oncol. Biol. Phys., 61, 10-3.

CHAPTER 4

OTG, A ZEBRAFISH MUTANT WITH p53-INDEPENDENT APOPTOSIS RESISTANCE AND T CELL MALIGNANCY PREDISPOSITION

Lynnie A. Rudner[1], Katherine B. Gibbs[1], Martha I. Garcia[3], Lance Batchelor[1], Nathan Sweeney[1], Alexis Davis[1], Cicely Jette[1], J. Kimble Frazer[1,2], and Nikolaus Trede[1,2*]

[1]Department of Oncological Sciences, The University of Utah, Salt Lake City, Utah, [2]Department of Pediatrics, The University of Utah, Salt Lake City, Utah; [3]University of Texas at Brownsville

* JKF and NST share senior authorship of this work

*Corresponding Author: Nikolaus S. Trede MD, PhD
Huntsman Cancer Institute
2000 Circle of Hope
Salt Lake City, Utah 84112
Nikolaus.Trede@hci.utah.edu
Tel: 801-585 -0599

Abstract

Zebrafish (*Danio rerio*) T cell acute lymphoblastic leukemia (T-ALL) models are useful tools for studying human cancer. Several transgenic and mutant *D. rerio* lines have been shown to develop T-ALL. One line with recessive T-ALL predisposition, *oscar the grouch* (*otg*), was identified in a mutagenesis screen designed to uncover aberrant T cell development. We have previously shown that *otg*-derived T cell cancers emulate human T-ALL. This suggests that *otg* cancers might be susceptible to human T-ALL therapies. Patients with ALL and zebrafish from the transgenic *rag2::MYC-ER* line affected with T-ALL respond with apoptosis and remission to treatment with glucocorticoids and γ-irradiation. Both treatments failed or had only limited efficacy in decreasing the disease burden in *otg* mutants. We tested if the *otg* mutation also confers resistance to irradiation-induced apoptosis in zebrafish embryos. While DNA damage response is intact in *otg* mutant embryos, they exhibit diminished activation of caspase 3 and decreased apoptosis. Genetic manipulation of *otg* mutant individuals revealed that the defect lies in the intrinsic mitochondrial-induced apoptosis pathway.

Introduction

Lymphocytic malignancies are the most common diseases in pediatric oncology. Relative to most other leukemias and lymphomas of childhood, those derived from the T cell lineage are also more difficult to cure and their treatments are often accompanied by acute side effects and long-term health risks (Larson et al 1998, Pui 1998, Takeuchi et al 2002). An additional challenge in understanding these diseases is that T cell malignancies are molecularly heterogeneous, driven by complex combinations of genetic changes (Ferrando et al 2002). Knowledge of specific molecular alterations that can cause T lymphocyte transformation has principally come from the discovery of aberrant chromosomal translocations and activation of pathways in blast cells from T-ALL patients (Armstrong and Look 2005, Pui et al 2004). While several informative translocations have been described (Teitell and Pandolfi 2009), most T-ALL

cases lack such cytogenetic changes (De Keersmaecker et al 2006, Harrison and Foroni 2002), making the causative events less transparent. Recent studies have identified NOTCH1 activation in over 50% of human T-ALL patient samples and cell lines (Weng et al 2004), and further studies have identified the *c-MYC* proto-oncogene as a direct target of NOTCH1 (Palomero et al 2006). While these reports provide important insights into a subset of T-ALL, lesions in a large number of T-ALL cases have undoubtedly not yet been determined. Therefore, discovery of additionally pathogenic mechanisms is pivotal to both clinical medicine and scientific understanding to refine prognosis and treatment of T cell malignancies.

The idea that apoptosis might have a role in the treatment of malignancies was first suggested by Kerr et al who observed extensive nonnecrotic cell death after cancers were treated with cytotoxic agents (Kerr et al 1972, 1994). Consequently, defective apoptosis is one of the pillars of tumorigenesis (reviewed in (Lowe and Lin 2000)). For example, in lymphoproliferative cancers *bcl-2* was identified as a promoter of cell survival by blocking programmed cell death (Hockenbery et al 1990, Lowe and Lin 2000, McDonnell et al 1989, Vaux et al 1988). In addition to over-expression of BCL2, inactivation of tumor suppressor genes such as *p53* and *Fas,* and their effector genes (*bax, apaf-1, casp9* and others) has been shown to cause apoptosis resistance in many different cancer types (Allan and Clarke 2009, Fadeel et al 2008, Mione and Trede 2010). Defects in apoptosis can contribute to treatment failure (reviewed in (Andreasson et al 2001) as the mechanism of action of many chemotherapeutic agents involves induction of apoptosis.

Zebrafish have recently become popular models for the study of human cancers, including hematological neoplasia (Amatruda and Zon 1999, Meeker and Trede 2008, Mione and Trede 2010)}. Five zebrafish models with T cell cancer predisposition have been described to date. Transgenic lines with lymphocyte-specific mis-expression of human NOTCH1 and murine MYC (mMYC) both develop T-ALL and T-LBL (Chen et al 2007, Langenau et al 2003). In a chemical mutagenesis screen, we identified three additional *D. rerio* lines (*srk*, *hlk*, *otg*) with

heritable germline mutations that also display highly penetrant T cell malignancy phenotypes (Frazer et al 2009). All of these ALL-prone lines have lymphocyte-specific GFP reporters, facilitating assessment of therapeutic interventions by fluorescence microscopy. Here, we used two of these T cell malignancy-prone lines, transgenic human *rag2::MYC-ER* (hMYC) and *otg* (Frazer et al 2009), to study response to common apoptosis-inducing T-ALL treatments. We report that one of these models, *otg*, has a defect in the intrinsic apoptosis pathway. Understanding the pathogenic mechanism of this zebrafish model stands to advance our understanding of the diverse molecular events that drive human T-ALL.

Results

Differential glucocorticoid sensitivity of zebrafish T-ALL models. The success of ALL treatment is based on the use of multimodal chemotherapy. Dexamethasone (DXM), a synthetic corticosteroid, plays an essential role in nearly all therapy combinations due to its ability to block cell cycle progression and induce apoptosis in ALL cells (Ploner et al 2005, Tissing et al 2003). DXM induces apoptosis by binding the glucocorticoid receptor (GCR), revealing its nuclear localization signal, and translocating with the GCR to the nucleus where the complex interacts with glucocorticoid response elements (GREs) leading to the transcriptional activation of proapoptotic genes (Tissing et al 2003). Sensitivity to glucocorticoids is therefore a major prognostic factor in human T-ALL (Arico et al 1995, Dordelmann et al 1999). The hMYC (A. Gutierrez, pers. communic.) and *otg* zebrafish models of T-ALL (Frazer et al 2009) share many common features with human T-ALL. We therefore wished to determine whether these models were sensitive to treatment with DXM, similarly to their human counterparts. We established a treatment regimen where a maximum of 10% of leukemic hMYC individuals succumbed in the early treatment phase, possibly due to tumor lysis syndrome (see Materials and Methods). Of 17 treated hMYC fish, 15 had responded by day 14, and 13 of 17 had achieved complete remission by day 21, after a week off treatment (Supplemental Table 4.1). We next tested the same

treatment protocol on 8 leukemic *otg* fish. Six of these showed no response to DXM, one had a delayed response (28 days vs. 14 days) and one fish responded within the same timeframe as hMYC individuals (Figure 4.1, Table 4.1).

Radiation therapy induces remission in zebrafish models of T-ALL. T-ALL is known for its exquisite sensitivity to irradiation, and radiation therapy has been used effectively in patients. Adult zebrafish respond to sublethal, single-dose γ-irradiation (20Gy) with T cell ablation within 72 hours and resume hematopoiesis 21 days after treatment (Langenau et al 2004, Traver et al 2004). To test the effectiveness of this treatment in our zebrafish models of T-ALL we conducted single-dose irradiation trials to induce remission as assessed by fluorescence microscopy (Langenau et al 2004, Traver et al 2004) (Figure 4.2a). Both hMYC*,* and *otg* fish remitted with a single dose of 20Gy. However, while this dose was sufficient to prevent relapse in all hMYC affected fish for at least 60 days, relapse occurred in *otg* fish as early as 10 days after treatment.

Next we sought to determine the minimum single irradiation dose necessary to achieve a complete remission in hMYC leukemic fish. To that end, we exposed affected hMYC fish to varying doses of γ-irradiation: 2 each at 17.5Gy, 15Gy, 12.5Gy, 10Gy, 7.5Gy, 5Gy. Exposure to 10Gy or greater resulted in complete remission at 72 hours post-treatment for all 8 leukemic individuals, whereas exposure to 7.5Gy or 5Gy only induced remission in 25% (Figure 4.2b). We therefore chose single exposure to 10Gy to treat affected hMYC*,* and *otg* fish. As expected, 100% of hMYC fish remitted with this treatment regimen and remained in remission for at least 49 days after treatment (n=7). By contrast, only 83% of *otg* fish achieved remission at this dose (n=6), and 60% of these had relapsed by 14 days after treatment (Figure 4.2c).

Otg embryos are resistant to irradiation-induced apoptosis. The marked decrease in radiation sensitivity of T-ALL in adult *otg* fish suggested a possible inherent resistance to irradiation-induced apoptosis in these animals. To test this, we used two different assays. First, 30 hours post-fertilization (hpf) embryos were exposed to high dose γ-irradiation, and apoptosis was scored by phenotypic changes in the shape of their tail as described previously (Parant et al

2010). Second, we exposed 18hpf embryos to 12.5Gy of γ-irradiation followed by acridine orange staining (Sidi et al 2008) to distinguish apoptosis from other forms of cell death. In *otg* heterozygote incrosses approximately one-quarter (429/1867, 23%) of the embryos exhibited no change in tail phenotype after treatment with 100Gy, indicating resistance to apoptosis, similar to *p53* mutant embryos (Fig 4.3a). Similarly, approximately one-quarter (26%) of offspring from *otg* heterozygous crosses also excluded acridine orange following 12.5Gy of γ-irradiation, indicating resistance to apoptosis (Fig 4.3b).

As γ-irradiation activates the intrinsic mitochondrial apoptotic pathway, we tested the integrity of the intrinsic mitochondrial pathway. *otg* embryos were exposed at 24hpf to 8Gy of γ-irradiation, as described previously (Jette et al 2008) and apoptotic cells were revealed with an antibody to activated-human Caspase-3. Using this assay, we observed that 45 out of 167 embryos (26.9%) produced from the mating of a known *otg* heterozygous pair (Fig 4.3c) had only weak induction of *caspase 3*, while three quarters of the embryos had wild type levels. In summary, all three assays confirm that irradiation-induced apoptosis, culminating in the activation of *caspase 3*, is impaired in *otg* mutant embryos.

otg embryos have a defect in the intrinsic apoptosis pathway. Gamma-irradiation triggers the intrinsic apoptotic pathway in zebrafish (reviewed in (Eimon and Ashkenazi 2010). A well studied cascade of events, this pathway can be broken into three main phases: double-strand break repair regulated by the accumulation and localization of the γ-phosphorylated histone H2Ax (γ-H2Ax); the response of p53 and BCL-2 family members (including Puma, Bax, Bad, and Bak) to permeabilize the outer mitochondrial membrane; and cytochrome *c* release followed by binding to APAF-1 and caspase-9 to form a holoenzyme that activates caspase-3 through proteolytic cleavage, resulting in cell-wide proteolysis and DNA cleavage (Eimon and Ashkenazi 2010).

To identify at which level the *otg* mutation exerts its effect, we investigated all three phases. For intact double strand breaks repair we visualized the recruitment of γ-H2Ax. The

presence of γ-H2Ax has been shown to culminate at 30 minutes after irradiation and decrease thereafter (Sedelnikova et al 2002). As exaggerated repair activity can lead to apoptosis resistance in B-chronic lymphocytic leukemia (B-CLL) (Deriano et al 2005), particular attention was paid to the time-course of H2Ax phosphorylation. Using a polyclonal antibody directed against γ-phosphorylated H2Ax, we examined 30hpf *otg* embryos at 10, 20, 30, and 40 minutes following 100gy irradiation. Similarly to wild type controls, all *otg* embryos exhibited γ-H2Ax staining in cells of the neural tube beginning at 10 minutes post irradiation, with maximum signal at 30 minutes post irradiation (Figure 4.4a). Similarly to control embryos, γ-H2Ax signal faded at 40 minutes post irradiation in *otg* embryos, indicating an appropriate denouement of response to double-stranded breaks (data not shown).

To ascertain if the mutation responsible for apoptotic resistance is distinct from p53, we performed complementation testing. Fish heterozygous for both *p53* and *otg* do not develop leukemia nor are they resistant to apoptosis at the expected frequency. In addition, we utilized the Chk1 inhibitor Gö6976 to block the inhibitory pathway that prevents activation of caspase 2 after irradiation. This Chk1 inhibitor has been previously shown to restore apoptotic sensitivity to irradiation-induced apoptosis in *p53* mutants (Sidi et al 2008). While a nontoxic dose of Gö6976 (1 μM) restored a complete apoptotic response to radiation in *p53* mutants, no restoration of apoptosis, as detected by acridine orange, was achieved in *otg* embryos (Figure 4.4b, Figure 4.4c), indicating that the mutation responsible for irradiation resistance in *otg* is not due to a mutation in *p53*.

Irradiation activates puma *transcription and protein expression in* otg *mutants.* Following DNA damage by γ-irradiation, caspase-3 cleavage is dependent on *p53* activation of the BH3-only gene *puma* but not other BH3-only proteins such as *Bik, Bmf1, Bid* or *Noxa* (Kratz et al 2006). This suggests that similarly to humans (Erlacher et al 2005) Puma is the primary initiator of the intrinsic apoptosis response in zebrafish (Erlacher et al 2005). To test the

expression of *puma* in *otg* embryos, we performed quantitative (q) RT-PCR analysis of *puma* 6 hours after irradiation with 12.5Gy at 18hpf. In both wild type and *otg* embryos, γ-irradiation induced a greater than 12-fold increase in *puma* mRNA expression (Figure 4.5a). To address if *puma* mRNA in *otg* embryos is functionally deficient, we injected wild type and *otg* embryos with 10ng/μL of mRNA encoding *puma* at the one-cell stage of development, and followed their development during the first 2 hpf as described previously (Jette et al). Injection of puma had a profound effect on both wild type and *otg* embryos with very few surviving past gastrulation (Figure 4.5b). Injecting a range of doses of z*puma* mRNA (1-10ng/μL) we observed no difference in the response of *otg* mutant and wild type embryos, suggesting that factors downstream of *puma* are intact, and their activation by exogenous *puma* injected at the one-cell stage is sufficient to induce apoptosis regardless of genotype.

The ability of *puma* mRNA to induce apoptosis in *otg* embryos, coupled with the increased level of endogenous *puma* mRNA as measured by qRT-PCR in these embryos after γ-irradiation (Figure 4.5a) may be explained by a mis-sense or non-sense mutation in the *puma* gene which leads to dysfunctional or degraded protein. Comparison of the coding sequence (including the 5' and 3' UTRs and the untranslated exons 1, 4 and 5) of *puma* cDNA derived from *otg* embryos and radiation-sensitive wild type embryos revealed no mutations that would result in an amino acid changes or a premature stop codon in these regions. Next, we tested whether in addition to expression of mRNA, Puma protein was detectable in *otg* fish. To induce a vigorous response, we irradiated wild type, *p53* mutant, and *otg* mixed clutches at 24hpf with 100Gy, followed by Western blot experiments on protein lysates with a polyclonal anti-zebrafish Puma antibody. As expected, Puma protein levels were increased after high-dose irradiation in wild type embryos. *otg* embryos identified after irradiation by the straight/curled tail assay showed an increase in Puma protein after irradiation that was comparable to the increase seen in a pool of mixed homozygous wild type and heterozygous siblings (Figure 4.6). The neural tube is the major anatomical area of irradiation-induced apoptosis induction of 30hpf embryos and is

extremely difficult to study in isolation. We therefore examined Puma expression in isolated brains and spinal cords from irradiated adult homozygous *otg* fish and wild type controls. Western blotting for Puma protein in these samples showed no difference in Puma protein between wild type and *otg* samples (Figure 4.6), suggesting that irradiation resistance in *otg* mutants is not due to defects in Puma protein sequence or levels.

Discussion

While the treatment of leukemias has improved greatly in recent years, success in curing T-ALL in particular is still challenging. Treatment of T-ALL is more aggressive, resulting in increased toxicity and potential long-term sequelae. More targeted therapies and a better understanding of the pathogenic mechanisms at work in T-ALL are required to improve treatment results and diminish side effects. To better understand the molecular mechanisms driving the pathogenesis of T-ALL, we studied a line of zebrafish, *otg,* that we previously identified in a mutagenesis screen as having a recessive hereditary predisposition to T-ALL (Frazer et al 2009). In the present study, we show that *otg* is resistant to treatment with treatments known to be effective in humans: dexamethasone and whole body irradiation. We find that this resistance to apoptosis ultimately results in a block of the intrinsic apoptosis pathway culminating in a loss of caspase 3 activation. Finally, we show that this mutation is not due to a loss of activity of *tp53* or its direct downstream targets. However, over-expression of one such effector, *puma,* can rescue apoptosis in *otg* embryos.

The observation that the injection of *puma* mRNA into *otg* zebrafish results in a restoration of apoptosis, but that no mutation in the *puma* gene can be found, creates a paradox surrounding the mechanism behind the *otg* phenotype. Recently, new findings regarding phosphorylation as a post-translational modification of human PUMA (Fricker et al 2010) suggest that yet another level of regulation maintains the delicate balance of this key protein. In that study, Fricker et al showed that phosphorylated PUMA undergoes increased turnover and had

repressed cell death potential. This therefore suggests that the phosphatase responsible for dephosphorylating PUMA may be key player in promoting apoptosis if conserved across species, and a loss of function in this phosphatase in zebrafish might result in decreased apoptotic potential in the presence of *puma* activation as seen in *otg* embryos. Our observations that over-expression of zebrafish *puma* mRNA can restore apoptosis in *otg* embryos argues against a defect in this phosphatase. However, since this phosphatase has not yet been identified, and its kinetics are therefore unknown, it is possible that the overexpression of *puma* mRNA may bypass the need for its proper function, resulting in apoptosis even in the face of a defective phosphatase.

BAD, another proapoptotic member of the BCL2 protein family, promotes cell death by binding to and preventing the prosurvival functions of BCL-xL and BCL-2 (Yang et al 1995) BAD also acts to displace PUMA from BCL-2 or BCL-xL allowing BAX to move to the mitochondrial membrane, and directly activating cytochrome C ((Kim et al 2006). Additionally, previous studies have shown that the overexpression of *bad* in wild type zebrafish (by RNA injection) can promote increased radiation sensitivity (Jette et al 2008). However, gene overexpression of *bad* in *otg* mutants did not result in restoration of irradiation-induced apoptosis (data not shown). In zebrafish, Bad protein function is regulated by the phosphorylation status of serines 84 and 103. Phosphorylation prevents proapoptotic function and dephosphorylation allows Bad to initiate proapoptotic activity (Jette et al 2008) by dissociating from 14-3-3 in the cytosol, and moving to the mitochondrial membrane to inactivate Bcl-XL or Bcl-2 (Yang et al 1995). A number of different phosphatases have been identified that dephosphorylate BAD in human cell lineages. These include PP1a in IL-2/IL-4 dependent T cell lines (Ayllon et al 2000), and PP2a in a prolymphocytic cell line (Chiang et al 2003). If dephosphorylation were inhibited in *otg* embryos due to a loss of function of the phosphatase responsible for this activity in zebrafish embryos, radiation-induced apoptosis would be expected to be impaired, as we observe here. We are currently exploring this possibility. This work will lead to an increased

understanding of the mechanism of irradiation-induced apoptosis, and a possible link between this pathway and the development of T cell malignancy.

The lack of activated caspase 3 expression in *otg* embryos could be the result of a loss of function in any of the myriad components of the intrinsic apoptosis pathway which culminates in the caspase cascade. The post-mitochondrial signaling arm of this pathway is well studied in the zebrafish, and the players engaged after mitochondrial activation are well elucidated (Eimon and Ashkenazi 2010. We have sequenced cDNAs derived from acridine orange-negative otg embryos and did not observe any mutations in the coding regions of caspase 3a, caspase 9, xaip , zaif or Apaf-1. This does not completely rule out a primary defect in post-mitochondrial signaling, and a mutation in other genes responsible for activating the cascade (e.g. birc family members) could explain the irradiation resistance seen in otg. A second pathway known to activate caspase 3 in response to irradiation is sphyngo,myelinase induction of ceramide production, a second messenger that initiates caspase 3-mediated apoptosis. Defects in generating ceramide have been shown to lead to apoptosis following γ-irradiation {Kolesnick, 2003 #96, Kolesnick and Fuks 2003) and to leukemia (Kim et al 2008). We have not found a mutation in the neutral sphyingomyelinase 2 or acid sphyngomyelinase 3/4 genes of otg mutants, but defects in any of the other factors in this pathway may be responsible for the loss of irradiation sensitivity seen in *otg*.

Since the mutated gene responsible for the *otg* phenotype has not yet been identified, the genetic explanation for the dual phenotype of *otg* (leukemic predisposition and apoptosis resistance) remains an exciting mystery. Although *otg* was originally identified based on a leukemic predisposition phenotype in the adult, subsequent studies revealed an embryonic irradiation resistance phenotype that bolsters the impact of this mutation. Gaining a more comprehensive understanding of apoptosis-induction and the loss of apoptotic potential are becoming critical to the fields of cancer pathogenesis and treatment. For these reasons, *otg* is poised to be instrumental in informing diagnosis, prognosis, and treatment of leukemia.

Materials and methods

Zebrafish transgenic lines. The *otg* line of zebrafish was identified in a mutagenesis screen performed on *lck*::EGFP zebrafish on the WIK background as described previously (Frazer et al 2009). *rag2::hMYC-ER* zebrafish were a gift from Alejandro Gutierrez (DFCI, Boston, MA).

Imaging of adult leukemic zebrafish. Fluorescent imaging of adult leukemic zebrafish was done on an Olympus MVX10 microscope (Center Valley, PA). Images were taken using a Spot Insight 14.2 color mosaic camera (Diagnostic Imaging, Sterling Heights, MI) and Spot 4.6 software with the following color capture settings: Red:1; Green:2.5; Blue: 2.8

Dexamethasone treatment of adult leukemic zebrafish. Dexamethasone (DXM) was delivered by adding the drug directly to the fish water. Adult fish were kept in 1L bottles in 500mL of fish water (pH 7.2, conductivity of 500 μs,). Water was changed daily for 2 weeks with replacement of drug with each water change during the first 2 weeks, and fish were then placed back in water without drug after the treatment period. A high death rate (>75 %) was observed at initial DXM doses beyond 4μg/mL (10μM) (see Supplemental Table 1). As nonleukemic fish treated with the same dose survived without incident, we attributed the high death rate of leukemic fish to tumor lysis. We therefore established the following protocol using incremental increases of DXM dose: 0.5 μg/mL DXM for 7 days, then 2.0 μg/mL for 3 days, then 4.0 μg/mL for 4 days. Complete remission was defined as a total loss of recordable GFP signal as determined by our imaging settings (see above). A response to dexamethosone was defined as a decrease in GFP signal easily discernible by eye.

Radiation treatment of adult leukemic zebrafish. Adult zebrafish were placed, in ultracentrifuge bottles containing 250mL of fish water, in a ^{137}Cs source irradiator (Mark I-30 Irradiator, J.L. Shepherd and Associates, CA) and exposed to 6.25 Gy/minute. To achieve an exposure of 20Gy, fish were exposed to the source for 3.2 minutes.

Radiation treatment of zebrafish embryos. For high-dose irradiation (IR), embryos were placed in a ^{137}Cs source irradiator (Mark I-30 Irradiator, J.L. Shepherd and Associates, CA) and exposed to 25 Gy/minute for a total of 100Gy. For low-dose irradiation, embryos were exposed to 6.25 Gy/minute. Apoptosis was assayed at 6 hours following IR treatment by soaking embryos in 50 µg/mL of Acridine Orange (Sigma, St. Louis, Missouri) for 45 minutes and subsequent de-staining by washing in embryo water 5x 5mins.

Whole-mount zebrafish caspase-3 assay. After irradiation, embryos were fixed and prepared for staining as described previously (Jette et al 2008) with minor modifications. Anti-activated human Caspase-3 primary antibody was used at 1:500 dilutions (BD Biosciences, San Jose, CA) and goat anti-rabbit IgG Alexa Fluor 488 (Invitrogen, Carlsbad, CA) was used as a secondary antibody at 1:200.

Whole-mount zebrafish γ-H2Ax immunofluorescenc. γ-phosphorylated zebrafish histone H2Ax (γ-H2Ax) was detected using a polyclonal anti-γ-H2Ax antibody (1:500) that was generously provided by James Amatruda (University of Texas Southwestern, Dallas, TX), and an Alexa 488-conjugated secondary goat anti-rabbit antibody (1:1,000; Invitrogen, Carlsbad, CA). Staining was done according to Rhodes et al 2009 with minor modifications.

Embryo treatment with Chk1 *inhibitor, Gö6976*. Immediately before IR, 18-hpf embryos were dechorionated and transferred to fresh egg water containing 1% DMSO, with or without Gö6976 (1µM; Calbiochem, Gibbstown, NJ). Embryos were exposed to the inhibitor for 6 hrs, transferred to fresh egg water, rinsed in embryo water five times each for 5 min, and labeled with AO as described above.

Quantitative RT-PC. Analyses were performed using the Roche Lightcycler 480 II qRT-PCR system according to manufacturers instructions. All experiments were performed in triplicate, and normalized against the constitutively expressed zebrafish gene *efl*α. Primers for *puma* used were those published in (Parant et al 2010). Their sequences are listed below:

Ef1α_F: 5'-ctggaggccagctcaaacat-3'
Ef1α_R: 5'-atcaagaagagtagtaccgctagcattac-3'
Puma_F: 5'-acgctgtcttccttcagagg-3
Puma_R: 5'-cctgcagaaattcccagag-3'

Microinjections. Zebrafish one-cell stage embryos were injected with 10ng/μL (approximately 30pg/embryo), 3ng/μL (approximately 10pg/embryo), or 1ng/μL (approximately 3pg/embryo). To control for variation in the survival of embryos after the mechanical stress of injection, 0ng/μL mRNA (injection of dye only) control was included with each set of embryos injected. Surviving embryos were counted at 2h, 4h, and 24h after injection.

Sequencing of puma *coding regions.* RNA from pooled acridine orange-positive and -negative embryos was extracted using Trizol Reagent (Invitrogen, Carlsbad, CA) and cDNA was created using iscript cDNA from Bio-Rad (Hercules, CA). cDNA from *otg* and wild type embryos was amplified using the following primer sets and sent for immediate sequencing after nucleotide cleanup using QIAGEN PCR purification kit (Valencia, CA) at MC Labs, South San Francisco, CA:

Puma 5'UTR and untrans ex 1_F: 5' tgaaaggactttgctgtcatc 3'
Puma 5'UTR and untrans ex _R: 5' gtggtgcagagagagtgctg 3'
Puma Translated F: 5' tgtatgtggagcaggctaactg 3'
Puma Translated R: 5' cctgcagaaaaatcccagag 3'
Puma untrans exon 4_F: 5' acgctgtcttccttcagagg 3'
Puma untrans exon 4_R: 5' attgccaggtttttgtaccg 3'
Puma untrans exon 5A_F: 5' gggatcttgatctttcctcca 3'
Puma untrans exon 5A_R: 5' cgggggatttacatgatgac 3'
Puma untrans exon 5B_F: 5' tgcttcacatgcaagaatca 3'
Puma untrans exon 5B_R: 5' cgctcaataaattagcttgtgct 3'
Puma untrans exon 5C, 3'UTR_F: 5' acccctctccccatgataaa 3'
Puma untrans exon 5C, 3'UTR_R: 5' tcaactgactaacaataacaacacaaa 3'

Western blotting: Pooled embryos were dechorionated, then collected into phosphate buffered saline (1xPBS), and repeatedly cooled on ice for 5 minutes, agitated , and washed with 1xPBS 3 times to remove attached. De-yolked embryos were lysed using RIPA buffer containing benzonase (Novagen, Gibbstown, NJ) and protease inhibitors cocktail (Sigma, St. Louis, MO) Protein levels were assessed using a Bradford assay, and 50μg of protein was loaded into each

lane of a 15% SDS-PAGE gel. The gel was run at 120V for 70 minutes in 1x SDS buffer and transferred to a PVDF membrane for 2 hours at 100V at room temperature in a Bio-Rad transfer apparatus. Rabbit polyclonal anti-zebrafish Puma (a gift from Cicely Jette, Univ. of Utah) was used at 1:250 dilution, and a donkey anti-rabbit HRP-conjugated secondary antibody (Bio-Rad) was used at 1:10,000 dilution. Anti-histone H3 antibody (Abcam, Cambridge, MA) was used as a loading control at 1:2000.

References

Allan LA, Clarke PR (2009). Apoptosis and autophagy: Regulation of caspase-9 by phosphorylation. *FEBS J* **276:** 6063-6073.

Amatruda JF, Zon LI (1999). Dissecting hematopoiesis and disease using the zebrafish. *Dev Biol* **216:** 1-15.

Andreasson P, Schwaller J, Anastasiadou E, Aster J, Gilliland DG (2001). The expression of ETV6/CBFA2 (TEL/AML1) is not sufficient for the transformation of hematopoietic cell lines in vitro or the induction of hematologic disease in vivo. *Cancer Genet Cytogenet* **130:** 93-104.

Arico M, Basso G, Mandelli F, Rizzari C, Colella R, Barisone E *et al* (1995). Good steroid response in vivo predicts a favorable outcome in children with T-cell acute lymphoblastic leukemia. The Associazione Italiana Ematologia Oncologia Pediatrica (AIEOP). *Cancer* **75:** 1684-1693.

Armstrong SA, Look AT (2005). Molecular genetics of acute lymphoblastic leukemia. *J Clin Oncol* **23:** 6306-6315.

Ayllon V, Martinez AC, Garcia A, Cayla X, Rebollo A (2000). Protein phosphatase 1alpha is a Ras-activated Bad phosphatase that regulates interleukin-2 deprivation-induced apoptosis. *The EMBO journal* **19:** 2237-2246.

Chen J, Jette C, Kanki JP, Aster JC, Look AT, Griffin JD (2007). NOTCH1-induced T-cell leukemia in transgenic zebrafish. *Leukemia* **21:** 462-471.

Chiang CW, Kanies C, Kim KW, Fang WB, Parkhurst C, Xie M *et al* (2003). Protein phosphatase 2A dephosphorylation of phosphoserine 112 plays the gatekeeper role for BAD-mediated apoptosis. *Mol Cell Biol* **23:** 6350-6362.

De Keersmaecker K, Lahortiga I, Graux C, Marynen P, Maertens J, Cools J *et al* (2006). Transition from EML1-ABL1 to NUP214-ABL1 positivity in a patient with acute T-lymphoblastic leukemia. *Leukemia* **20:** 2202-2204.

Deriano L, Guipaud O, Merle-Beral H, Binet JL, Ricoul M, Potocki-Veronese G *et al* (2005). Human chronic lymphocytic leukemia B cells can escape DNA damage-induced apoptosis through the nonhomologous end-joining DNA repair pathway. *Blood* **105:** 4776-4783.

Dordelmann M, Reiter A, Borkhardt A, Ludwig WD, Gotz N, Viehmann S *et al* (1999). Prednisone response is the strongest predictor of treatment outcome in infant acute lymphoblastic leukemia. *Blood* **94:** 1209-1217.

Eimon PM, Ashkenazi A (2010). The zebrafish as a model organism for the study of apoptosis. *Apoptosis* **15:** 331-349.

Erlacher M, Michalak EM, Kelly PN, Labi V, Niederegger H, Coultas L *et al* (2005). BH3-only proteins Puma and Bim are rate-limiting for gamma-radiation- and glucocorticoid-induced apoptosis of lymphoid cells in vivo. *Blood* **106:** 4131-4138.

Fadeel B, Ottosson A, Pervaiz S (2008). Big wheel keeps on turning: apoptosome regulation and its role in chemoresistance. *Cell Death Differ* **15:** 443-452.

Ferrando AA, Neuberg DS, Staunton J, Loh ML, Huard C, Raimondi SC *et al* (2002). Gene expression signatures define novel oncogenic pathways in T cell acute lymphoblastic leukemia. *Cancer Cell* **1:** 75-87.

Frazer JK, Meeker ND, Rudner L, Bradley DF, Smith AC, Demarest B *et al* (2009). Heritable T-cell malignancy models established in a zebrafish phenotypic screen. *Leukemia* **23:** 1825-1835.

Fricker M, O'Prey J, Tolkovsky AM (2010). Phosphorylation of Puma modulates its apoptotic function by regulating protein stability
. *Cell Death & Disease* **1**.

Harrison CJ, Foroni L (2002). Cytogenetics and molecular genetics of acute lymphoblastic leukemia. *Rev Clin Exp Hematol* **6:** 91-113; discussion 200-112.

Hockenbery D, Nunez G, Milliman C, Schreiber RD, Korsmeyer SJ (1990). Bcl-2 is an inner mitochondrial membrane protein that blocks programmed cell death. *Nature* **348:** 334-336.

Jette CA, Flanagan AM, Ryan J, Pyati UJ, Carbonneau S, Stewart RA *et al* (2008). BIM and other BCL-2 family proteins exhibit cross-species conservation of function between zebrafish and mammals. *Cell Death Differ* **15:** 1063-1072.

Kerr JF, Wyllie AH, Currie AR (1972). Apoptosis: a basic biological phenomenon with wide-ranging implications in tissue kinetics. *Br J Cancer* **26:** 239-257.

Kerr JF, Winterford CM, Harmon BV (1994). Apoptosis. Its significance in cancer and cancer therapy. *Cancer* **73:** 2013-2026.

Kim H, Rafiuddin-Shah M, Tu HC, Jeffers JR, Zambetti GP, Hsieh JJ *et al* (2006). Hierarchical regulation of mitochondrion-dependent apoptosis by BCL-2 subfamilies. *Nat Cell Biol* **8:** 1348-1358.

Kim WJ, Okimoto RA, Purton LE, Goodwin M, Haserlat SM, Dayyani F *et al* (2008). Mutations in the neutral sphingomyelinase gene SMPD3 implicate the ceramide pathway in human leukemias. *Blood* **111:** 4716-4722.

Kolesnick R, Fuks Z (2003). Radiation and ceramide-induced apoptosis. *Oncogene* **22:** 5897-5906.

Kratz E, Eimon PM, Mukhyala K, Stern H, Zha J, Strasser A *et al* (2006). Functional characterization of the Bcl-2 gene family in the zebrafish. *Cell Death Differ* **13:** 1631-1640.

Langenau DM, Traver D, Ferrando AA, Kutok JL, Aster JC, Kanki JP *et al* (2003). Myc-induced T cell leukemia in transgenic zebrafish. *Science* **299:** 887-890.

Langenau DM, Ferrando AA, Traver D, Kutok JL, Hezel JP, Kanki JP *et al* (2004). In vivo tracking of T cell development, ablation, and engraftment in transgenic zebrafish. *Proc Natl Acad Sci U S A* **101:** 7369-7374.

Larson RA, Dodge RK, Linker CA, Stone RM, Powell BL, Lee EJ *et al* (1998). A randomized controlled trial of filgrastim during remission induction and consolidation chemotherapy for adults with acute lymphoblastic leukemia: CALGB study 9111. *Blood* **92:** 1556-1564.

Lowe SW, Lin AW (2000). Apoptosis in cancer. *Carcinogenesis* **21:** 485-495.

McDonnell TJ, Deane N, Platt FM, Nunez G, Jaeger U, McKearn JP *et al* (1989). bcl-2-immunoglobulin transgenic mice demonstrate extended B cell survival and follicular lymphoproliferation. *Cell* **57:** 79-88.

Meeker ND, Trede NS (2008). Immunology and zebrafish: spawning new models of human disease. *Dev Comp Immunol* **32:** 745-757.

Mione MC, Trede NS (2010). The zebrafish as a model for cancer. *Dis Model Mech* **3:** 517-523.

Palomero T, Lim WK, Odom DT, Sulis ML, Real PJ, Margolin A *et al* (2006). NOTCH1 directly regulates c-MYC and activates a feed-forward-loop transcriptional network promoting leukemic cell growth. *Proc Natl Acad Sci U S A* **103:** 18261-18266.

Parant JM, George SA, Holden JA, Yost HJ (2010). Genetic modeling of Li-Fraumeni syndrome in zebrafish. *Dis Model Mech* **3:** 45-56.

Ploner C, Schmidt S, Presul E, Renner K, Schrocksnadel K, Rainer J *et al* (2005). Glucocorticoid-induced apoptosis and glucocorticoid resistance in acute lymphoblastic leukemia. *J Steroid Biochem Mol Biol* **93:** 153-160.

Pui CH (1998). Recent advances in the biology and treatment of childhood acute lymphoblastic leukemia. *Curr Opin Hematol* **5:** 292-301.

Pui CH, Relling MV, Downing JR (2004). Acute lymphoblastic leukemia. *N Engl J Med* **350:** 1535-1548.

Rhodes J, Amsterdam A, Sanda T, Moreau LA, McKenna K, Heinrichs S *et al* (2009). Emi1 maintains genomic integrity during zebrafish embryogenesis and cooperates with p53 in tumor suppression. *Mol Cell Biol* **29:** 5911-5922.

Sedelnikova OA, Rogakou EP, Panyutin IG, Bonner WM (2002). Quantitative detection of (125)IdU-induced DNA double-strand breaks with gamma-H2AX antibody. *Radiat Res* **158:** 486-492.

Sidi S, Sanda T, Kennedy RD, Hagen AT, Jette CA, Hoffmans R *et al* (2008). Chk1 suppresses a caspase-2 apoptotic response to DNA damage that bypasses p53, Bcl-2, and caspase-3. *Cell* **133:** 864-877.

Takeuchi J, Kyo T, Naito K, Sao H, Takahashi M, Miyawaki S *et al* (2002). Induction therapy by frequent administration of doxorubicin with four other drugs, followed by intensive consolidation and maintenance therapy for adult acute lymphoblastic leukemia: the JALSG-ALL93 study. *Leukemia* **16:** 1259-1266.

Teitell MA, Pandolfi PP (2009). Molecular genetics of acute lymphoblastic leukemia. *Annu Rev Pathol* **4:** 175-198.

Tissing WJ, Meijerink JP, den Boer ML, Pieters R (2003). Molecular determinants of glucocorticoid sensitivity and resistance in acute lymphoblastic leukemia. *Leukemia* **17:** 17-25.

Traver D, Winzeler A, Stern HM, Mayhall EA, Langenau DM, Kutok JL *et al* (2004). Effects of lethal irradiation in zebrafish and rescue by hematopoietic cell transplantation. *Blood* **104:** 1298-1305.

Vaux DL, Cory S, Adams JM (1988). Bcl-2 gene promotes haemopoietic cell survival and cooperates with c-myc to immortalize pre-B cells. *Nature* **335:** 440-442.

Weng AP, Ferrando AA, Lee W, Morris JPt, Silverman LB, Sanchez-Irizarry C *et al* (2004). Activating mutations of NOTCH1 in human T cell acute lymphoblastic leukemia. *Science* **306:** 269-271.

Yang E, Zha J, Jockel J, Boise LH, Thompson CB, Korsmeyer SJ (1995). Bad, a heterodimeric partner for Bcl-XL and Bcl-2, displaces Bax and promotes cell death. *Cell* **80:** 285-291

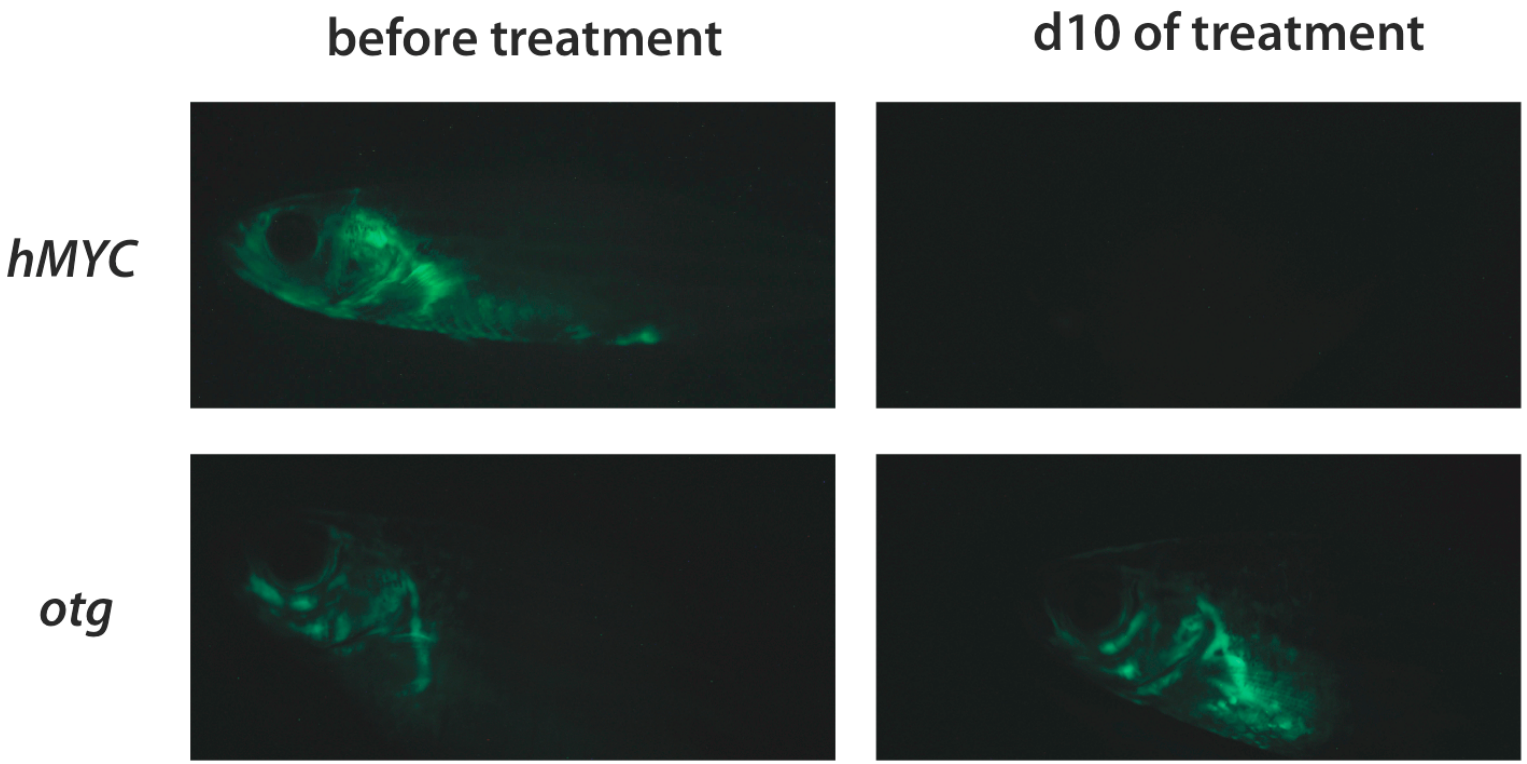

Figure 4.1. ***otg*** **leukemic fish respond poorly to dexamethasone treatment.** Leukemic hMYC (n=17) and *otg* fish (n=8) were treated with dexamethasone for 14 days. Dosing was incremental: 0.5 µg/mL DXM for 7 days, 2.0 µg/mL for 3 days, and 4.0 µg/mL for 4 days. 15/17 hMYC fish responded by 14 days after the start of treatment, while only 2/8 *otg* responded. Representative images of the two treatment groups are shown.

Figure 4.2. Single dose radiation treatment of hMYC **and *otg* leukemic fish.** (a) Representative fluorescent images of hMYC and *otg* leukemi fish treated with a single dose of 20Gy of γ-irradiation . While both fish achieve complete remission from this single dose, the *otg* fish relapsed by 10 days post treatment and the hMYC fish did not relapse until 60 days after irradiation. (b) hMYC fish were treated with a number of different doses to determine the smallest single dose able to induce remission in all fish. This dose was determined to be 10Gy. (c) Leukemic hMYC (n=7) and otg (n=6) were treated with a single 10Gy dose of γ-radiation. A graph of relapse percentages shows that all of the hMYC fish achieved remission with this dose, while only 83% of the *otg* fish achieved complete remission. Additionally, nearly all hMYC fish either remained in complete remission throughout the 60-day study (5/7) with 2 fish relapsing at 49 and 60 days after treatment. Of the 5 *otg* fish who attained remission, 2 relapsed as early as 12 days after treatment, while all had relapsed by 60 days.

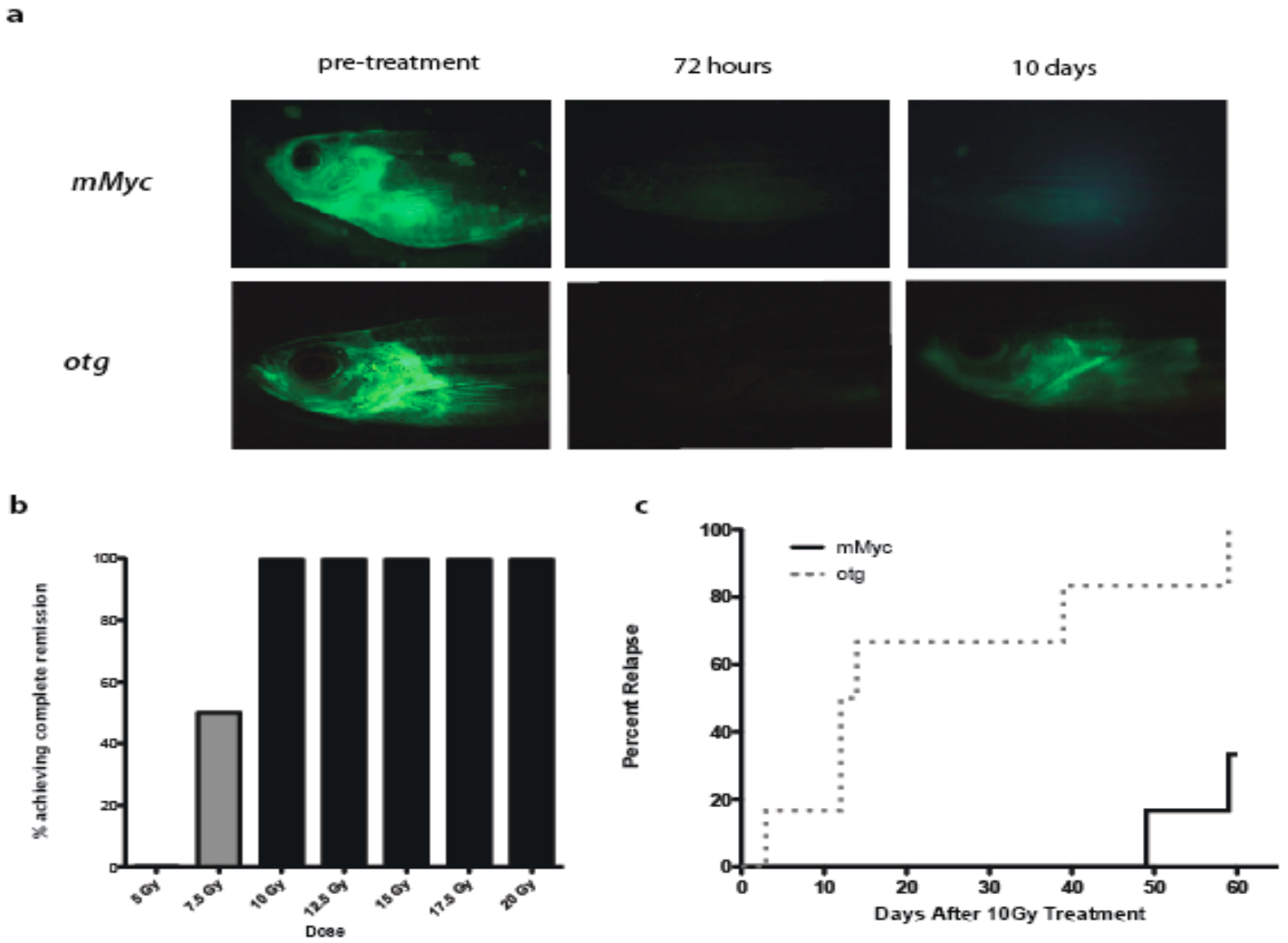
a
pre-treatment
72 hours
10 days
mMyc
otg
b
% achieving complete remission
100
80
60
40
20
0
5 Gy
7.5 Gy
10 Gy
12.5 Gy
15 Gy
17.5 Gy
20 Gy
Dose
c
Percent Relapse
100
80
60
40
20
0
mMyc
otg
0
10
20
30
40
50
60
Days After 10Gy Treatment

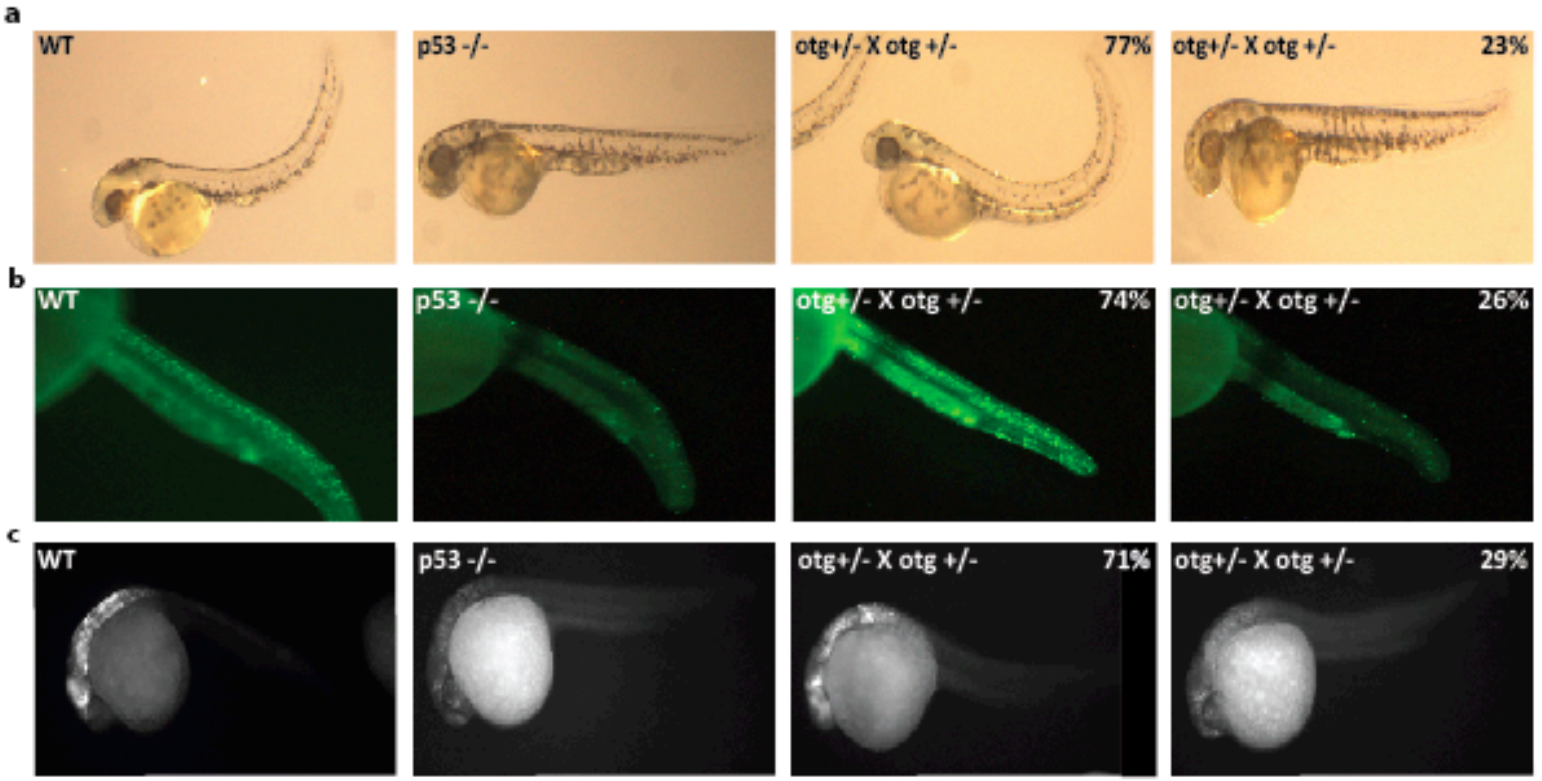

Figure 4.3. Demonstration of resistance to irradiation-induced in *otg* zebrafish embryos. Embryos at 30hpf (a) or 18hpf (b,c) wild type, *p53*$^{-/-}$ and mixed *otg* heterozygous embryos were exposed to 100Gy (a) or 12.5Gy (b,c) of γ–irradiation. After 6 hours, embryos in (a) were sorted based on tail curl phenotype. In (b), following irradiation, embryos were treated with acridine orange at 50ug/mL and sorted based on acridine orange staining in the head and tails. In clutches from *otg*$^{+/-}$ parents, 74% of offspring had high levels of acridine orange staining, and 26% had low levels. In (c) embryos 6 hp irradiation were fixed and stained with a polyclonal anti-human activated caspase 3 antibody. After staining, embryos from *otg*$^{+/-}$ incrosses were sorted based on fluorescence with 71% of embryos having high levels of anti-activated caspase 3 stain, and 29% having low levels

Figure 4.4. Double strand break repair and Chk1 signaling are normal in *otg* mutant zebrafish embryos. (a) 30hpf *otg* embryos were irradiated with 100Gy then fixed at 10, 20, 30, or 40 minutes after irradiation and stained with a polyclonal anti-γH2Ax antibody. Recruitment of γH2Ax increased after irradiation and reached a maximum at 30 minutes post exposure. No difference was detected between *otg* embryos and wild type embryos. (b) *p53*$^{-/-}$ and *otg* embryos were irradiated at 18hpf with 12.5Gy then treated with the chk1 inhibitor Gö6976 for 6 hours and s.2tained with acridine orange. (c) While *p53*$^{-/-}$ embryos were re-sensitized to irradiation-induced apoptosis after Gö6976 treatment, *otg* embryos were not.

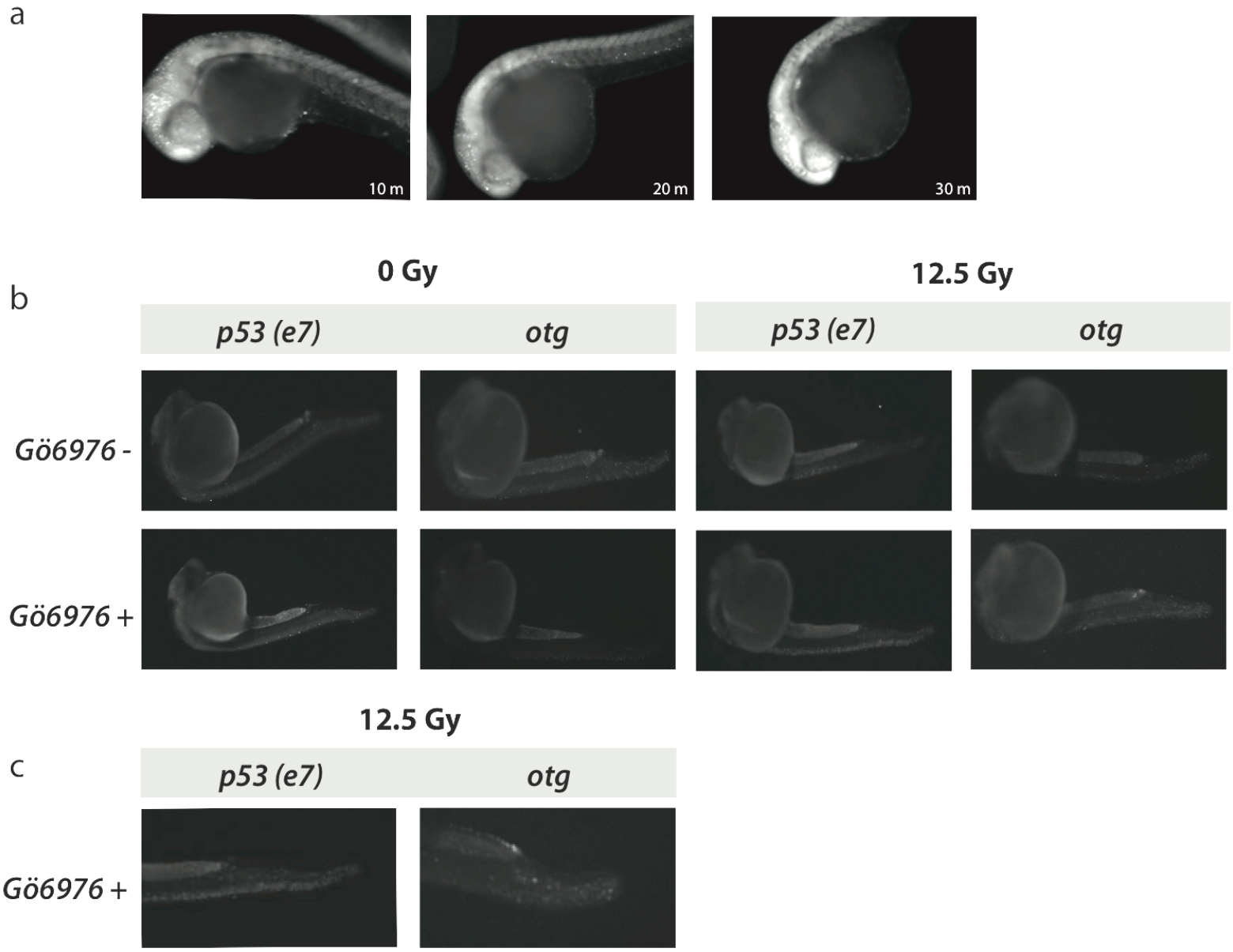
a
10 m
20 m
30 m
b
0 Gy
12.5 Gy
p53 (e7)
otg
p53 (e7)
otg
Gö6976 -
Gö6976 +
c
12.5 Gy
p53 (e7)
otg
Gö6976 +

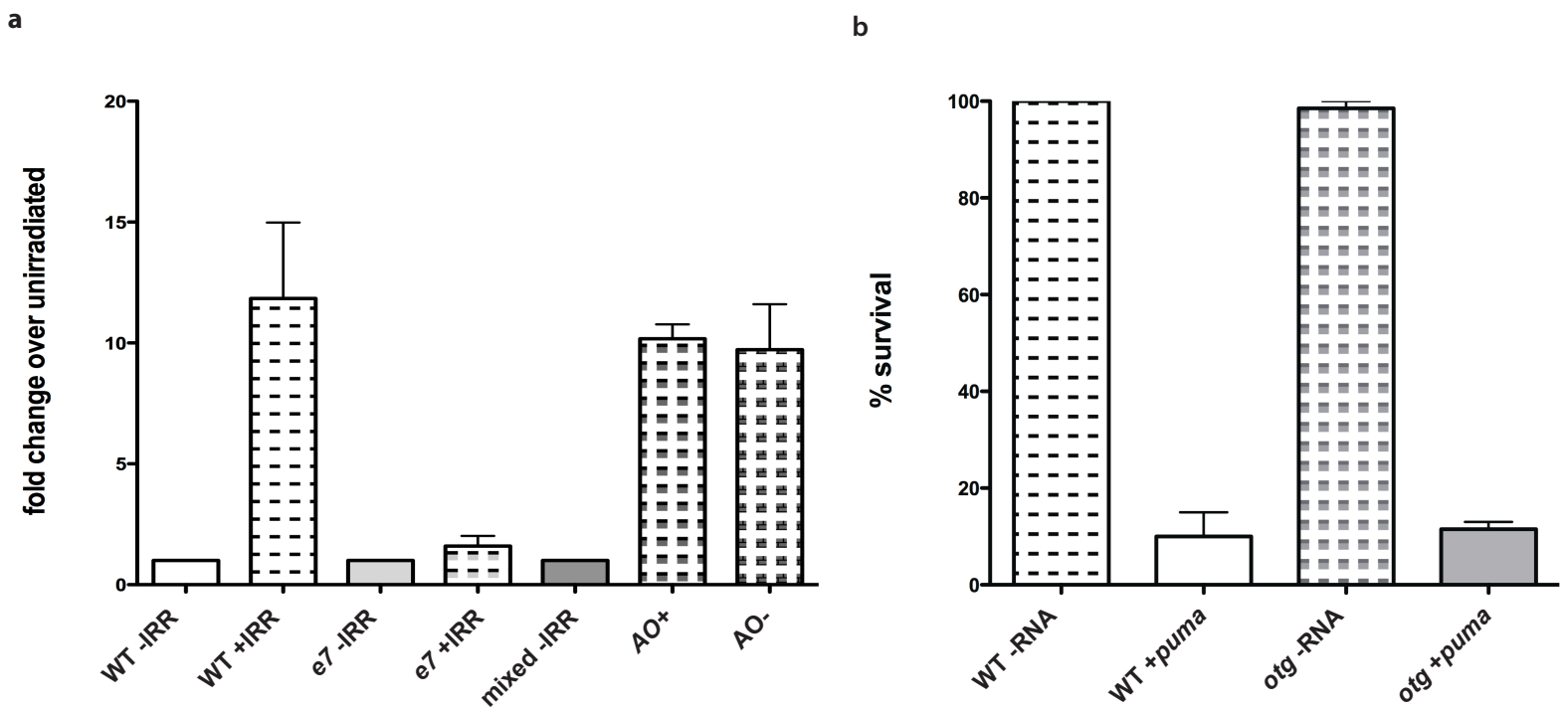

Figure 4.5. *puma* mRNA expression and induction of apoptosis are normal in *otg* embryos. (a) 18hpf wild type and *otg* embryos were irradiated with 12.5Gy, and 6 hours after irradiation *puma* mRNA expression was analyzed by qRT-PCR. Irradiation induced the expression of *puma* mRNA in both, wild type and *otg* embryos, at greater than 12 times baseline levels. (b) When *puma* mRNA was injected into single cell *otg* embryos, apoptosis ensued and embryos became degraded within 2 hours, an effect that mirrored that in wild type embryos.

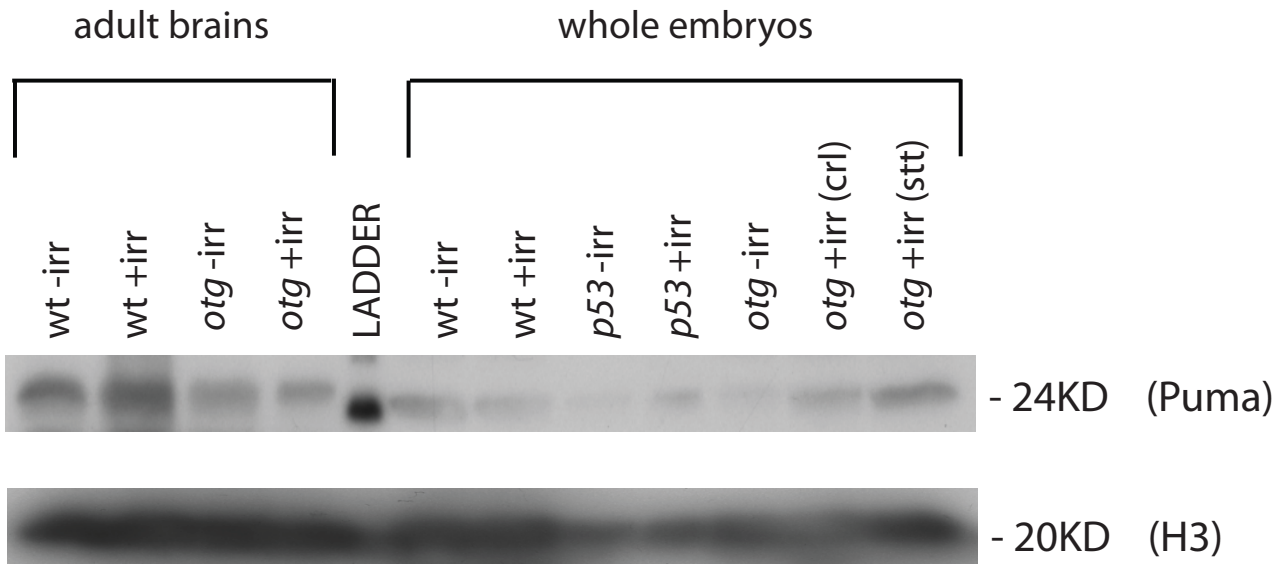

Figure 4.6. PUMA protein expression is normal in *otg* adults and embryos after irradiation. Wild type and *otg* adults and 24hpf embryos were irradiated with 100Gy and protein lysates were prepared 8 hours after irradiation. Puma protein was detected by probing with a rabbit anti-zebrafish polyclonal antibody. Adult brains and whole embryos of both wild type and *otg* fish showed expression of Puma protein, regardless of genotype. Zebrafish Puma protein is approximately 24kD, and histone H3 was used as a loading control (20kD).

Table 4.1. Dexamethasone treatment of hMYC and otg leukemic fish

Fish	strain	d14 response	d21 response	d28 response
5-10	hMYC	CR	CR	VGPR
5-11	hMYC	VGPR	VGPR	CR
5-12	hMYC	VGPR	VGPR	VGPR
5-13	hMYC	CR	CR	VGPR
5-14	hMYC	VGPR	VGPR	VGPR
5-15	hMYC	GPR	GPR	GPR
6-15	hMYC	GPR	GPR	GPR
6-16	hMYC	VGPR	VGPR	VGPR
7-1	hMYC	died d1	n/a	n/a
7-2	hMYC	VGPR	VGPR	CR
7-3	hMYC	PR	Rel	Rel
8-1	hMYC	died d9	n/a	n/a
8-2	hMYC	CR	n/a	n/a
8-3	hMYC	CR	CR	n/a
9-1	hMYC	VGPR	PR	PR
9-2	hMYC	CR	CR	CR
9-3	hMYC	VGPR	n/a	n/a
7-1	*otg*	NR	n/a	n/a
7-2	*otg*	NR	NR	NR
7-3	*otg*	NR	NR	n/a
7-4	*otg*	PR	NR	NR
8-1	*otg*	NR	NR	NR
8-2	*otg*	NR	NR	NR
9-1	*otg*	CR	PR	PR
9-2	*otg*	NR	NR	NR

NR = no response; PR = partial response; GPR = good partial response; VGPR = very good partial response; CR = complete remission; n/a = not applicable due to death by time-point

Supplemental Table 1. Titration of Dexamethasone Exposure in hMYC Zebrafish

No. of Fish	Exposure (µg/ml)	Death Rate (%)	Response Rate By d21
4	250	4 (100%)	
4	100	4 (100%)	
4	10	3 (75%)	3
4	2	1 (25%)	4
4	1	0	4
9	1(7d) + 4(7d)	2 (22%)	9
6	1(7d) + 2(3d) + 4(4d)	3 (50%)	6
6	1qOD(7d) + 2(3d) + 4(4d)	3 (50%)	6
17	0.5(7d) + 2(3d) + 4(4d)	2 (12%)	15

CHAPTER 5

SHARED ACQUIRED GENOMIC CHANGES IN ZEBRAFISH AND HUMAN T-ALL

Lynnie A. Rudner[1], Kim H. Brown[2], Kimberly P. Dobrinski[2], Diana F. Bradley[1], Jonathan Downie[1], Nathan D. Meeker[3], Alexandra Smith[1], Martha Iveth Garcia[4], Alejandro Gutierrez[5], Charles Mullighan[6], A. Thomas Look[7], James R. Downing[8], Joshua D. Schiffman[9], Charles Lee[10], Nikolaus Trede[11] and J. Kimble Frazer[12]

[1]Department of Oncological Sciences, University of Utah, Salt Lake City, UT; [2]Department of Pathology, Brigham and Women's Hospital, Boston, MA; [3]Department of Pediatrics, University of Utah, Salt Lake City, UT; [4]University of Texas, Brownsville, Brownsville; [5]Dana Farber Cancer Institute, Somerville, MA; [6]Dept. of Pathology, MS #342, St. Jude Children's Rsch. Hosp., Memphis, TN; [7]Pediatric Oncology, Dana-Farber Cancer Institute, Boston, MA; [8]Pathology, St Jude Children's Research Hospital, Memphis, TN; [9]Pediatric Hematology/Oncology, University of Utah, Salt Lake City, UT; [10]Pathology, Harvard Medical School-BWH, Boston, MA; [11]Department of Pediatrics/Department of Oncological Sciences, University of Utah, Salt Lake City, UT; [12]Department of Pediatrics/Department of Oncological Sciences, University of Utah, Salt Lake City

Corresponding Author: J. Kimble Frazer MD, PhD
Huntsman Cancer Institute
2000 Circle of Hope
Salt Lake City, Utah 84112
Kimble.frazer@hsc.utah.edu
Tel: 801-587-5599

Abstract

T cell acute lymphoblastic leukemia (T-ALL) is a challenging entity with high rates of induction failure and relapse. To discover genetic changes occurring in T-ALL, and those contributing to relapse, we studied zebrafish (*Danio rerio*) T-ALL samples using array comparative genomic hybridization (aCGH). We performed aCGH on 17 T-ALLs, representing 4 zebrafish T-ALL models, and evaluated similarities between humans and zebrafish by comparing all *D. rerio* genes with copy number aberrations (CNAs) to a cohort of 75 published human T-ALLs analyzed by aCGH. Within these *D. rerio* CNAs, we identified 893 genes with human homologues and found significant overlap (63%) with the human dataset. In addition, when we restricted our analysis to primary T-ALLs (14 zebrafish and 61 human samples), 10 genes were recurrently altered in >3 zebrafish samples and $\geq$4 human T-ALL cases, suggesting a conserved role for these loci in T-ALL transformation across species. We also conducted iterative allo-transplantations with 3 zebrafish malignancies. This technique selects for particularly aggressive disease, results in shorter survival times in successive transplant rounds, and models refractory and relapsed human T-ALL. Fifty-five percent of original CNAs were preserved after serial transplantation, demonstrating shared clonality between each primary and passaged leukemia. Additionally, T-ALLs acquired an average of 34 CNAs during passaging. Genes in these loci may underlie the enhanced malignant behavior of these neoplasias. We also compared genes found in CNAs of passaged zebrafish malignancies to human aCGH results from 50 T-ALL patients who failed induction, eventually relapsed, or already had relapsed. Again, many genes (88/164) overlapped in both datasets. Additionally, 9 genes altered in 2 of 3 passaged *D. rerio* samples were also found in several human T-ALL cases. These results suggest that zebrafish and human T-ALLs are similar at the genomic level, and are governed by factors that have persisted throughout evolution.

Introduction

Genomic alterations are a prominent feature of cancer, and include aneuploidy, chromosomal translocations, and focal amplifications and deletions. Some changes foster oncogenic transformation, while others favor the outgrowth of specific sub-clones in an already established neoplasia (Mullighan et al 2008). Gain or loss of certain genes can promote tumor development, metastasis, drug resistance, or other clinically pertinent features. Finally, specific genomic changes associated with a particular malignancy type may correlate with prognosis (Armstrong and Look 2005). Consequently, the identification of recurrent genomic anomalies contributes to our understanding of cancer.

To detect acquired CNAs, aCGH has been widely applied to human cancers (Pinkel and Albertson 2005) and is likewise amenable to model organisms (Hodgson et al 2001, Maydan et al 2007, Thomas et al 2007). Recently, zebrafish (*Danio rerio*) aCGH genomic platforms have become available. An initial *D. rerio* array contained 286 BAC clones enriched for homologous human oncogene and tumor suppressor sequences, with an approximate 5 Mb resolution (Freeman et al 2009). Newer high-density oligonucleotide arrays based on more accurate genomic assemblies (Peterson and Freeman 2009), have even greater resolution.

As vertebrates, zebrafish share most human genes and these genes usually have conserved actions. Specifically, many *D. rerio* homologues of human oncogenes and tumor suppressors also have the same function, making this organism an excellent model to study human cancers (Mione and Trede 2010). Supporting this, several transgenic zebrafish lines that mis-express mammalian oncogenes develop near-identical malignancies to humans (Chen et al 2007, Langenau et al 2003, Langenau et al 2007, Patton et al 2005, Sabaawy et al 2006). Moreover, in studies of zebrafish cancers, CNAs with putative *D. rerio* oncogenes and tumor suppressors are readily detected (Freeman et al 2009).

For zebrafish to be an optimal model to study human cancer, the genes in *D. rerio* CNAs must be pertinent to human disease. CNAs containing homologous genes from the same tumor

type across both species may identify unappreciated players in human neoplasia. To test this hypothesis, we performed aCGH on 17 zebrafish T-ALL samples and compared results to aCGH findings in human T-ALL (Gutierrez et al 2010a, Mullighan et al 2007, Mullighan et al 2008). We concentrated on recurrently-altered genes in both human and zebrafish cancers, and those genes shared by leukemias with particularly malignant clinical behavior. Collectively, these analyses show a striking overlap between T-ALL CNA genes across species, and support zebrafish as a model pertinent to human leukemogenesis and disease progression.

Results and discussion

We used aCGH to detect somatically-acquired CNAs in 17 zebrafish T-ALLs. These represent cancers from 4 *D. rerio* genetic models: 1 transgenic line mis-expressing murine *c-Myc* (*mMyc*) (Langenau et al 2005) and 3 mutant lines with heritable T-ALL predisposition (*hlk*, *srk*, *otg*) (Frazer et al 2009). Genomic DNA of non-malignant tissue from each cancer-bearing fish was used as a hybridization control to eliminate detection of inherited germline copy number variants (CNVs). T cell receptor (TCR) loci on chromosomes 2 and 17 served as internal controls (Supp. Figure 1), as deletions normally occur in these regions during T cell receptor recombination. (Haire et al 2000, Meeker et al 2010, Schorpp et al 2006). TCR deletions and other CNAs from wild-type *D. rerio* T cells (pooled from 25 zebrafish) were eliminated from consideration in subsequent analyses, as they are unlikely oncogenic (processing algorithm detailed in Supplemental Materials and Methods).

Using two zebrafish aCGH platforms, a total of 840 cancer-specific CNAs were detected comprised of 335 amplifications and 505 deletions, averaging 49.4 total CNAs per sample (Supp. Table 5.1, Supp. Figure 5.2a in Supp. Files). Eight T-ALLs were hybridized to a NimbleGen oligonucleotide array; a higher-density Agilent array was used for 9 other *D. rerio* samples. Amplifications and deletions averaged 197 and 135 kb, respectively. Depictions of all 17

zebrafish T-ALL genomes and pooled normal T cells are shown in Supplemental Figures 5.1 and 5.3 (please see Supp. Files).

We investigated 3 *D. rerio* cancers by aCGH using a unique approach only possible in an animal model. We iteratively passaged these T-ALLs (one leukemia from each of the *srk, hlk*, and *otg* lines) by serial allo-transplantation [(Frazer et al 2009, Rudner et al 2010) and Figure 1a]. Our prior studies have shown that iterative transplantation of small numbers of cells ($1x10^5$) selects for aggressive disease, with recipient survival times declining in subsequent rounds. We hypothesize that *in vivo* passaging favors aggressive sub-clones comprising a minor fraction of the original malignancy. It may also select for new mutations that promote more aggressive disease features. In another zebrafish T-ALL model, individual cells have been shown to act as leukemic stem cells to transmit disease (Smith et al 2010). This approach would eliminate clonal selection and optimize isolation of new mutations. However, because clonal evolution and new mutations are both integral to relapse in human patients (Choi et al 2007, Mullighan et al 2008, Panzer-Grumayer et al 2005), we opted to impose a 100,000 cell bottleneck. We believe that using a small number of donor cells allows both processes to occur, mimicking the clinical scenario of human T-ALL relapse where rare clones repopulate the leukemic pool as suggested previously (Ren et al 2009).

We compared these 3 "passaged" T-ALLs to their "primary" counterparts. In these 6 cancers, new CNAs were observed that could be linked to aggressive clinical behavior (Figure 5.1b and Supp. Figure 5.3 in Supp. Files). Overall, serially-transplanted T-ALLs had a comparable number of CNAs (62.0 vs. 51.3; Supp. Table 5.2). Many CNAs of *de novo* T-ALLs (55%) were preserved in their passaged counterpart, demonstrating the clonal relationship between paired leukemias. Serially-transplanted cancers lost 45% of CNAs present in the primary, which may indicate that these were "passenger" events that did not contribute to oncogenesis. In addition, this phenomenon suggests the outgrowth of a dominant clone (or clones) lacking some CNAs present in the original. Passaged clones display more aggressive *in*

vivo behavior [(Frazer et al 2009, Rudner et al 2010) and Figure 1a], and genetic changes in derivative cancers may identify loci responsible for this phenotypic drift. In this study, we detected 101 new CNAs (54% of CNAs in serially-transplanted T-ALLs), that are putatively linked to increased aggressiveness.

To explore similarities in genomic instability between *D. rerio* and human T-ALL, we examined aCGH results from 75 human T-ALL samples obtained from 61 patients. These patients were from 3 cohorts: Children's Oncology Group Study P9404, n=40; Dana Farber Cancer Institute Acute Lymphoblastic Leukemia Consortium Protocol 00-01, n=7; St. Jude Cancer Research Hospital (SJCRH) patients treated from 1995-2003, n=14 (Gutierrez et al 2010a, Mullighan et al 2007). The SJCRH cohort also contributed aCGH results from the same 14 patients using DNA acquired at relapse. In total, these 75 T-ALL samples had 1578 CNAs (mean 24.2/genome), with 510 amplifications and 1068 deletions (Supp. Figure 5.2b in Supp. Files and Supp. Table 5.1). The prevalence of CNAs and relative frequency of deletions vs. amplifications were quite similar in human and zebrafish T-ALLs (Supp. Table 5.1). Zebrafish CNAs were smaller and more abundant than those in human T-ALLs, but these differences likely derive from disparate genome sizes, inaccuracy of the *D. rerio* genomic assembly, and varying probe densities in the different hybridization platforms used.

To compare the two datasets, we focused on "CNA genes" common to human and zebrafish T-ALL. To identify homologous genes shared by both species' CNAs, we first identified every known *D. rerio* gene located within all 840 CNAs of our 17 zebrafish malignancies. From this list, we removed genes located in aneuploid chromosomes or other lesions >3 Mb, and from CNAs seen in normal T cells. Overall, 29% (5/17) of *D. rerio* T-ALLs had at least one trisomy, and others had large amplifications or deletions that we also excluded (details in Supp. methods). This degree of genomic instability was similar to human T-ALLs, where 25% (19/75) were aneuploid. This paring resulted in a list of 943 genes from CNAs of one or more *D. rerio* T-ALL (Supp. Table 5.3). We then manually ascertained whether human

homologues existed for these 943 genes using online databases and search tools (Supp. methods). Over 98% (n=926) of these genes had human counterparts, permitting a thorough cross-species comparison and emphasizing the high conservation between these two vertebrates.

We compared this list to CNA genes of the 75 human T-ALLs described above. Of the 926 zebrafish CNA genes, 33 were seen in human germline CNVs and removed from analysis (see Supp. Methods), leaving 893 homologous gene pairs. Of these 893 *D. rerio* genes, 558 (62.5%) were also amplified or deleted in at least 1 human T-ALL (Table 5.1). Because human studies used single nucleotide polymorphism microarrays, loss of heterozygosity (LOH) was also detected in human T-ALL cohorts. If copy-neutral LOH events were also considered, even greater overlap was seen between the *D. rerio* and human datasets (597/893; 66.9%).

Because many human genes occurred in at least one T-ALL CNA, the significance of this concordance is diminished. Therefore, we focused only on genes recurrently altered in both *D. rerio* and human T-ALL. We compared CNA genes present in more than 1 zebrafish T-ALL to human homologues present in multiple cases (Table 5.1). Of the 558 CNA genes in T-ALLs of both species, 253 were seen in 2 or more *D. rerio* samples, and of these, 94 (37.2%) also occurred in at least 2 human T-ALLs. Applying these same criteria more stringently, 65 CNA genes were found in $\geq$3 zebrafish cancers, with 26/65 (40%) occurring in at least 2 human T-ALLs and 15/65 (23.1%) seen in $\geq$5 human cases. The intersection of these two datasets holds great potential to discover key genes fundamental to T cell malignancy.

In the prior analysis, we identified recurring CNA genes from primary, passaged, and relapsed T-ALLs of both species. We next refined this dataset by restricting our comparison to only primary T-ALLs. Of the 75 human samples, 61 were primary T-ALLs. We compared CNA genes from these cases to those in our 14 zebrafish primaries. From our initial set of 926 zebrafish CNA genes, 768 genes derived from primary cancers. Of these, 472 (61.5%) occurred in at least one human primary T-ALL CNA (Table 5.1). We next concentrated on recurrent CNA genes from *D. rerio* and human T-ALL. Nearly half of these 472 shared CNA genes (218; 46.2%) were

seen in multiple human cases (Table 5.1). To distinguish the most promising candidates, we identified CNA genes seen in multiple human and *D. rerio* primaries. Ten genes occurred in ≥3 zebrafish and ≥4 human T-ALLs (Supp. Table 5.4). This short list may represent unrecognized oncogenic factors in T-ALL, as their repeated occurrence in CNAs of these divergent species is unlikely to be coincidental. CNAs of these 10 genes were not only recurrent, but also focal, further suggesting that these genes may be oncogenic drivers. High resolution depictions of all zebrafish CNAs seen involving 4 of these genes are shown in Figure 5.2 (please see Supp. Files).

One of these genes, *TGFBR1* (seen in 5 *D. rerio* and 7 human samples), has already been implicated in T-ALL by aCGH (Remke et al 2009). Other genes with established roles in T-ALL [*NOTCH1, PHF6, HES1*; (Van Vlierberghe et al 2010, Weng et al 2004, Weng et al 2006)] occurred as focal CNAs in single zebrafish samples. Additionally, CNAs containing the T-ALL oncogenes *LYL1*, *TAL1*, *TAL2*, *HES6*, *MLL4*, and *JAK2* were also seen, but were excluded from our analysis since they derived from large chromosomal gains. However, despite these similarities in T-ALL biology, the other 9 recurring genes in both species (Supp. Table 5.4) are not yet recognized as important factors in T-ALL, although they are frequently rearranged in human cases (Gutierrez et al 2010a, Gutierrez et al 2010b, Mullighan et al 2007, Remke et al 2009).

Curiously, several genes with known oncogenic properties in human T-ALL, such as *CDKN2A, CDKN2B, PTEN, LEF1, WT1,* and *MYB*/*AHI1*, were not seen in zebrafish. *CDKN2A*, the gene most often deleted in human T-ALL (Sulong et al 2009), is not present in *D. rerio*, so its absence from our analysis was expected; the absence of *CDKN2B* deletions may suggest differences between the two species. Additionally, genomic rearrangements are only one means to disrupt normal gene function, and loci absent from CNAs may still be perturbed by other mechanisms. The absence of CNAs involving *MYB*/*AHI1, LEF1, PTEN*, and *WT1* from 17 *D. rerio* T-ALLs is not statistically compelling, as CNAs of these genes are infrequent in human cases (<12%). Moreover, both *PTEN* and *WT1* are duplicated *in trans* in the zebrafish genome.

This redundancy may obviate their roles as lynchpins in *D. rerio* T-ALL, as deletion of all 4 copies of either tumor suppressor is unlikely. Notably, CNAs of PTEN-induced putative kinase 1 (*pink1*) occurred repeatedly in *D. rerio* (3/17; 17.6%), possibly representing an alternative mechanism to disrupt Pten function. Finally, 2 other CNA genes in *D. rerio* T-ALL, *prkca* and *tfdp1*, were not found in the 75 human cases used for comparison, but CNAs of their homologues have been reported in other human T-ALLs (Remke et al 2009).

As a final comparison, we identified CNA genes from serially-passaged zebrafish T-ALLs and analyzed them with respect to relapsed human cases. Amplified and deleted genes of passaged, but not primary, T-ALLs may explain transformed cells' acquisition of new aggressive features. Our transplantation model creates highly malignant T-ALLs, and uses *in vivo* selection, which preserves biologic constraints absent in cell culture. In this respect, our experimental system mimics aspects of clinical relapse [(Frazer et al 2009, Rudner et al 2010), and Figure 5.1a].

We passaged 3 T-ALLs (1 *hlk*, 1 *srk*, and 1 *otg*) until each cancer rapidly engrafted and killed all recipients (in the 3 series, recipient death occurred 14.7 days earlier, on average, in the final round: 13.2 vs. 27.9 days). Final-passage and primary leukemic samples were then analyzed by aCGH to detect newly-acquired CNAs (Figure 5.1b and Supp. Figure 5.3 in Supp. Files) that contained a total of 164 *D. rerio* genes with human homologues. Remarkably, 9 of the 164 genes were altered in 2 passaged T-ALLs (Supp. Table 5.4), a significant finding as these leukemias derived from different mutant lines. Furthermore, 8 of these 9 genes were not seen in any *D. rerio* primary T-ALL, suggesting they may not be required for oncogenesis. Rather, these genes are predicted to contribute to malignant progression by our assay.

We also compared these 164 genes to the human dataset. Because passaged cancers represent the most aggressive zebrafish T-ALLs, we focused on human cases with the worst outcomes – induction failures and relapses. Cancers in these human cases persisted despite multi-agent treatment, and their CNA genes may be candidates contributing to therapeutic failure.

Specifically, we evaluated CNA genes from samples of patients who achieved remission but later relapsed (n=27), relapsed samples themselves (n=14), and 9 patients who failed induction (Table 2). In aggregate, these 50 samples had CNAs of 88/164 (53.7%) genes from our passaged T-ALLs. All of the 9 recurring genes from passaged zebrafish T-ALLs were also present as human CNA genes. In fact, all 9 genes were still coincident when we limited analysis to only the 23 worst cases (14 relapses and 9 induction failures). Moreover, 8 of the 9 genes occurred in multiple cases of poor outcome human T-ALL, with 6/9 seen in $\geq$5 cases (Supp. Table 5.4). Remarkably, CNAs of these genes were common in relapsed and induction failure cases, but rarely occurred in 25 cases that achieved event free survival (Supp. Table 5.4). Thus, CNAs of these loci correlate strongly with T-ALL treatment failure.

These 9 genes, encountered repeatedly in CNAs from aggressive disease in both species, may be prognostic factors in human T-ALL. Additionally, CNAs of these loci may not only predict therapeutic failure, but also identify pathways governing poor outcome at the molecular level. Together with the 10 recurring CNA genes shared by primary zebrafish and human T-ALLs, our cross-species comparisons have identified a short list of genes of potential importance to T cell malignancy. Further testing is needed to interrogate this premise, but our data clearly suggest that critical genetic similarities exist between these species' cancers, and that fundamental properties governing oncogenesis and disease progression have persisted over eons of evolution.

Conflict of interest

The authors declare no conflict of interest.

Acknowledgements

The authors wish to thank Brett Milash and Ken Boucher for expert bioinformatics and statistical assistance, respectively. NST was supported by NIAID award R21-AI079784 and the

Huntsman Cancer Foundation. JKF was supported by Eunice Kennedy Shriver NICHD award K08-HD053350, the CHRC at the University of Utah, and the PCMC Foundation. Huntsman Cancer Institute core facilities supported by NCI P30-CA042014 also contributed to this work.

References

Armstrong SA, Look AT (2005). Molecular genetics of acute lymphoblastic leukemia. *J Clin Oncol* **23:** 6306-6315.

Chen J, Jette C, Kanki JP, Aster JC, Look AT, Griffin JD (2007). NOTCH1-induced T-cell leukemia in transgenic zebrafish. *Leukemia* **21:** 462-471.

Choi S, Henderson MJ, Kwan E, Beesley AH, Sutton R, Bahar AY *et al* (2007). Relapse in children with acute lymphoblastic leukemia involving selection of a preexisting drug-resistant subclone. *Blood* **110:** 632-639.

Frazer JK, Meeker ND, Rudner L, Bradley DF, Smith AC, Demarest B *et al* (2009). Heritable T-cell malignancy models established in a zebrafish phenotypic screen. *Leukemia* **23:** 1825-1835.

Freeman JL, Ceol C, Feng H, Langenau DM, Belair C, Stern HM *et al* (2009). Construction and application of a zebrafish array comparative genomic hybridization platform. *Genes Chromosomes Cancer* **48:** 155-170.

Gutierrez A, Dahlberg SE, Neuberg DS, Zhang J, Grebliunaite R, Sanda T *et al* (2010a). Absence of biallelic TCRgamma deletion predicts early treatment failure in pediatric T-cell acute lymphoblastic leukemia. *J Clin Oncol* **28:** 3816-3823.

Gutierrez A, Sanda T, Ma W, Zhang J, Grebliunaite R, Dahlberg S *et al* (2010b). Inactivation of LEF1 in T-cell acute lymphoblastic leukemia. *Blood* **115:** 2845-2851.

Haire RN, Rast JP, Litman RT, Litman GW (2000). Characterization of three isotypes of immunoglobulin light chains and T-cell antigen receptor alpha in zebrafish. *Immunogenetics* **51:** 915-923.

Hodgson G, Hager JH, Volik S, Hariono S, Wernick M, Moore D *et al* (2001). Genome scanning with array CGH delineates regional alterations in mouse islet carcinomas. *Nat Genet* **29:** 459-464.

Langenau DM, Traver D, Ferrando AA, Kutok JL, Aster JC, Kanki JP *et al* (2003). Myc-induced T cell leukemia in transgenic zebrafish. *Science* **299:** 887-890.

Langenau DM, Feng H, Berghmans S, Kanki JP, Kutok JL, Look AT (2005). Cre/lox-regulated transgenic zebrafish model with conditional myc-induced T cell acute lymphoblastic leukemia. *Proc Natl Acad Sci U S A* **102:** 6068-6073.

Langenau DM, Keefe MD, Storer NY, Guyon JR, Kutok JL, Le X *et al* (2007). Effects of RAS on the genesis of embryonal rhabdomyosarcoma. *Genes & development* **21:** 1382-1395.

Maydan JS, Flibotte S, Edgley ML, Lau J, Selzer RR, Richmond TA *et al* (2007). Efficient high-resolution deletion discovery in Caenorhabditis elegans by array comparative genomic hybridization. *Genome Res* **17:** 337-347.

Meeker ND, Smith AC, Frazer JK, Bradley DF, Rudner LA, Love C *et al* (2010). Characterization of the zebrafish T cell receptor beta locus. *Immunogenetics* **62:** 23-29.

Mione MC, Trede NS (2010). The zebrafish as a model for cancer. *Dis Model Mech* **3:** 517-523.

Mullighan CG, Goorha S, Radtke I, Miller CB, Coustan-Smith E, Dalton JD *et al* (2007). Genome-wide analysis of genetic alterations in acute lymphoblastic leukaemia. *Nature* **446:** 758-764.

Mullighan CG, Phillips LA, Su X, Ma J, Miller CB, Shurtleff SA *et al* (2008). Genomic analysis of the clonal origins of relapsed acute lymphoblastic leukemia. *Science* **322:** 1377-1380.

Panzer-Grumayer ER, Cazzaniga G, van der Velden VH, del Giudice L, Peham M, Mann G *et al* (2005). Immunogenotype changes prevail in relapses of young children with TEL-AML1-positive acute lymphoblastic leukemia and derive mainly from clonal selection. *Clin Cancer Res* **11:** 7720-7727.

Patton EE, Widlund HR, Kutok JL, Kopani KR, Amatruda JF, Murphey RD *et al* (2005). BRAF mutations are sufficient to promote nevi formation and cooperate with p53 in the genesis of melanoma. *Curr Biol* **15:** 249-254.

Peterson SM, Freeman JL (2009). Cancer cytogenetics in the zebrafish. *Zebrafish* **6:** 355-360.

Pinkel D, Albertson DG (2005). Comparative genomic hybridization. *Annu Rev Genomics Hum Genet* **6:** 331-354.

Remke M, Pfister S, Kox C, Toedt G, Becker N, Benner A *et al* (2009). High-resolution genomic profiling of childhood T-ALL reveals frequent copy-number alterations affecting the TGF-beta and PI3K-AKT pathways and deletions at 6q15-16.1 as a genomic marker for unfavorable early treatment response. *Blood* **114:** 1053-1062.

Ren M, Li X, Cowell JK (2009). Genetic fingerprinting of the development and progression of T-cell lymphoma in a murine model of atypical myeloproliferative disorder initiated by the ZNF198-fibroblast growth factor receptor-1 chimeric tyrosine kinase. *Blood* **114:** 1576-1584.

Rudner LA, Frazer JK, Trede NS (2010). Modeling human hematologic malignancies in zebrafish: A review. *Current Trends in Immunology*.

Sabaawy HE, Azuma M, Embree LJ, Tsai HJ, Starost MF, Hickstein DD (2006). TEL-AML1 transgenic zebrafish model of precursor B cell acute lymphoblastic leukemia. *Proc Natl Acad Sci U S A* **103:** 15166-15171.

Schorpp M, Bialecki M, Diekhoff D, Walderich B, Odenthal J, Maischein HM *et al* (2006). Conserved functions of Ikaros in vertebrate lymphocyte development: genetic evidence for distinct larval and adult phases of T cell development and two lineages of B cells in zebrafish. *J Immunol* **177:** 2463-2476.

Smith AC, Raimondi AR, Salthouse CD, Ignatius MS, Blackburn JS, Mizgirev IV *et al* (2010). High-throughput cell transplantation establishes that tumor-initiating cells are abundant in zebrafish T-cell acute lymphoblastic leukemia. *Blood* **115:** 3296-3303.

Sulong S, Moorman AV, Irving JA, Strefford JC, Konn ZJ, Case MC *et al* (2009). A comprehensive analysis of the CDKN2A gene in childhood acute lymphoblastic leukemia reveals genomic deletion, copy number neutral loss of heterozygosity, and association with specific cytogenetic subgroups. *Blood* **113:** 100-107.

Thomas R, Duke SE, Bloom SK, Breen TE, Young AC, Feiste E *et al* (2007). A cytogenetically characterized, genome-anchored 10-Mb BAC set and CGH array for the domestic dog. *J Hered* **98:** 474-484.

Van Vlierberghe P, Palomero T, Khiabanian H, Van der Meulen J, Castillo M, Van Roy N *et al* (2010). PHF6 mutations in T-cell acute lymphoblastic leukemia. *Nat Genet* **42:** 338-342.

Weng AP, Ferrando AA, Lee W, Morris JPt, Silverman LB, Sanchez-Irizarry C *et al* (2004). Activating mutations of NOTCH1 in human T cell acute lymphoblastic leukemia. *Science* **306:** 269-271.

Weng AP, Millholland JM, Yashiro-Ohtani Y, Arcangeli ML, Lau A, Wai C *et al* (2006). c-Myc is an important direct target of Notch1 in T-cell acute lymphoblastic leukemia/lymphoma. *Genes & development* **20:** 2096-2109.

Figure 5.1. Serial transplantation shows clonal evolution of aggressive disease. T-ALL cells from 1 donor *otg* fish were sequentially passaged through 5 iterations of irradiated hosts. 1 x10^5 cells were transplanted into each recipient. (a) Kaplan-Meier survival curves for engrafted fish are plotted [1st host cohort, n=11 (red); 2nd cohort, n=8 (blue); 5th cohort, n=10 (green); rounds 3 and 4 are not shown for clarity]. One fish from each cohort (not plotted) was sacrificed to be the donor for the next transplant series. Recipients had statistically significant differences in mean survival duration for each transplant round (p values listed in figure). (b) Partial genomic representations (Chromosomes 18-25) of the *otg* primary T-ALL donor and a 5th passage T-ALL. aCGH results are normalized to non-malignant tissue DNA of the original donor. Red lines depict deletions, green lines reflect amplifications, and line lengths correspond to heterozygous vs. homozygous deletions. Most CNAs are common to both samples, demonstrating clonality. CNAs gained or lost in 5th passage may reflect selection of a sub-clone that was a minor population of the original T-ALL and/or new CNA events. Some new CNAs may underlie the more malignant phenotype of the 5th passage. Copy number analysis and figure graphics were created using Nexus5 Copy Number software.

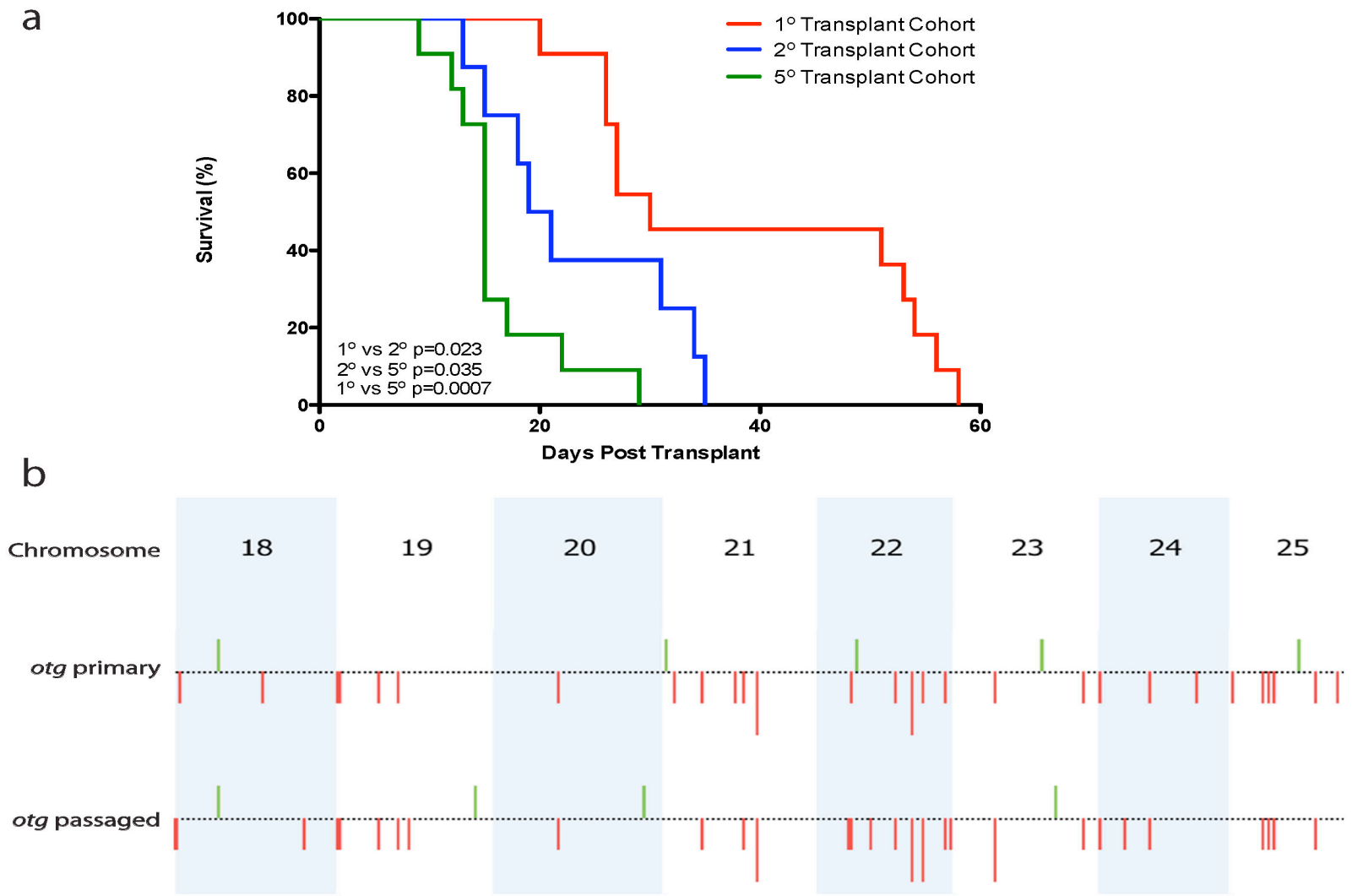
a
100
80
60
40
20
0
Survival (%)
0
20
40
60
Days Post Transplant
1° Transplant Cohort
2° Transplant Cohort
5° Transplant Cohort
1° vs 2° p=0.023
2° vs 5° p=0.035
1° vs 5° p=0.0007
b
Chromosome
18
19
20
21
22
23
24
25
otg primary
otg passaged

Table 5.1. Shared CNA Genes in Zebrafish and Human T-ALL

Shared CNA Genes in 17 *D. rerio* and 75 Human T-ALLs

Occurrence in CNAs of 17 *D. rerio* T-ALLs:	**≥1 *D. rerio* T-ALL**	**Only 1 *D. rerio* T-ALL**	**≥2 *D. rerio* T-ALLs**	**≥3 *D. rerio* T-ALLs**	**≥4 *D. rerio* T-ALLs**	**≥5 *D. rerio* T-ALLs**
# of genes with human homologues	893	640	253	65	26	6
# in human T-ALL, gain or loss only (% of total)	558 (62.5%)	395 (61.7%)	163 (64.4%)	38 (58.5%)	19 (73.1%)	4 (66.7%)
# in human T-ALL, gain, loss, or LOH (% of total)	597 (66.9%)	414 (64.7%)	183 (72.3%)	45 (69.2%)	20 (76.9%)	5 (83.3%)
Occurrence in CNAs of 75 human T-ALLs:						
shared genes in ≥1 human T-ALL	558	395	163	38	19	4
shared genes in ≥2 human T-ALLs	347	253	94	26	11	3
shared genes in ≥5 human T-ALLs	126	86	40	15	7	2
shared genes in ≥6 human T-ALLs	77	50	27	9	7	2

Shared CNA Genes in 14 *D. rerio* and 61 Human Primary T-ALLs

Occurrence in CNAs of 14 *D. rerio* primary T-ALLs:	**≥1 *D. rerio* T-ALL**	**Only 1 *D. rerio* T-ALL**	**≥2 *D. rerio* T-ALLs**	**≥3 *D. rerio* T-ALLs**	**≥4 *D. rerio* T-ALLs**
# of genes with human homologues	768	528	240	63	25
# in human T-ALL, gain or loss only (% of total)	472 (61.5%)	326 (61.7%)	146 (60.8%)	35 (55.6%)	18 (72.0%)
# in human T-ALL, gain, loss, or LOH (% of total)	505 (65.8%)	344 (65.2%)	161 (67.1%)	42 (66.7%)	19 (76.0%)
Occurrence in CNAs of 61 human primary T-ALLs:					
shared genes in ≥1 human T-ALL	472	326	146	35	18
shared genes in ≥2 human T-ALLs	218	150	68	24	11
shared genes in ≥4 human T-ALLs	93	72	21	10	7

Table 5.2. Shared CNA Genes of Passaged *D. rerio* T-ALL and Poor-Outcome Human T-ALL

Occurrence in passaged *D. rerio* T-ALLs (n=3):	**≥1 *D. rerio* T-ALL**	**Only 1 *D. rerio* T-ALL**	**2 *D. rerio* T-ALLs**
# of genes with human homologues	164	155	9
Poor Clinical Outcomes (all non-EFS cases; n=50)			
# of genes shared by poor-outcome human T-ALL CNAs; gain or loss only (% of total)	76 (46.3%)	70 (45.2%)	6 (66.7%)
# of genes shared by poor-outcome human T-ALL CNAs; gain, loss, or LOH (% of total)	88 (53.7%)	79 (51.0%)	9 (100%)
Destined-to-Relapse (DFCI, COG, or SJCRH cases who would relapse; n=27)			
# of genes shared by destined-to-relapse human T-ALL CNAs; gain or loss only (% of total)	48 (29.3%)	42 (27.1%)	6 (66.7%)
# of genes shared by destined-to-relapse human T-ALL CNAs; gain, loss, or LOH (% of total)	54 (32.9%)	47 (30.3%)	7 (77.8%)
Poorest Clinical Outcomes (n=23) [induction failures (n=9) and relapsed T-ALL samples (n=14)]			
# of genes shared by poorest-outcome human T-ALL CNAs; gain or loss only (% of total)	69 (42.1%)	64 (41.3%)	5 (55.6%)
# of genes shared by poorest-outcome human T-ALL CNAs; gain, loss, or LOH (% of total)	83 (50.6%)	74 (47.7%)	9 (100%)

Supplemental material

Leukemic cell isolation and FACS. GFP^+ leukemic tissues were dissected under fluorescent microscopy into Zebrafish Kidney Stromal media. Single cell suspensions were made by pipetting, filtering through SmallParts 35 m filters (Miramar, FL, USA), and final passing through 70m Filcon filters (Becton Dickinson, San Jose, CA, USA) before analysis. Flow cytometry and fluorescence-activated cell sorting (FACS) were as described (Frazer, Meeker Rudner et al. 2009) using a BD FACSVantage instrument (Becton Dickinson). GFP intensity, forward- and side-scatter were used for gating. Cells were collected into Zebrafish Kidney Stromal media.

Serial transplantation. Tumors were dissected and cells prepared as above. GFP^+ cells were FACS-purified, diluted in Zebrafish Kidney Stromal media and concentrations confirmed by hemocytometer counts. Using a ^{137}Cesium source, hosts were irradiated with 25 Gy, and intra-peritoneally injected 2 days later with 1x 10^5 of FAC-sorted GFP^+ cells in injection volumes of 10 ul. Recipients were monitored by serial fluorescence microscopy to follow engraftment and disease progression.

Array comparative genome hybridization and imaging. After FACS collection, total genomic DNA was extracted from collected cells as well as individual matched tail clips using the DNeasy Blood & Tissue Kit (Qiagen Inc., Valencia, CA). DNA collected from the tail clips was used as a reference (i.e. cancerous test vs. non-cancerous control) to determine CNVs using a self-self hybridization to reduce potential inter-individual effects. After heat denaturation, genomic DNA (500 ng) from the test and reference sample was labeled with Cy5-dCTP or Cy3-dCTP by random priming using the BioPrime Labeling Kit (Invitrogen, Carlsbad, CA), in which fluorescently labeled nucleotides are incorporated during genomic DNA replication. Unincorporated nucleotides were removed using Amicon Ultra 0.5 mL 30K filters (Millipore) prior to the determination of DNA concentration and dye incorporation. For array hybridization,

3.5 µg of labeled tumor DNA was co-precipitated with 3.5 µg of reference DNA at a total volume of 79 µl, 25 µl of herring sperm DNA, 26 µl of blocking agent and 130 µl of hybridization solution were combined and denatured at 95°C for 3 minutes. Samples were then pre-hybridized at 37°C for 30 minutes before being placed on custom Agilent zebrafish arrays. Arrays were placed in individual hybridization chambers and hybridized for 40 hours at 65°C.

After hybridization, the cover slips were removed by placing the slide into Oligo aCGH wash buffer I. Slides were then transferred into a second container of Oligo aCGH wash buffer I at room temperature containing a stir bar at 120 RPMs and washed for 3 minutes. Following the first wash slides were transferred to a preheated container of Oligo aCGH wash buffer II at 37°C circulating as above for 1 minute. Slides were then slowly removed from the solution to prevent streaking and placed directly into the scanner for processing. A two-color scan of the arrays was conducted using the Agilent G2565CA Microarray Scanner System with SureScan High Resolution Technology (Agilent Technologies, Inc., Santa Clara, CA) at a 3 µm resolution. Images were then analyzed using Agilent Feature Extraction software which normailizes the Cy3 and Cy5 fluorescence intensities across the array and quantifies each DNA probe for color intensities and background intensity to produce Cy3/Cy5 $\log_2$ ratios.

Array analysis. Copy-number analysis using the Rank Segmentation algorithm and group comparisons were performed employing the BioDiscovery Nexus Copy Number 5.0 software (BioDiscovery, El Segundo CA, USA). Copy-number analysis was performed using a significance threshold (p- value) of 1x10-6 and a minimal grouping of 3 affected adjacent probes. Thresholds for gains and losses were set such that aneuploidies were recordable, and deletions in the T cell receptor regions were visible in at least 90% of samples.

For zebrafish analysis, Nexus-produced CNA calls were refined by removal of regions of "self-self" hybridization, when > 3Mb were amplified or deleted, or where CNAs were also present in normal zebrafish T lymphocytes.

Sample	Event	Boundaries
hlk 1	trisomy	chr 6
srk 3	trisomy	chr 8
srk 3	amplification	chr23:0-4,075,864
otg 1	trisomy	chr 23
hlk 4	trisomy	chr 6
hlk 4	trisomy	chr 21
hlk 4	trisomy	chr 23
hlk 4	amplification	chr1:19,044,570-24,073,766
mMyc	trisomy	chr 19

A gene list was created first by identifying genes altered in these CNAs on both the NimbleGen and Agilent platforms, and then cross referencing them to Zv6 and Zv8, respectively, to determine the most current official zebrafish gene names. Each zebrafish gene was then cross referenced to the NCBI human genome database 36.1 or sequence-searched by BLAST to determine a homologous human gene. Zebrafish genes who share homology with a single human gene were only counted once. The human gene list was then used to analyze human T-ALL datasets by using the "Query" function of Nexus 5.

Human Datasets: Two human T-ALL datasets were used. The first dataset includes 47 patients treated on Children's Oncology Group study P9404 or Dana-Farber Cancer Institute study 00-01 clinical trials. Among these 25 experienced event free survival, 9 showed induction failure, and 13 eventually relapsed (Gutierrez et al. 2010a). The second was paired primary and relapse samples from 14 T-ALL treated at St Jude Children's Research Hospital between 1993 and 2005 (Mullighan et al. 2007). Eight of these 14 patients also contributed a germline sample for aCGH, and genes found to be altered in these germline samples were not included in the comparison with zebrafish T-ALLs.

Supplemental Table 5.1. CNAs Observed in Zebrafish and Human T-ALLs

17 Zebrafish T-ALLs	**Total CNAs**	**Amplifications**	**Deletions**
Nimblgen (n=8)	176	117	59
average (range)	22.0 (4-68)	14.6 (1-54)	7.4 (2-14)
average size (bp)		210,165	72,810
Agilent (n=9)	664	218	446
average (range)	73.8 (28-143)	24.2 (7-81)	49.6 (22-105)
average size (bp)		189,639	143,276
Summary (n=17)	840	335	505
average	49.4	19.7	29.7
average size (bp)		196,808	135,044

75 Human T-ALLs	**Total CNAs**	**Amplifications**	**Deletions**
Agilent 244K (n=47)	509	130	379
average (range)	17.8 (9-35)	3.4 (0-11)	14.4 (9-25)
average size (bp)		2,661,949	4,108,918
Affymetrix 500K (n=8) or snp6 (n=20)	1069	380	689
average (range)	35.3 (3-90)	11.6 (0-37)	25.1 (3-72)
average size (bp)		1,759,019	1,914,300
Summary (n=75)	1578	510	1068
average	24.2	6.4	18.3
average size (bp)		1,989,178	2,693,102

Supplemental Table 5.2. Zebrafish Primary and Passaged T-ALL CNAs

	Primary T-ALLs (n=3)	**Passaged T-ALLs (n=3)**
Total # of CNAs	154	186
Average # of CNAs (range)	51.3 (31-89)	62.0 (28-119)
Primary-only CNAs (% of total)	69 (45%)	n/a
Average # of CNAs (range)	23.0 (15-34)	
Passaged-only CNAs (% of total)	n/a	101 (54%)
Average # of CNAs (range)		33.7 (17-64)
Shared Primary and Passaged CNAs	85 (55%)	85 (46%)
Average # of CNAs (range)	avg. 28.3 (11-55)	avg. 28.3 (11-55)

Supplemental Table 5.3. Algorithm for Identifying *D.rerio* CNA Genes with Human Homologues

Algorithm Processing Step		***D. rerio* T-ALL CNA Genes**
NimbleGen platform (8 samples)		311
	(+)	
Agilent platform (9 samples)		759
	(=)	
# of Genes in ≥1 CNA on either platform		1070
	(-)	
# of Genes present in CNAs on both platforms		127
	(=)	
Total # of unique CNA genes		943
	(-)	
Genes lacking human homolgues		15
Genes not found on human genome build 36.1		2
	(=)	
D. rerio CNA genes with human homologues		926
	(-)	
Genes with human germline CNVs		33
	(=)	
Analyzable homolgous gene pairs		893

Supplemental Table 5.4. Recurrent CNA genes in *D. rerio* and Human T-ALLs

Shared and recurrent CNA genes in zebrafish (n=14) and human (n=61) primary T-ALLs

***D. rerio* gene**	**# of *D. rerio* T-ALLs with gene in CNA**	**Human gene**	**# of human T-ALLs (n=61) with gene in CNA (inc. LOH)**	**# of human EFS T-ALLs (n=25) with gene in CNA (inc. LOH)**	**# of human poor-outcome primary T-ALLs (n=36) with gene in CNA (inc. LOH)**
col15a1	5 (35.7%)	*COL15A1*	5 (6)	4 (4)	1 (2)
tgfbr1b	5	*TGFBR1*	5 (6)	4 (4)	1 (2)
lrp6	4 (28.6%)	*LRP6*	6 (7)	3 (3)	3 (4)
zgc:158374	4	*MANSC1*	6 (7)	3 (3)	3 (4)
osr2	4	*OSR2*	6 (6)	2 (2)	4 (4)
zgc:66488	4	*FBXO43*	6 (6)	2 (2)	4 (4)
pus7	4	*PUS7*	4 (4)	2 (2)	2 (2)
matn4	3 (21.4%)	*MATN2*	4 (4)	2 (2)	2 (2)
zgc:65779	3	*RNF170*	4 (6)	2 (2)	2 (4)
zgc:77727	3	*TOR1A*	4 (4)	3 (3)	1 (1)

Shared and recurrent CNA genes of passaged zebrafish (n=3) and poorest-outcome human (n=23) T-ALLs

***D. rerio* gene**	**# of *D. rerio* T-ALLs with gene in CNA**	**Human gene**	**# of human T-ALLs (n=75) with gene in CNA (inc. LOH)**	**# of human EFS T-ALLs (n=25) with gene in CNA (inc. LOH)**	**# of human poor-outcome T-ALLs (n=50) with gene in CNA (inc. LOH)**
zgc:153606	2 (66.7%)	*C7orf60*	7 (7)	1 (1)	6 (6)
zgc:158222	2	*AHCYL2*	6 (7)	1 (1)	5 (6)
zgc:114085	2	*ERGIC1*	6 (7)	1 (1)	5 (6)
flt4	2	*FLT4*	6 (7)	1 (1)	5 (6)
ckmt1	2	*CKMT1A*	0 (5)	0 (0)	0 (5)
ckmt1	2	*CKMT1B*	0 (5)	0 (0)	0 (5)
zgc:112384	2	*WBP4*	2 (2)	0 (0)	2 (2)
katnb1	2	*KATNB1*	3 (3)	1 (1)	2 (2)
zgc:113984	2	*HIST2H3C*	0 (1)	0 (0)	0 (1)

CHAPTER 6

CONCLUSION

Treatment for acute lymphoblastic leukemia (ALL) overall has improved dramatically over the past 50 years. With the advent of current multi-agent chemotherapy, survival of pediatric patients with many forms of ALL has improved from single digits to over 80% (Silverman and Sallan 2003), but T-ALL lags behind with pediatric cure rates of only 70% (Pui 1998) and adult survival <40% (Larson et al 1998, Takeuchi et al 2002).

The underlying etiology of T-cell malignancies is driven by a complex combination of genetic changes (Ferrando et al 2002.) Specific molecular alterations that are responsible for lymphocyte oncogenesis has come from the discovery of aberrant chromosomal translocations and activation of particular pathways in blast cells of ALL patients (Armstrong and Look 2005, Pui and Evans 1998). While a number of contributing translocations have been described (Ferrando and Look 2000) most cases still are not explained by these cytogenetic aberrations (Graux et al 2006, Harrison and Foroni 2002). Transcription factor mis-expression has also been implicated in T-ALL (Ferrando et al 2002) but the genetic lesions underlying this dysregulation are still unidentified.

Considerable evidence suggests that genetic modifiers can act as risk factors for leukemia, but few heritable mutations conferring this risk are actually known (Goldgar et al 1994). Identification of the loci responsible for these familial cases could help explain the mechanisms underlying malignancies of the same type. This has been a challenge to do in human

pedigrees, with their small sample sizes. Therefore, animal models of heritable leukemic predisposition were needed.

Zebrafish are becoming a well-accepted model in which to study cancer, particularly hematological neoplasias, since the immune systems of humans and zebrafish are strikingly similar (Amatruda and Zon 1999, Trede et al 2004). Prior to studies done in our lab, two transgenic models have used cell-specific over-expression of mammalian proto-oncogenes (NOTCH and MYC) to induce zebrafish T-ALL (Chen et al 2007, Langenau et al 2003). These cancers faithfully recapitulate human disease that originate in the thymus and possibly kidney marrow and spread to peripheral blood. Although these models are innovative, they are restricted in scope to the known cancer pathways used to create them.

My thesis project has continued to prove the suitability of zebrafish in the study of immunologic cancers. It consists of work that identifies and characterizes three new hereditary models of T-ALL in the zebrafish (Frazer et al 2009). In addition, it delineates the pathway dysregulated in one of these heritable models. Finally, my work has shown that genomic studies done in our models can to cross boundaries between model-organisms and humans in order to identify potentially important, but as yet unstudied, factors that may underlie oncogenesis and relapse in T-ALL.

Our approach to unravel unknown genetic lesions underlying T-cell malignancy through a mutagenesis screen in the zebrafish is novel. To facilitate detection of T cell over-proliferation, we used a *D. rerio* line that fluorescently reports T cells due to the $p56^{lck}$::EGFP transgene (Frazer et al 2009). In this work, we reported identification of three different zebrafish mutants that all develop heritable T-cell malignancy. We showed that each faithfully recapitulates human T cell disease in onset, invasion pattern, and morphology, and that their neoplastic cells are clonal and transplantable. Moreover, cells from each malignancy can also be transplanted serially (Frazer et al 2009, Rudner et al 2010), suggesting the presence of leukemia-initiating cells (LICs).

Once identified and characterized, these zebrafish models of T cell malignancy have proved useful in understanding the pathways involved in oncogenesis of T-ALL. My thesis work has focused on determining the factors that contribute to disease progression in *otg* fish. Due to the similarities we observed between *otg* and human T-ALL, we were able to test therapies that are used in humans to better understand whether the same pathways are altered in this disease, and to open the doors for testing preclinical compounds in the future. By testing the efficacy of DXM and single dose irradiation treatment (XRT), both of which induce apoptosis in T-ALL, I determined that some zebrafish T-ALL lines are susceptible to these human therapies, while the T-ALL of *otg* fish is more resistant and relapses sooner. Next, I determined that *otg* embryos are also resistant to whole-body radiation, suggesting that the mutation underlying *otg* creates a global block in apoptosis. By examining the intrinsic apoptosis pathway carefully, my thesis work has narrowed the possible candidates underlying this mutation to a block in post-mitochondrial caspase 3-mediated apoptosis.

A mutation in any of a number of factors might result in the phenotype exhibited by *otg* embryos, as well as correlate with a predisposition to leukemia. Resistance to glucocorticoid treatment has been observed in ALL in humans, and studies have linked the upregulation of glycolysis in these leukemic cells to prednisolone resistance (Hulleman et al 2009). An alteration in this pathway may underlie *otg*. Additionally, in T-ALL particularly, expression levels of the GLUT1 glucose transporter, ATP citrate lyase, a critical enzyme in tumors that links glucose metabolism to lipid synthesis and hexokinase II, responsible for coordinating metabolic and apoptotic pathways at the mitochondrial membrane have also been observed to be significantly correlated with steroid resistance (Beesley et al 2009).

Other pro-apoptotic factors may also be responsible. Bad, a pro-apoptotic member of the Bcl-2 family of proteins, has been shown previously to enhance sensitivity to radiation-induced apoptosis in zebrafish embryos (Jette et al 2008). A loss of function of this factor might occur by a direct mutation, or by a loss of function of the phosphatase required for its activation. Once

activated, Bad allows for activation of post-mitochondrial apoptosis to occur. This cascade, beginning with the activation of cytochrome C, and culminating with the effector caspases 9 and 3 is very well studied in both mammals (Eimon and Ashkenazi 2010), however assays to investigate mitochondrial activation and cytochrome c mobilization in zebrafish are just beginning to be developed (Kim et al 2008). While we have determined that the sequence of a number of post-mitochondrial apoptosis factors are normal in *otg* embryos (including *apaf-1, xiap, casp9, casp3*) the possibility exists that correct message may not be translated into a functional protein. An investigation of the localization and accumulation of these proteins by immunohistochemistry or western blotting may shed light on whether this transition is occurring productively in *otg* embryos after radiation treatment.

While identifying an aberrant pathway that disrupts signaling and results in a particular phenotype is a useful first step toward understanding the underlying mechanism caused by a mutation, it is rare that this type of investigation leads to the discovery of the underlying mutation present in a mutant. During my thesis work, I have made a number of attempts to map the gene responsible for the two *otg* phenotypes: leukemia and resistance to irradiation-induced apoptosis. My first strategy utilized restriction-site associated DNA (RAD) mapping techniques followed by parallel and multiplexed sample sequencing of the RAD tag libraries of 16 adult leukemic fish. Two subsequent attempts relied on classical PCR-based microsatellite mapping techniques in radiation resistant embryos. Neither approach has so far yielded a map position, but we have recently begun to use one of the few zebrafish isogenic lines, CG-1 (Mizgireuv and Revskoy 2006) in an attempt to decrease intra-strain polymorphisms and increase the number of informative microsatellite markers. An approach that has been used recently to map zebrafish mutants sensitive to radiation-induced apoptosis is RNA-based deep sequencing (Cicely Jette, unpublished). Once performed it is possible to narrow down possible candidates by assuming that single base-pair mutations (the type prevalent in ENU mutagenesis) will result in the formation of

a STOP codon. This is another technique we could use in an attempt to identify the mutation responsible for the phenotypes we observe in *otg*.

Although the gene responsible for *otg* has not yet been identified, the fact that the T-ALL in these animals faithfully recapitulates the human disease suggests that the underlying genetic mechanisms may be shared between the two species. This would make zebrafish an optimal model to study human ALL. As part of my thesis, I linked a number of genomic aberrations seen in zebrafish T-ALL models with those human samples. To do this, we utilized the technique of array comparative genome hybridization (aCGH) and compared copy number aberrations (CNAs) in 17 zebrafish T-ALLs with those in 75 human samples. This allowed us to compare genomic aberrations in both primary, and relapsed human disease with spontaneously occurring, as well as the more aggressive serially transplanted, zebrafish T-ALLs. In our investigation of primary T-ALLs, we examined 14 zebrafish samples and 75 human samples. From those, we identified 10 genes who were altered in at least 3 zebrafish samples and at least 4 human samples (Figure 6.1). One of these genes, TGFBR1, has been previously identified as having a potential role in T-ALL, but the other 9 genes: *COL15A1*, *FBXO43*, *OSR2*, *MATN2, LRP6*, *MANSC1*, *PUS7*, *RNF170*, and *TOR1A* have never, to our knowledge, been associated with the transformation or leukemogenesis in T-ALL.

In addition to examining primary T-ALLs in humans and zebrafish, We focused on leukemias with particularly malignant clinical behavior. In addition to the 10 gene discussed above, we identified 6 genes encountered repeatedly in CNAs from aggressive disease in both specie (Figure 6.2). The genes amplified or deleted in aggressive disease may prognosticate therapeutic failure, or identify mis-regulated pathways governing poor outcome at the molecular level. These 6 genes are: *C7orf60, AHCYL2*, *ERGIC1, FLT4*, *CKMT1A* and *CKMT1B*. While all have potential as candidates, the fact that loss of *ACHYL2* function has been associated with both colon and lung cancer (ME et al 2006) suggests that its function mediating *P53* contributes to cancer progression. Additionally, this enzyme has been shown to play a role in altered methionine

metabolism and global DNA methylation in liver cancer (Calvisi et al 2007). Overall, these cross-species comparisons have identified a short list of genes whose potential importance for T cell malignancy will be explored in future studies.

Taken together, my PhD thesis work has contributed to a better understanding of T-ALL, and how zebrafish models of this disease can be used to improve our understanding of the molecular mechanisms underlying this disease in humans. This work started with the identification and characterization of three new models of heritable, spontaneously occurring, zebrafish T-ALL. In addition, the molecular pathway dysregulated in one of these models, *otg*, has been identified and studied, narrowing down the possible responsible candidates. Finally, this work has taken a global approach using aCGH, and examined genome losses and gains in both zebrafish, and human, forms of the disease. This comparison has identified a number of genes that may potentially underlie transformation of T-ALLs, or the development of particularly aggressive disease. As an MD/PhD student, my motivation for bench science has always been the acquisition of knowledge that contributes to improvement in diagnosis, prognosis, and treatment when returning to the bedside of our patients. By developing zebrafish as a model to study a challenging clinical entity such as T-ALL, we have begun to bridge this gap.

References

Amatruda JF, Zon LI (1999). Dissecting hematopoiesis and disease using the zebrafish. *Dev Biol* **216:** 1-15.

Armstrong SA, Look AT (2005). Molecular genetics of acute lymphoblastic leukemia. *J Clin Oncol* **23:** 6306-6315.

Beesley AH, Firth MJ, Ford J, Weller RE, Freitas JR, Perera KU *et al* (2009). Glucocorticoid resistance in T-lineage acute lymphoblastic leukaemia is associated with a proliferative metabolism. *Br J Cancer* **100:** 1926-1936.

Calvisi DF, Simile MM, Ladu S, Pellegrino R, De Murtas V, Pinna F *et al* (2007). Altered methionine metabolism and global DNA methylation in liver cancer: relationship with genomic instability and prognosis. *Int J Cancer* **121:** 2410-2420.

Chen J, Jette C, Kanki JP, Aster JC, Look AT, Griffin JD (2007). NOTCH1-induced T-cell leukemia in transgenic zebrafish. *Leukemia* **21:** 462-471.

Eimon PM, Ashkenazi A (2010). The zebrafish as a model organism for the study of apoptosis. *Apoptosis* **15:** 331-349.

Ferrando AA, Look AT (2000). Clinical implications of recurring chromosomal and associated molecular abnormalities in acute lymphoblastic leukemia. *Semin Hematol* **37:** 381-395.

Ferrando AA, Neuberg DS, Staunton J, Loh ML, Huard C, Raimondi SC *et al* (2002). Gene expression signatures define novel oncogenic pathways in T cell acute lymphoblastic leukemia. *Cancer Cell* **1:** 75-87.

Frazer JK, Meeker ND, Rudner L, Bradley DF, Smith AC, Demarest B *et al* (2009). Heritable T-cell malignancy models established in a zebrafish phenotypic screen. *Leukemia* **23:** 1825-1835.

Goldgar DE, Easton DF, Cannon-Albright LA, Skolnick MH (1994). Systematic population-based assessment of cancer risk in first-degree relatives of cancer probands. *J Natl Cancer Inst* **86:** 1600-1608.

Graux C, Cools J, Michaux L, Vandenberghe P, Hagemeijer A (2006). Cytogenetics and molecular genetics of T-cell acute lymphoblastic leukemia: from thymocyte to lymphoblast. *Leukemia* **20:** 1496-1510.

Harrison CJ, Foroni L (2002). Cytogenetics and molecular genetics of acute lymphoblastic leukemia. *Rev Clin Exp Hematol* **6:** 91-113; discussion 200-112.

Hulleman E, Kazemier KM, Holleman A, VanderWeele DJ, Rudin CM, Broekhuis MJ *et al* (2009). Inhibition of glycolysis modulates prednisolone resistance in acute lymphoblastic leukemia cells. *Blood* **113:** 2014-2021.

Jette CA, Flanagan AM, Ryan J, Pyati UJ, Carbonneau S, Stewart RA *et al* (2008). BIM and other BCL-2 family proteins exhibit cross-species conservation of function between zebrafish and mammals. *Cell Death Differ* **15:** 1063-1072.

Kim MJ, Kang KH, Kim CH, Choi SY (2008). Real-time imaging of mitochondria in transgenic zebrafish expressing mitochondrially targeted GFP. *Biotechniques* **45:** 331-334.

Langenau DM, Traver D, Ferrando AA, Kutok JL, Aster JC, Kanki JP *et al* (2003). Myc-induced T cell leukemia in transgenic zebrafish. *Science* **299:** 887-890.

Larson RA, Dodge RK, Linker CA, Stone RM, Powell BL, Lee EJ *et al* (1998). A randomized controlled trial of filgrastim during remission induction and consolidation chemotherapy for adults with acute lymphoblastic leukemia: CALGB study 9111. *Blood* **92:** 1556-1564.

ME LL, Vidal F, Gallardo D, Diaz-Fuertes M, Rojo F, Cuatrecasas M *et al* (2006). New p53 related genes in human tumors: significant downregulation in colon and lung carcinomas. *Oncol Rep* **16:** 603-608.

Mizgireuv IV, Revskoy SY (2006). Transplantable tumor lines generated in clonal zebrafish. *Cancer research* **66:** 3120-3125.

Pui CH (1998). Recent advances in the biology and treatment of childhood acute lymphoblastic leukemia. *Curr Opin Hematol* **5:** 292-301.

Pui CH, Evans WE (1998). Acute lymphoblastic leukemia. *N Engl J Med* **339:** 605-615.

Rudner LA, Frazer JK, Trede NS (2010). Modeling human hematologic malignancies in zebrafish: A review. *Current Trends in Immunology*.

Silverman LB, Sallan SE (2003). Newly diagnosed childhood acute lymphoblastic leukemia: update on prognostic factors and treatment. *Curr Opin Hematol* **10:** 290-296.

Takeuchi J, Kyo T, Naito K, Sao H, Takahashi M, Miyawaki S *et al* (2002). Induction therapy by frequent administration of doxorubicin with four other drugs, followed by intensive consolidation and maintenance therapy for adult acute lymphoblastic leukemia: the JALSG-ALL93 study. *Leukemia* **16:** 1259-1266.

Trede NS, Langenau DM, Traver D, Look AT, Zon LI (2004). The use of zebrafish to understand immunity. *Immunity* **20:** 367-379.

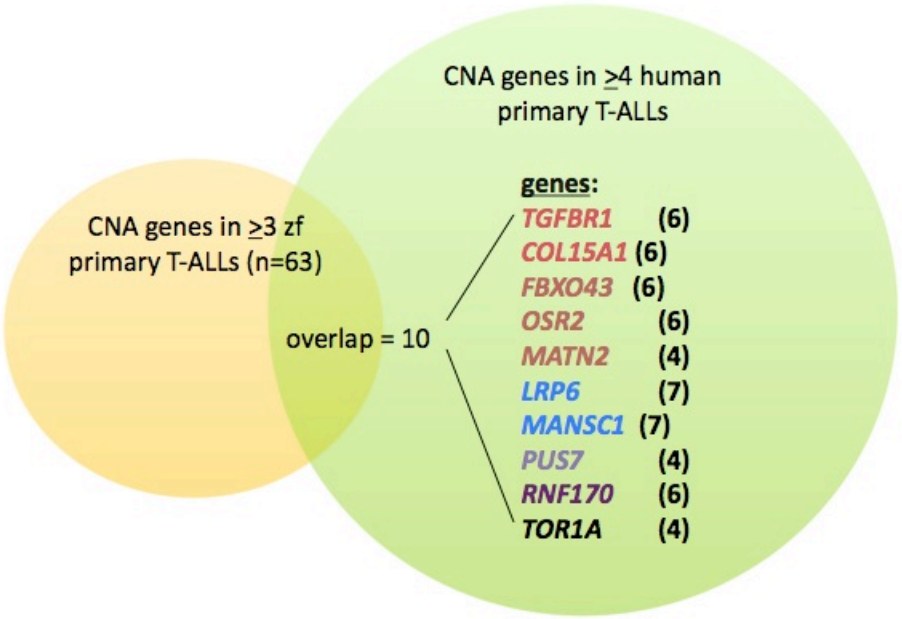

Figure 6.1 Recurrent shared CNA genes in primary zebrafish and human T-ALLs. Ten CNA genes were altered in ≥3 primary zebrafish T-ALLs (orange) and ≥4 primary human T-ALLs" (green). The gene names are listed, and colored text groups the genes by CNAs which include them.

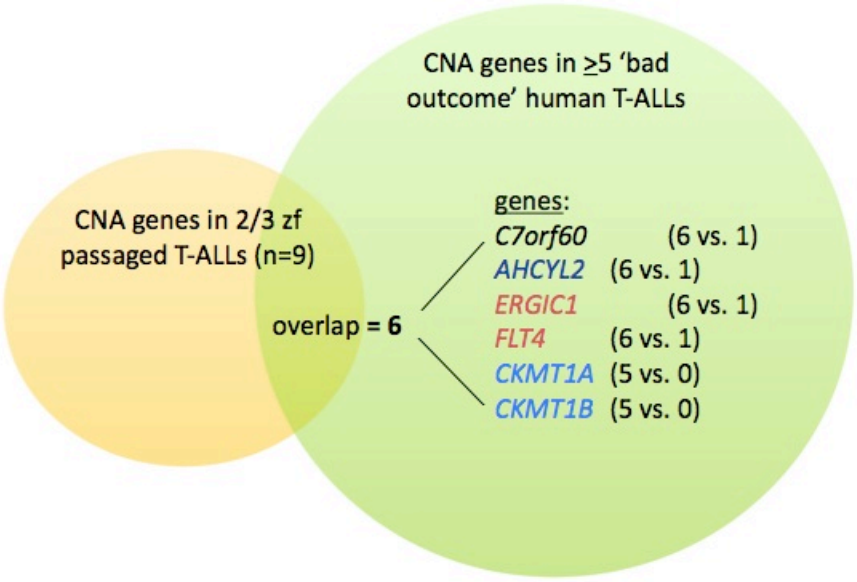

Figure 6.2. Recurrent shared CNA genes in passaged zebrafish or "bad outcome" human T-ALLs. Six CNA genes were altered in 2 passaged zebrafish T-ALLs (orange) and ≥5 human T-ALLs with "bad outcome" (green). The gene names are listed, and the number of bad outcome human samples vs. EFS human samples where the gene was altered is in parentheses. Colored text groups the genes by CNAs which include them.